YIELDING AND STRESS– STRAIN BEHAVIOUR OF SAND

by

Khaled Belkheir

(Ingenieur d'etat en Genie Civil, U.S.T.O)

Thesis submitted for the degree of

Master of science

Department of Civil Engineering

University of Glasgow

April 1993

ProQuest LLC.
789 East Eisenhower Parkway
P.O. Box 1346
Ann Arbor, MI 48106 – 1346

To my father Said

and in the memory of my Mother Yamina

CONTENTS

pages

ACKNOWLEDGEMENTS

SUMMARY

CHAPTER I : Introduction 1

CHAPTER II : REVIEW OF PLASTICITY THEORY AND ITS APPLICATION FOR SOILS

2-1 : Introduction 4

2-2 : Experimental testing of plasticity theory for soil 6

2-3 : Review of experimental evidence of plasticity 9

2-3-1 : Experimental yield curve 9

2-3-2 : Plastic potentials 13

2-3-3 : Hardening laws 14

CHAPTER III : APPARATUS AND TESTING PROCEDURES

3-1 : Hydraulic triaxial apparatus and instrumentation 18

3-1-1 : Hydraulic triaxial apparatus 18

3-1-2 : Operation of the apparatus 19

3-1-3 : Instrumentation 21

3-2 : Material used 23

3-3 : Sample preparation 24

3-3-1 : Sample preparation procedure 25

3-3-2 : Sample saturation procedure 27

3-4 : Test technique 29

3-5 : Shear box apparatus and instrumentation 29

3-5-1 : Instrumentation 30

3-5-2 : Test technique 30

CHAPTER IV : EXPERIMENTAL RESULTS

4-1 : Standard drained compression tests 32

4-2 : Stress dilatancy 36

4-3 : Stress probes 40

4-4 : Shear box tests 46

CHAPTER V : A CONSTITUTIVE MODEL FOR SAND IN TRIAXIAL COMPRESSION

5-1 : Introduction 49

5-2 : Elastic properties 50

5-3 : Shear yield with its corresponding plastic potential functions 53

5-3-1: Shear yield function 55

5-3-2: Plastic potential function 56

5-3-3: Experimental findings 58

5-3-4: Shear hardening law and flow rule for sand 60

5-3-4-1: Shear hardening law 60

5-3-4-1-1: New shear hardening law 64

5-3-4-2: A new flow rule for sand 66

5-4: Volumetric yield with its corresponding plastic potential functions 68

5-4-1: Volumetric yield surface 68

5-4-2: Volumetric hardening law 69

5-5 : Total plastic response 71

5-6 : Control of parameters 72

5-7 : Performance and predictions of the model 76

5-8 : Limitation of the model 79

CHAPTER VI : CONCLUSION

6-1 : Introduction 82

6-2 : Extension to general stress states 85

6-3 : Suggestions for future work 88

FIGURES

REFERENCES

ACKNOWLEDGEMENTS

The work described in this thesis was carried out in the Department of Civil Engineering at Glasgow University.

The Author wishes to thank his supervisor, Professor David Muir Wood, Cormack Professor of Civil Engineering for his invaluable advice and suggestions and for the time he has devoted in many discussions and in the revision of the manuscript of this thesis.

I am also grateful to Professor A. Drescher for the interest he has shown to my work and for his suggestions during his stay at Glasgow University.

Appreciations are extended to Mr T.W. Finlay and Dr P. Smart for his help in setting up the optical microscope.

The help of W. Henderson, T. Montgomery and I. Dickson has been indispensable in sorting out the problems encountered in the laboratory.

Many thanks also to my friends and fellow research students, M. Ould Khaoua, M. Zerroukat, T. Ould Kada, Dr A. Bensalem, Dr H.K. Jassem, Dr L. Dingfu and Wei Hu.

SUMMARY

The object of this work has been to gain an understanding of sand behaviour when subjected to a change of stress.

The testing procedure involved development of a pluviation method of sample preparation and a saturation method using the initial vacuum technique.

Experimental testing has been carried out in a Bishop and Wesley triaxial cell.

The tests involved conventional drained triaxial tests and stress probes around an anisotropic stress state on saturated Lochaline sand.

A group of shear box tests were used merely to compare the angles of frictions that have been obtained both in the triaxial tests and shear box tests and also to test the available stress dilatancy relationships e.g Taylor (1948).

The first type of tests was used to derive some of the ingredients of incremental plasticity theory (flow rules etc..) and elastic parameters.

The second type of tests was used to see the relationship between different constant stress increment ratios and strain increment ratios, in other words the study of the dependency of the strain increment ratio on stress path. The effect of stress state on strain increment ratio was also studied.

A model has been developed based on the concept of double hardening which uses two mechanisms of yielding, a shear yielding and a volumetric yielding.

This model uses a new flow rule for shear yielding that is able to take into account the stress level and initial density dependency of the resulting stress strain relationships.

This model gives very good predictions and simulates most of the features observed in the triaxial compression. It is also able to determine the incremental response and the yielding properties of sand when subjected to probings in different directions.

CHAPTER I

INTRODUCTION

The various models proposed to predict the stress– strain behaviour of soils are based on a wide range of concepts.

No mathematical model can completely describe the complex behaviour of real soils. Each soil model aims to predict certain phenomena, describe the essential features and ignore or disregard what is considered to be less important. Thus these models or constitutive relations for soils become very limited when confronted with situations when the features that have been disregraded become dominant.

Obviously a number of tests need to be performed in order to identify the parameters of a given soil in a set of constitutive equations. Hence an integration of tests and theoretical studies of constitutive relations is required.

The physical properties and mechanical behaviour of soils are far from being well understood.

Experiments should be conducted so that realistic simulation of in situ conditions is achieved.

New testing techniques and equipment need to be developed accounting for a more uniform distribution of stress and strain throughout the sample.

In order to define completely the stress state for an element of any continuous material, six independent components of stress need to be specified. In other words

six degrees of freedom would be desirable in testing equipment. However most laboratory test apparatus have two or at best three degrees of freedom, we can cite among these testing apparatus:

- Conventional triaxial apparatus: two degrees of freedom

- Simple shear apparatus : two degrees of freedom

- Directional shear cell : three degrees of freedom

- Hollow cylinder : four degrees of freedom

- True triaxial : three degrees of freedom

During the recent past, several types of sophisticated equipment have been developed with accompanying testing techniques to study the behaviour of soils. This has been mainly due to the following reasons:

- The increasing demand for a large variety of information and parameters which can be used to describe the behaviour of a given soil in a set of constitutive equations.

- Realistic experimental simulation of in situ conditions and better understanding of soil behaviour require development of new testing techniques and equipment that has capabilities exceeding those of conventional apparatus.

- The explosion in the number of electronic tools aimed at better measurements, better reading and better processing of data obtained during laboratory testing.
Moreover identification of phenomena such as anisotropy in granular soil and the

separation of the effects of anisotopy from other features that contribute to the behaviour of the soil, require the use of experimental devices that are capable of producing rotation of principal axes with respect to reference axes of the material. In the past, it was not possible to achieve such tasks with conventional apparatus e.g triaxial apparatus.

We can divide these new testing apparatus into two groups:

- those which produce rotation of principal axes such as simple shear apparatus; hollow cylinder apparatus and directional shear apparatus

- those which have fixed principal axes and can produce only a jump rotation of 90 degrees such as hollow cylinder (when no torque is applied to the sample, but different inside and outside pressures); and multiaxial cubical apparatus.

However in this present research work, experiments were conducted in the triaxial apparatus using a versatile equipment (Bishop and Wesley cell) which permits one to follow a wide range of stress paths in compression and extension. The tests were exclusively limited to the case of compression. Stress probes at two different initial states were carried out in order to investigate the local response of Lochaline sand to stress changes and compare it with the prediction of plasticity theory. A model has been developed within the framework of incremental plasticity using two sets of yield surfaces. The critical state conditions have also been incorporated in the constitutive equations. The model has been shown to give a good agreement with the experimental observations. A group of shear box tests have also been conducted in order to compare the strength of this saturated Lochaline sand obtained using the shear box and triaxial apparatuses.

CHAPTER II

REVIEW OF PLASTICITY THEORY AND ITS APPLICATION FOR SOIL

2– 1 INTRODUCTION

Theoretical modelling for soils is over two centuries old, starting probably from the analyses of failure mechanisms of soil masses. In these analyses, the soil was idealised as a rigid – perfectly plastic solid, and simple calculations led to an estimation of the ultimate loads that would cause collapse without any attempt to predict the magnitude of deformation of the soil before failure. These analyses used perfect plastic models in which the yield locus is fixed in stress space and is therefore identical to the failure locus.

Whilst useful for applications to stability problems (slope stability, retaining wall, bearing capacity of footings, etc), perfect plasticity is not suitable for the study of stress strain relations at working loads and before failure is reached. One deficiency of this perfect plasticity model when used to predict the deformations of soils arises because for granular materials the Mohr– Coulomb failure criterion was treated as

both yield envelope and plastic potential and the normality condition then implies an unacceptably large rate of dilation at failure, with the angle of dilation being equal to the angle of internal friction. It is clear from experimental observation that soils are not rigid before failure.

The limitations of perfect plasticity theory led Drucker, Gibson and Henkel (1957) to make a major advance in the application of the theory of plasticity to soil by introducing the concept of work hardening theory of plasticity. The idea put forward by these workers was that the isotropic compression curve is a work hardening stress strain relationship, and can be associated with successive yield envelopes. The model proposed by these research workers was incomplete and did not achieve a full synthesis of soil behaviour.

However, the introduction of the concept of work hardening plasticity, led the Cambridge soil mechanics group led by Roscoe to add an additional feature to this concept, the idea of critical states proposed by Roscoe et al (1958).

This has led to the development of the Cam – clay model (Schofield and Wroth (1968)) which instead of being based on the Mohr – Coulomb failure criterion, uses a basic energy equation which specifies how any externally applied energy is divided between that part stored and that dissipated. This Cam – clay model provides a way of fitting the pre – failure behaviour of soil. An extensive number of models has been suggested since the publication of this model, each trying to match a new aspect of soil behaviour. The Cam–Clay model although not particularly suited for sand does provide understanding of soil behaviour and many models have used similar principles and may predict the existence of critical states and make statements about dissipation of energy which are then artificially linked to the work hardening theory of plasticity.

The Cam–clay model is unsatisfactory in its description of the mechanical behaviour of sand because:

–(a)– sands show yielding controlled primarily by stress ratio so that the Cam–clay yield locus is not a correct shape.

–(b)– sand does not seem to follow the principle of normality of plastic strain increment to yield loci.

(c)– Hardening effects in sand seem to be mainly linked with distortional strains.

In this thesis a model for the behaviour of sand in triaxial compression is developed which overcomes these disadvantages and matches many of the observed features of sand response.

Unfortunately, models developed for sand which are expressed entirely in terms of isotropic hardening plasticity theory do not fit unloading behaviour of sand. Soil shows hysteretic and non linear behaviour below the yield locus. Plasticity models may be expanded and modified to accommodate many aspects of soil behaviour. Some of these extensions are mentioned in Chapter 5 under possibilities for future work.

2–2 Experimental Testing of Plasticity Theory for Soil

The application of plasticity theory to soils is a subject which has been studied extensively during the last forty years of this century and is still a topic which must be examined critically.

Testing the validity of plasticity theory requires tests conducted at working loads below failure so that deformations of the material, which may include recoverable deformations and irrecoverable deformations, can be assessed.

The simplest test that can be thought of is a test in which the soil is loaded,

unloaded and reloaded. The character of the response observed shows that under small unloading– reloading cycles the response of soil is of the general type predicted by plasticity theory. Such tests could, for example, be isotropic compression tests or shear tests. However, if the magnitude of the cycles of loading, unloading and reloading is increased, the soil starts showing hysteretic response. The amount of hysteresis may increase with the number of cycles in a way which conventional theory of plasticity does not account for. Limited experimental information is given on the hardening of the material.

However, tests of this sort have provided extensive information about plasticity theories for soil. In the case of sand such, tests involving monotonic loading with increasing stresses have provided experimental evidence of stress dilatancy relationships.

Such tests are certainly not sufficient in proclaiming the validity of the application of plasticity theory for soil since they do not check the form of the yield locus which is one of the central ideas of incremental plasticity theory and the behaviour of this yield locus lies at the heart of the theory. Its position indicates when yield will begin thus causing plastic deformations. Tatsuoka and Ishihara (1974a) performed shear tests in which a sample is first loaded (at constant cell pressure) and unloaded (at constant cell pressure). After reducing the mean effective stress while maintaining the shear stress constant, the sample is reloaded again and the stress strain relationship allows a yield point to be detected. This investigation is continued with further probes in order to trace a series of segments of individual yield curves. However this type of investigation is very lengthy and disregards the effect of hardening of the first probes which may significantly alter the shape of the yield surface or segment of yield surface detected by the later probes; the tests always cross the yield locus in the same direction, so that there is no attempt to study the effect of change of direction of probing on the yield curve.

Testing normality and local slope of yield locus has been done in the past for a

clay by Lewin and Burland (1970). They performed tests on clay involving stress probes to see whether the direction of the strain increment vector was independent of the direction of the stress increment. Their results show a dependency of the direction of strain increment vector on the applied stress path.

Stress probing of the type conducted by Lewin and Burland (1970) is an alternative to investigate the yield curve provided that strain and stress measurements are accurate.

In Lewin's tests samples were subjected to identical stress histories, and then subjected to a series of small stress probe tests in which the probe was made in a different direction for each test. If series of stress probes with loading and unloading are carried out, the strain response gives detailed information about the elastic and plastic properties. Investigation into the yielding properties of sand under greater range of stress histories, stress states and stress probes directions is required in order to test more rigorously the applicability of the predictions of plasticity theory to soil.

In this research work, stress probe tests have been conducted in which samples were subjected to identical stress histories, and then subjected to a series of small stress probe tests at two different stress ratio states, in which the probe was made in a different direction for each test. The effect of change of direction of stress increment and stress state on the resulting direction of strain increment vector has been studied. The effect of stress history has not been investigated so that evidence of kinematic hardening which develops with stress history (this evidence is available in the literature) cannot be produced here.

The disadvantage with stress probes is that they require several samples to be prepared and provide only a few discrete points which may be difficult to interpret (particularly for stress paths involving unloading). An alternative to that has been suggested by Houlsby (1981). He suggested stress cycle tests in which the same

information as given by stress probes using several identical samples can be gathered using a single test only on a single sample.

2– 3 Review of Experimental Evidence of Plasticity

In order to predict the deformation of sand using an elasto– plastic model, firstly the elastic response of the material must be assessed, then a yield function, a plastic potential and a hardening law have to be defined. Among these functions, the yield function represents the shape of the yield curve in a stress space which distinguishes stress states which can be reached elastically from those which can only be reached after plastic deformation (or cannot be reached at all). Therefore it is necessary to investigate the yield characteristics of sand in order to evaluate the stress strain behaviour of sand which has experienced complicated stress histories during loading, unloading and reloading processes.

2– 3– 1 Experimental yield curve

The investigation of the shape of the yield curve of sand was first carried out by Poorooshasb et al (1966,1967). The shape of yield curve for isotropically conmpressed dense sand was investigated by an experimental test program consisting of multi– stage triaxial compression tests in which loading, unloading and reloading cycles shown in Fig 2.1 were repeated several times.

Fig 2.2 shows the resulting stress strain curves together with the yield points. The initiation of yielding was determined as the state of stress associated with a marked change in slope of the stress strain curves. The yield curves in the triaxial plane were found to be approximately straight lines (see fig 2.3) at constant stress ratio

and they were found not to coincide with the shape of plastic potential curves.
Barden et al (1969) performed plane strain tests with multi– stage stress paths with confining pressures ranging from 30– 7000 kPa in order to examine the shape of the yield curve for dense sand. Their results show that under plane strain conditions at fairly low stress levels, the shape of yield curves was approximated by the previous maximum value of the stress ratio. At high mean stress levels, particle crushing occurs and this complicates the yield behaviour.
These workers also showed that the yield surface did not coincide with the plastic potential surface.

Tatsuoka and Ishihara (1974a) carried out several triaxial compression tests with multi– stage stress paths on sand having several different densities. The test results show (Fig 2.4) that the experimental yield curves for loose, medium dense and dense sand are slightly curved lines.
It was concluded that the yield curves could be determined uniquely independently of previous stress history but dependent to some extent on the densities of the sample.

Khatrush (1987) performed triaxial tests using internal devices to measure the deformations. The method followed in the detection of occurrence of yielding was based on the idea that when the sample is subjected to unload reload cycles along the same stress path, the sample does not yield until a stress ratio close to the previous maximum stress ratio is exceeded. This worker went on to say that this is valid whatever the stress level at which unloading take place. The experimental yield locus was found to agree with the one suggested by Tatsuoka et al (1974a). The validity of the proposed shape of the yield locus was examined by performing a multi stage stress path. The type of stress path sequence is shown in fig 2.5 (a). It can be seen that after a yield locus has been obtained by loading / unloading / reloading path 1, the other two unloading– reloading paths 2 and 3 were located within the

elastic domain which is below the yield locus. The shear strains corresponding to these tests as shown in fig 2.5 (b) indicate no further irrecoverable strains occuring on the second and third loading. The effect of stress history on the shape of the yield locus was also studied by performing three triaxial stress paths. In the first (see fig 2.6 (a)) the sample was loaded in compression along a constant stress ratio OA, unloaded along the same stress path, then reloaded along a higher constant stress ratio path OB. The second sample (see fig 2.6 (a)) was also loaded in compression but with the opposite sequence of loading to the first. Thus the sample was loaded along a higher constant stress ratio path OB, unloaded along the same path, then reloaded at a lower stress ratio. In the third test (see fig 2.6 (c)) the same sequence of cycles of loading was applied but in extension.

It can be seen in fig 2.6 (a) that there is a continuous increase in the plastic shear strains on reloading along a higher constant stress ratio path, whereas there is no sign of development of plastic shear strains on reloading along a lower constant stress ratio path (see fig 2.6 (b)). Similar results were observed in extension, see fig 2.6 (c). Stress reversals were also performed by this worker in order to investigate the effect of these on the shape of yield locus. Evidence from the results of some complex stress paths indicates that the shape of the yield locus after stress reversal was not significantly affected and remains unchanged.

Although these reviewed yield curves represent reasonably the yield properties of sands under shear stresses, they fail to describe the yield properties associated with development of volumetric strains for example in isotropic compression. For this reason, another yield function was proposed to describe the volumetric strains due to isotropic compression.

The shape of the yield envelope for compression of sand does not seem to be well determined. Some experimental data obtained by Miura et al (1982a;1984) indicate that the shape is broadly similar to that given by the various Cam–Clay type theories.

Although more complex shapes have been suggested, it is likely that the modified Cam– clay ellipse could be used for describing the compression of a sand as well as clay (Wroth and Houlsby (1985)). There is clear evidence (Miura et al (1984)) that even at low stress ratios sand exhibits non associative flow, however sufficient accuracy can probably be obtained by using an associative flow rule at low stress ratios, since the compression strains in sand are relatively small.

It is to be noted that most of the experimental findings that are available in the literature were restricted to isotropically compressed sands. Little evidence seems to be available about the shape of yield locus for anisotropically compressed sands which may have important effects on the deformation of sand; in addition to the fact that in situ stress states are generaly anisotropic. Yasufuku et al (1991) performed series of tests in order to study the yield characteristics of an anisotropically compressed sand at both low and high stress levels. Tests of type A, B, and C (see fig2.7 (a), fig2.7 (b) and fig2.7 (c) respectively) were performed at low and high stress levels. In tests of type A, the samples were anisotropically compressed to point A (along a constant stress ratio path) and were then unloaded to point B, along the same constant stress ratio path. From the common point B, eight stress paths of constant stress increment ratios were applied. In tests of type B, the samples were isotropically compressed to A and unloaded to B from which eight stress paths of constant stress increment ratios were applied. Tests of type C are the same as tests of type A except that they were conducted on the extension side of the p': q plane. These types of tests B and C are merely conducted in order to investigate the effect of stress history on the shape of the yield curve (proportional loading path history). These research workers concluded that for tests of type A it can be said that the overall shape of both yield curves in the low and high stress levels is roughly similar. The shape of these yield loci for anisotropically compressed sand is an approximately elliptical one (see fig2.8 (a) and fig2.8 (b)), which are not symmetrical about the

isotropic stress axis. For tests of type B and C, it was found that both yield curves were elliptical but considerably different from each other in shape (see fig2.3 (a) and fig2.3 (b)).

This then appears to suggest that the shape of yield curve is dependent on the stress history experienced by the soil; in other words the shape of the yield locus has a kinematic nature dependent on the stress history.

2–3–2 Plastic potentials

Plastic potentials are used to describe the mechanism of plastic deformation that occurs when the soil yields. The normal to the plastic potential surface that passes through the current stress state indicates the direction of the corresponding plastic strain increment vector.

The relationship between plastic strain increment ratio and stress ratio is known as a flow rule controlling the mechanism of deformation. The shape of the plastic potential is usually expressed in the form of a flow rule relating directions of plastic strain increments to the current stress state.

Whilst the experimental determination of the form of flow rules is reasonably well established, although there is some uncertainty concerning the assumed elastic response, it has been noted already that the shape of yield curve is less easy to determine experimentally because it relies partly on indirect evidence (indistinct yield point in stress strain relationships and hardening of the yield locus between successive probes). However, on the basis of experimental evidence it seems that the yield surface and plastic potential function do not have the same shape, thus implying that the condition of normality cannot apply for sand.

One of the most successful flow rules proposed for sand is the stress dilatancy relationship proposed by Rowe (1962). The derivation of flow rules for granular

materials is frequently based on considerations of the dissipation of energy in plastic work. For instance the original Cam-clay flow rule which fits well the behaviour of sand in the triaxial plane is based on the simple hypothesis that the incremental plastic work dW_p is given by

$$dW_p = M.p'.d\epsilon_q^p \quad (2.1)$$

where M = critical state stress ratio

$d\epsilon_q^p$ is the incremental plastic shear strain

If use is made of any flow rules based on assumptions of work dissipation, and resulting in relationships between the stress ratio and strain increment ratio, then the characteristic state (the stress ratio at which the volumetric strain rate is instantaneously zero), the line of phase transformation (the stress ratio at which the rate of change of mean effective stress in undrained tests is instantaneously zero) and the critical state (the stress ratio at which there is continuous shearing at constant volume and effective stresses) are forced to be at the same stress ratio.

However, these flow rules are not appropriate for the strains associated with low stress ratio compression. The plastic strains on isotropic compression may be modelled quite accurately by a hardening law which depends on a power function of the mean effective stress. Lade (1977) reports values which imply that the equivalent plastic modulus depends on the mean effectve stress to a power between 0.12 and 0.74. The data of Lee and Seed (1967) (see fig2.10) show that at very high pressures compression lines for sand, are like those of clays, approximately straight in $v-\ln p'$ space.

2-3-3 Hardening laws

The prediction of plastic strain magnitude is equivalent to establishing the

hardening law. When loading proceeds, the yield locus expands. The link between this expansion of the yield locus and development of plastic strains is also the hardening law. Under general conditions of stress, predictions of the magnitude of plastic strains becomes very difficult.

Often the hardening law is derived from a constant cell pressure triaxial test, which a priori does not guarantee the applicability of the same law to a different stress path.

At the onset of loading, as the deformation proceeds the yield locus expands and the hardening function is positive. If the failure locus is reached the hardening function becomes negative, the yield locus contracts and the material softens. Eventually, the critical state is reached after large deformations.

For sand, a hardening law that is dependent on the plastic shear strain is appropriate for explaining the stress strain relationships due to shear loading.

The earliest approach, is to fit a hyperbola to the shear stress : strain curve. This method originates with the work of Kondner and Zelasko (1963) and is widely accepted as providing a reasonable fit to the data. Vermeer (1978) adapts this approach to plasticity and fits a hyperbola to a plot of stress ratio versus shear strain. However this approach is not totally satisfactory in the sense that it does not allow any softening to occur and hence the material continuously hardens until the stresses reach certain asymptotic values. Other approaches are taken by other research workers in order to simulate softening of the soil. These approaches are extensively described in Chapter 5.

Other workers (Tavenas et al (1979), Yasufuku et al (1991) among others) have defined hardening by use of strain energy contours which have been found experimentally to have the same shape as the yield locus, so that energy serves as a parameter for describing the expansion of the yield locus.

It has been tacitly implied that most of the models reviewed above use an isotropic

hardening rule, few other models use both kinematic and isotropic hardening rules which describe the change of the size and shape of the yield locus, which may be more realistic but need new concepts to be introduced within the framework of plasticity, like for instance bounding surface or multiple yield surfaces (concepts which will be outlined in Chapter 5).

Evidence for the kinematic nature of the hardening of the yield locus has been produced by some workers.

Jardine (1992) show data of effective stress paths and strains during triaxial compression of samples which have been unloaded one dimensionnaly to various overconsolidation ratios. The truly elastic response was shown to extend up to a shear strain of 0.01 per cent. Jardine (1992) attempted to describe the stress strain behaviour of soil by defining, in normalised stress space, an outer bounding surface and three characteristic zones which he termed KSYS's (kinematic sub– yield surfaces) (see fig2.11). It was assumed that a small inner yield surface exists which bounds a small region of truly elastically attainable effective stress states and which is carried around by the current stress state. A change of stress to a state lying inside zone I is associated with high stiffness; a change of stress to a state lying between zone II and zone III is associated with a lower stiffness; and a change of stress to a state lying beyond zone III (outer surface) is associated with major irrecoverable deformations. Jardine (1992) interpreted the stiffness data (see fig2.12) and contours of strain (see fig2.13) as indicating the changing position of the inner yield locus as the soil is unloaded.

The same approach has been taken by Alawaji et al (1990). Identical samples of sand with different stress histories were probed to discover the position of a current yield locus using a True Triaxial Apparatus. In these tests the contours of strains were treated as an indication of the size of the current yield locus. The shape of these strain contours has been approximated to circles. The centres of these circles can give the position of the current yield locus. If a link is imagined between the

current yield locus (centre of a circle) and the history of stresses that the sand has experienced, the change of position of the yield locus (translation) serves as a measure of kinematic translation of the yield locus.

In this Chapter, a selective review of plasticity theory and its application for soils has been given. The type of experimental programe for testing the predictions of plasticity theory for soil has also been outlined with particular emphasis on stress probe tests which provide a rigorous test for plasticity theory (effect of stress state, stress history (kinematic nature of the hardening of yield locus) and stress path dependency of the resulting stress– strain behaviour of sand).

The remainder of the dissertation is divided into four Chapters: Chapter III deals mainly with apparatus and testing procedures. A method of sample preparation has been developed using an air pluviation technique. A sample saturation procedure has also been developed based on the initial vacuum technique. Chapter IV is an experimental study of the way in which the predictions of plasticity theory may be tested experimentally, leading to a programe of simple conventional stress paths and stress probe which are used to study the effects of stress state and stress path dependency on the behaviour of sand. A Bishop and Wesley triaxial cell has been used in this study. The results of the tests are presented and interpreted in terms of elasticity and plasticity theory. In Chapter V a double hardening model is described within the framework of incremental plasticity theory and critical state conditions. The model is shown to perform well in conditions of monotonic change of stresses. Indications are given of how conventional plasticity theory may be extended in order to accommodate situations where stress reversals or cyclic loading are of primary concern. Finally, Chapter VI is divided into two parts: Part one is a summary of the constitutive model developed in this work. Part two deals with the study of factors that may influence the way in which the constitutive model should be extended to general states of stress.

CHAPTER III

APPARATUS AND TESTING PROCEDURES

3–1 Hydraulic triaxial apparatus and instrumentation

3–1–1 Hydraulic triaxial apparatus

Bishop and Wesley (1975) have described a hydraulically loaded triaxial cell which was developed at Imperial College and is intended to readily reproduce a wide range of stress path conditions in the laboratory.

Cylindrical samples of 38mm diameter can be tested in either axial compression and axial extension. Tests can be carried out either at controlled rates of loading or controlled rate of strain.

The design is based on experience gained at Imperial College through the use of the Bellofram rolling seal as a loading device (see fig 3.1).

The pedestal is mounted at the top of a loading ram, at the bottom of which is a piston and pressure chamber. The upper part is similar to the conventional triaxial cell except that the vertical load in a compression test is applied by moving the sample pedestal upwards from below and pushing the top cap against a stationary load cell which records the load. The Bellofram rolling seals are used to retain the cell fluid and the ram travels up and down in a rotolin linear bearing. The axial load is applied by increasing the chamber pressure.

The loading ram has a cross–arm attached to it which moves up and down in wide slots. The cross–arm has two rods attached to it and axial deflections can be measured with dial gauges or linear transducers mounted on the top of the cell.

In the present research work, some modifications have been made to the existing drainage lines because of occurrence of leakage. It is believed that the new configuration of drainage lines (see fig 3.2) will ensure the prevention of leakage. In the original configuration of drainage lines (see fig 3.1), both the drainage and the pore pressure leads from the sample pedestal are taken down the centre of the loading ram and out through slots, whereas the new configuration takes the drainage and pore pressures leads from the sample pedestal out through holes which are provided inside the cell. The new configuration also permits both bottom and top drainage of the sample.

3–1–2 Operation of the apparatus

When using this apparatus, the operator will generally desire to vary σ_a (the axial stress) and σ_r (the radial stress) in some controlled manner and measure the resulting deformation of the sample and the pore pressure response or volume change. However, the two pressures which can be controlled directly are the cell pressure (σ_r) and the pressure in the lower pressure chamber (pc). The value of σ_a

is dependent on both σ_r and pc and the key to the operation of the apparatus is the relationship between σ_a, σ_r and pc. This relationship is obtained by considering the equilibrium of the loading ram and could be expressed as:

$$\sigma_a = pc.(a/A) + \sigma_r.(1 - (a/A)) - W/A \quad (3.1)$$

where : A is the sample area, at the relevant stage of the test

a is the Bellofram seal area

W is the weight of the sample

Using equation (3.1) it is easy to determine the way in which pc must be varied in order to produce a required stress path. It is even more appropriate if eqn (3.1) is written in terms of stress change :

$$\Delta\sigma_a = \Delta pc.(a/A) + \Delta\sigma_r.(1 - (a/A)) \quad (3.2)$$

Since many stress paths are conveniently expressed in the form :

$$\Delta\sigma_r = k.\Delta\sigma_a \text{ (in term of total stresses)} \quad (3.3)$$

or $$\Delta\sigma'_r = k.\Delta\sigma'_a \text{ (in terms of effective stresses)} \quad (3.4)$$

by substituting eqn (3.3) in eqn (3.2) we obtain

$$\Delta pc = \Delta\sigma_r.(1 + (A/a).((1/k) - 1)) \quad (3.5)$$

or in drained tests with a constant back pressure u

$$\Delta pc = \Delta\sigma'_r.(1 + (A/a).((1/k) - 1)) \quad (3.6)$$

For any particular test it is easy to determine from eqn (3.6) the way in which pc should be varied in order to produce the required stress path.

At the start of a test a cell pressure is usually applied and the value of pc then adjusted so as to balance the cell pressure plus ram and sample weight. Controlling the test from this stage onward, the operator need only be concerned with stress changes.

In conventional triaxial apparatus, tests can be conducted only with constant rate of axial strain, in other words only strain controlled tests can be performed. Tests can be run using this present apparatus under either stress controlled or strain controlled loading.

Stress controlled tests can be performed by connecting the lower pressure chamber to a controllable pressure source (see fig 3.2).

Strain controlled loading can be performed by connecting the lower pressure chamber to a standard control cylinder with a screw–controlled piston which then provides a constant rate of flow source (see fig 3.2), the screw is rotated either manually as is the case in the present work or by an electric motor which can be connected to it.

3–1–3 Instrumentation

Four types of transducers were used as measuring devices namely, :

– Pressure transducers

– Load transducers

- Displacement transducers

- Volume change transducers

The measurements or information from these transducers are received by a Solartron Orion datalogger, which also provides a constant voltage source to energise each transducer (except displacement transducers).

- **Pressure transducers**

Three pressure transducers were used, a pore pressure transducer to measure the pore water pressure in the sample, a cell pressure transducer to measure the pressure of the fluid (water) in the cell and an axial pressure transducer to measure the pressure in the chamber beneath the cell. These transducers could be used at pressures in the range 0 - 1000 kPa.

- **Load transducer**

A submersible load transducer is used in this testing device. The outstanding advantage of the submersible transducer is the elimination of the effects of piston friction from the load measurements. The capacity of this transducer was 4.5 kN.

- **Displacement transducers**

Two LVDTs were used, one to monitor the axial deformation of the sample; the travel of this transducer was 50 mm, and the other to monitor the movement of the piston of the volume change device, the travel of that latter transducer was 35 mm.

- Volume change transducer

The volume change transducer shown in fig 3.3 was developed at Imperial College, London.

This device consists of a hollow thick walled brass cylinder containing a floating piston attached to a bellofram rolling seal at either end. Movement is measured by an externally mounted displacement transducer. A unit of 50 cm^3 capacity has been used in this study reading to 0.02 cm^3.

One advantage of this type of transducer is that pressurised air can be applied to the lower end as an alternative to water. The unit then serves as a pressurised air/water interface and a separate air/water bladder cell is not necessary.

These transducers can be used at back pressures up to 1400 kPa, but a minimum pressure of about 30 kPa is needed to expand the bellofram seals.

3- 2 Material used

The material used throughout this work was a fine saturated Lochaline sand. Sieve analyses were performed on the sand following the procedure described in B.S 1377 (1975). The resulting particle size distribution shown in fig 3.4 provides a fine uniform material for testing which would not segregate when formed into specimens, and for which membrane penetration would be negligible. The particle shapes were looked at using the optical microscope. The particle shape was found to be fairly rounded with the effective particle size, D_{50} of 0.21 mm and a coefficient of uniformity C_u = 1.40. The specific gravity was measured using the density bottle method which is described by K.H.Head (1984). The value of the specific gravity was found to be 2.65.

The maximum void ratio was determined by the procedure known as dry shaking

Head (1984), a method which consists of placing 1kg dry sand into a glass graduated cylinder, 2000cm^3, of approximately 75mm diameter to which is fitted a bung. The cylinder is shaken by inverting it a few times, to thoroughly loosen the sand. The cylinder is turned upside down and very quickly turned back again. The volume of sand is recorded on the graduated scale and subsequently the maximum void ratio is calculated.

The minimum void ratio was determined using the vibrating hammer procedure which consists of placing sand in a cylindrical metal mould in three approximately equal layers. Each layer is compacted for 5min using the electric vibrating hammer.

The dry mass is measured and subsequently the minimum void ratio is calculated. Those two methods have been described by K.H.Head (1984). The limiting void ratios were 0.84 and 0.51 respectively.

3– 3 Sample preparation

Testing of uniform samples under uniform states of stress and strain is required for fundamental studies of soil property characterisation. It is generally assumed that a specimen tested in the laboratory represents an infinitesimal element of a soil medium. It is necessary to be able to prepare series of identical homogeneous specimens for such studies in order that effects of stress history can be studied with effects of sample preparation eliminated.

The control of uniformity and the ability to replicate several specimens are difficult but very important. Several methods of reconstituting sand specimens have been used, the common objective in each method has been the control of average density. Uniformity is generally assumed, conscious efforts to verify uniformity by direct measurement of density over the height of reconstituted sample have been made only in a limited number of cases (Vaid et al (1988)). These measurements show that

specimens prepared by pluviation in air or water tend to be uniform: methods which require compaction by, for example, moist tamping produce samples that are less uniform. Basic principles of pluviation are given by Kolbuzewski (1948a, 1948b) and various modifications to the method are described in the literature (eg Mulilis et al (1977), Miura et al (1982b), Singh et al (1982), Chaney et al (1978) among others). With these techniques it is possible to prepare specimens having a wide range of relative densities (usually from 10 – 15 % to 90 – 95 %), thus avoiding the use of vibrations to obtain high densities as described by Bishop and Henkel (1962) for the funnel method. Improvements in saturation procedures make wet pluviation unnecessary. Specimens can be prepared dry and saturated subsequently (Baldi et al (1988)) as is the case in the present experimental programme. Pluviation of sand specimens is fast and thus particularly useful when large specimens are to be prepared. However, this method is not suitable for use with material having a large grain size distribution because particle segregation may occur, particularly when fines are present. In those circumstances a method such as tamping which has been described by Ladd (1978) may be more appropriate. Low vibration methods have also been shown to produce uniform sand samples (see Mulilis et al (1977)).

3– 3– 1 Sample preparation procedure

The technique for deposition used in this present research work is based on Kolbuszewski's principles. A pouring tower produces a rain of sand grains, and by altering the intensity of the raining and the height of fall, the density of the resulting deposit can be varied within a wide range. The deposition system is required to produce a rain of sand grains, the velocity and intensity of which can be varied over wide limits.

The velocity depends on the height of fall and so can be easily adjusted to control the intensity; this is achieved by means of a variable aperture hopper (see fig 3.5).

Essentially, this consists of a square plate which is perforated with a regular pattern of holes. This plate is called the base plate, two other plates are provided with the same pattern of holes. One of these, the control plate, rests on the base plate. The effective aperture and hence the flow of sand out of the hopper can be varied.
The other plate, the shutter plate, is placed immediately beneath the base plate and is used to start and stop the flow of sand. The vertical jets of sand issuing from the hopper are then dispersed into a uniform rain by a sieve mesh placed below the hopper (see fig 3.5).

The design consists of a cylindrical tower made of perspex at the top of which is fixed a container. Through this tower the three plates are fixed followed by a couple of meshes. It would be worth noting that in this design the height of deposition was kept fixed, since the terminal velocity of the sand was reached at a height of 30 cm, consequently the density produced was dependent only on the intensity of raining.
This does not seem to support the popular concept that the larger the height of fall, the higher the density deposited. Kolbuszewski (1948a) used heights of pouring up to 2m. Vaid et al (1988) noted that the influence of height of drop on densification seems to be most significant in a drop height range of about 0 to 30 cm for the sand they studied (see fig 3.6). Vaid et al (1988) also showed that the void ratio attained at a given height depends on the pouring rate and the mean particle size or gradation. These findings are consistent with the observations made by Mulilis et al (1977) and Miura and Toki (1982b).

In conclusion it can be said that the rate of pouring and height of drop are the controlling parameters for the void ratio obtained. The height of drop becomes insignificant when the terminal velocity is reached which corresponds to a height of 30cm for fine sand (for sand with mean particle size less than 0.4 it could even be less than 30cm).

The triaxial sand samples were directly prepared into the triaxial cell base, by fixing the tower along three guide rods which were attached to the triaxial cell through its

holes. The container was filled with dry sand, the shutter plate being in the closed position. The effective aperture size was selected so that the desired density can be obtained. A rubber membrane was put around the pedestal and sealed by two O rings, a split mould was assembled around it. The rubber membrane was rolled over the top of the split mould and a small vacuum was applied through the mould to hold the membrane tight against its inside. At that moment, the shutter plate was put in the open position and the sand was pluviated. As soon as the mould was filled, the shutter plate was closed and the top surface was gently levelled off by using a straight edge. The top cap was assembled and the rubber membrane was rolled up against it and sealed with two O rings. An initial vacuum was applied to give the sample rigidity and permit measurements of the initial dimensions of the sample. It is to be noted that this present method of levelling off the top surface of the deposited sand may loosen up the top end of the sample and results in a slightly non uniform distribution of the density over the height.

3-3-2 Sample saturation procedure

Saturation of sand specimens in laboratory investigations is necessary to provide reliable measurements of volume change and pore pressure. The saturation of samples by means of a back pressurising technique can easily involve an undesirably high back pressure. Some people have used this conventional method with intermediate flushing with carbon dioxide, which replaces the air and is then very soluble in water with which the sample is subsequently saturated. This method has been shown to lower the back pressure eventually required to maintain saturation.

In the research described here, it has been decided to apply the procedure which was developed by Rad and Clough (1984) that utilises equipment available in almost any geotechnical laboratory. This procedure as shown schematically in fig 3.7 consists of

the application of an initial vacuum of 98 kPa to the top of the initial dry specimen for a short time (5 min), then percolating deaired water through the specimen; water is drawn from the specimen into the lower reservoir of the vacuum pump until the specimen is nominally saturated. The vacuum inside the specimen is kept for a further period of 5 min in order to ensure a proper equilibrium inside the specimen. At this stage the vacuum is still of the order of 98 kPa.

The final stage is then a conventional back pressure technique. The degree of saturation is monitored in terms of Skempton's pore pressure parameter B, where a B value of 1 is taken to demonstrate complete saturation. However, it must be remembered that the parameter relevant for triaxial testing is the degree of saturation, which is related to B through the porosity and compressibility of the pore fluid and soil structure. The same value of B, say 0.95, may mean 99.9 % saturation in stiff soil, but only 96% in a soft soil (Black and Lee (1973)).

Therefore, some types of soils (very dense granular materials) may have a high percentage of saturation even though they show B values less than one.

Skempton's pore pressure coefficient was determined by applying the following procedure:

A relatively small cell pressure and back pressure (25 kPa) were applied initially to the Lochaline sand samples. Values of cell pressure increase and back pressure increase that have been applied to the sample were of the same order to ensure that the effective confining pressures were not exceeding 10kPa so that negligible volume changes occur. An increase in cell pressure was subsequently applied, the resulting increase in pore pressure being monitored (the bottom and top drainage lines were closed at this stage). The ratio of pore pressure change to cell pressure change which represents the B– value was calculated at each stage in order to check saturation. A B– value of 1 was achieved after the back pressure had reached a value of the order of 100 kPa. In other words, full saturation of the initially dry Lochaline sand samples has been obtained; thus in all the tests performed here the problems which are

encountered when using this parameter B did not arise in this present study. Using this technique, the back pressure needed to saturate the sample did not exceed 100 kPa which clearly shows by how much the vacuum technique is able to lower the back pressure by comparison with the use of the conventional technique on its own. We found this method very efficient, it ensures full saturation of the sample especially when the initial vacuum applied is high. According to Rad and Clough (1984) the vacuum procedure can be used for saturating different sands regardless of their initial water content, particle size, relative density, or level of cementation.

3- 4 Test technique

The samples prepared were 80mm long x 38mm diameter. The end platens were not lubricated or enlarged, however contact between the top cap and the load cell was improved so that no tilting will occur while shearing the specimen at large strains. Tilting was prevented by eliminating rotation of the top cap (see fig3.8) and this was done by clamping the top cap into the load cell. However this design of top cap connection was only used for a few tests, some of the later drained compression tests, so that in the major part of the testing programme tilting of the top cap of triaxial samples at large deformations is not prevented, and this may have some influence on the observed stress strain response at large strains.

3- 5 Shear box apparatus and instrumentation

The shear box apparatus was developed originally for the determination of the angle of shear resistance, φ, of sands. It has also been used for the measurement of residual shear strength of overconsolidated clays.

The ELE shear box apparatus used in this study, can accommodate specimens 60 mm square or 100 mm square. This apparatus comprises a rigid floor– mounted steel frame to which is attached the controlled drive unit, the shear box carriage, displacement dial gauge and loading hanger. A reversible loading jack connects the drive unit to the shear box carriage which is mounted on straight– line ball tracks. The vertical stress is applied to the specimen by adding weights to the hanger situated beneath the frame. A useful accessory is the counter– balanced lever loading device, which enables the loading to be increased by a ratio of 10:1. The driving control and gear box provide a wide range of speeds from 2.0 mm/min to 0.0005 mm/min. Load can be measured in both directions of shear by means of a load ring.

The layout of this apparatus is shown in fig 3.9.

3– 5– 1 Instrumentation

Three LVDTs were connected to the apparatus and used as measuring devices Two linear transducers were used to measure the horizontal displacement and vertical displacement respectively, the other transducer was used to measure the deflection of the load ring and subsequently deduce the load or shear force applied to the sample. In this machine, the maximum travel was 12mm and maximum shear force was 2kN. The information from these transducers was received by a Solartron Orion datalogger, which also provided a constant voltage source to energise each transducer.

3– 5– 2 Test technique

The material used was dry Lochaline sand; the samples were prepared by the pluviation method mentioned earlier in the previous sections. The relative density was

80%. The tests were carried out at the strain rate of 0.750 mm/min.

This shear box apparatus was used in order to compare the values of angle of friction obtained in the triaxial apparatus with that obtained in the direct shear box apparatus. For this reason, only very dense sand was tested at different normal stresses.

CHAPTER IV

EXPERIMENTAL RESULTS

4– 1 Standard drained compression tests

The permeability of sand is relatively high, implying that for sands, drainage times are typically very short and undrained situations rather rare. The undrained shear strength is therefore not a very important quantity, and emphasis is directed towards drained calculations using mobilised friction angle. Undrained situations may arise in the case of cyclic loadings or seismic loadings where liquefaction is a major concern.

Most sands encountered in engineering practice are medium to dense sands. So all tests were on a sand falling in this range of densities. The stress levels applied correspond to a range of 10 to 30m overburden which are realistic stress levels for civil engineering problems.

A series of twenty six standard drained compression tests was carried out at different cell pressures of 100, 200, 250, 300 kPa and relative densities of 60, 70, 75, 80%.

These tests were conducted at controlled stress almost to the peak shear stress and then continued at controlled strain up to large strains.

The samples were first consolidated under isotropic pressure for a period of one hour; this time was found sufficient for the volumetric compression of the sand samples to occur. After this compression has taken place, the shearing of the sand samples proceeds. Typical stress : strain and volume : strain results are shown in figs 4.1, 4.2, 4.3. For the sake of clarity not all the tests will be shown since the reason for carrying out such a large number of tests was to assess the reproducibility of the test results under the same conditions of initial density and stress level, thus only representative results are shown.

When the sample was sheared from its isotropic stress state, it starts compressing up to a point where the rate of volumetric deformation becomes instantaneously zero, and during this phase the volumetric deformations were not important. After passing that point, the sample starts expanding and the rate of volumetric deformation becomes important. Kirkpatrick (1961) suggested that the friction angle at the instant of maximum compression where the rate of volumetric deformation is instantaneously zero is equal to the constant volume friction angle φ_{cv}. If this turns out to be true, observation of the characteristic state of Habib and Luong (1978) and Luong (1979) or the phase transformation of Ishihara et al (1975) would easily permit the evaluation of φ_{cv} in the triaxial tests without having to reach large strains and attain the critical state where the rate of volumetric deformation together with the change of effective stresses are zero.

From the experimental results see fig4.4 (a) and fig4.4 (b), it was found that the mobilised angle of friction at the instant of maximum compression increases with increase in the stress level at a given density. This seems to suggest that this mobilised angle of friction may approximate the constant volume friction at high confining pressures. Negussey et al (1987) conducted some drained compression tests together with ring shear tests in order to compare the angle of friction at the

instant of maximum compression obtained from the triaxial tests and the constant volume friction which they obtained from the ring shear tests. Their findings (see fig4.5 and fig4.6) were that with initially loose conditions, the characteristic state and the critical state seem to be the same. However, at different initial densities for a given confining pressure it was found that φ_{mc} (characteristic state angle) decreases with increase in relative density. In the same manner, the effect of confining pressure was studied at a given initial density. The findings were that φ_{mc} increases with the confining stress level and approaches φ_{cv} at high confining pressures. Faruque and Zaman (1991) also came to the conclusion that the characteristic state and critical state are distinct and would merge when shearing occurs at high stress level or for initially loose conditions.

The difficulty encountered in defining the critical state, especially for dense sands has led to the assumption that critical state line and characteristic state line have the same slope in the p – q plane. If this assumption is made in a model, predicted volumetric strain exhibits substantial deviation from experimental observation (evidence will be produced ahead in Chap.V). Thus volumetric response for sand needs to be adequately addressed by incorporating into the constitutive equations for sand those features which suggest that the characteristic state and critical state are distinct.

Based on the findings of Negussey et al (1987), and the present shear box test results (to be shown later) the angle of constant volume friction was estimated both from the triaxial tests which have the highest confining pressure and the residual strength in the shear box test to be 30^0.

The peak strength has also been investigated in this research work for this fine Lochaline sand. The findings were that both the stress level and the initial density have an important role on the strength, that is the higher the stress level for a given initial density, the lower is the strength; the higher the initial density for a given stress level the higher is the strength. These conclusions are probably true

for the fairly low stress levels used in the present research, but for high stress levels this may not be true, as reported by Lee and Seed (1967). This then emphasises the need to define a state parameter that combines the stress level and initial density together as suggested by Been and Jefferies (1985, 1986).

The strength of sands may also be dependent on the angularity or shape of the particles. This fine Lochaline sand has been looked at under the optical microscope and the findings were that the particles were rounded which may explain the relatively low strength obtained. Vaid et al (1985) among others conducted triaxial tests on two different sands having the same particle size distribution but different angularities, rounded particles and angular particles respectively. The findings were that angular particles show more strength than the rounded particles at low stress level; at high stress level crushing occurs and angular particles are the most affected as an increase in fine content will occur and hence the strength is lowered.

It then appears logical to correlate the mechanical properties such as the strength of sand with an index of angularity so that samples of different mineralogy and angularities can be brought together.

The strength of sand is also dependent on the way the sand samples have been prepared (see Mulilis et al (1977)) but uniformity of the prepared sand samples plays an important role and the air pluviation method is the one which satisfies this requirement the best and hence if this method of sample preparation is standardised, this dependency of strength on the sample preparation method will be eliminated.

It may also be noted that the end restraint conditions (that is whether flexible or rigid end platens are used) together with the ratio of height to diameter have been found to affect the strength and uniformity of deformations (see Rowe and Barden (1964), Drescher and Vardoulakis (1982), Goto and Tatsuoka (1988) among others). These research workers found that the strength is dependent on the sample

slenderness (which is the ratio of initial height to initial diameter) and end conditions. They pointed out that for the purpose of achieving very uniform strain conditions, tests on very short samples with well lubricated ends may be needed. Goto and Tatsuoka (1988) concluded that the strength evaluated from tests conducted with rigid ends provided that the slenderness ratio is high, say 2.5 – 2.7 for dense sands as was the case for the present triaxial tests and 2.0 – 2.5 for loose sands, is very similar to the strength evaluated from tests conducted with lubricated ends and slenderness ratios of 2.1 – 2.6.

This then suggests the need to establish standardised procedures for triaxial testing which has not been effectively addressed since the publication of the book of Bishop and Henkel (1962).

4– 2 Stress dilatancy

The drained shearing resistance of a granular material can be represented by a single parameter, the mobilised angle of friction. It has been suggested that this parameter comprises three main components of shear resistance (Rowe (1962); Lee and Seed (1967)):

– Intrinsic sliding friction controlled by φ_μ, the angle of interparticle sliding.

– The resistance to dilation.

– The resistance to particle rearrangement.

Horne (1969) suggested a direct linkage of φ_μ and φ_{cv} (angle of shearing resistance at constant volume). As φ_μ is regarded conceptually as a material constant,

therefore φ_{cv} is unique. However consistent and reproducible measurements of φ_{cv} have been difficult to achieve and experimental and theoretical use of this parameter is virtually non– existent.

The magnitude of shear resistance required to resist dilation is dependent on packing density, stress level, grain shape and grain size distribution.

At very large strains, granular materials rearrange and shear at constant volume. φ_{cv} can be considered as an independent material property.

The triaxial device is not a suitable device for producing test results at large deformations due to the fact that it is virtually impossible to retain a uniformly deformed specimen in this region of large strains.

One of the earliest, and still one of the most accurate flow rules proposed for sand is the stress dilatancy relationship proposed by Rowe (1962).

This rule is usually expressed in the triaxial plane as :

$$R = K.D \quad (4.1)$$

where

$$R = \sigma_1'/\sigma_3' \quad (4.2) \quad \text{and} \quad D = -2\delta\epsilon_3/\delta\epsilon_1 \quad (4.3)$$

K being a constant

This relationship between stress ratio and strain increments simply expresses the well established empirical relationship that at stress ratios lower than some value K, a sand will compress, and at higher stress ratios it will dilate.

K is related to the constant volume friction by the following equation

$$K = (1+\sin\varphi_{cv})/(1-\sin\varphi_{cv}) \quad (4.4)$$

Using parameters for volumetric and distortional stress and strain Wood (1990) has expressed Rowe's stress dilatancy relationship as follows:

$$\delta\epsilon_p/\delta\epsilon_q = 9(M-\eta)/(9+3M-2M\eta) \qquad (4.5)$$

$$\text{with } \sin\varphi_{cv}' = 3M/(6+M) \qquad (4.6)$$

Rowe's stress dilatancy relationship has been shown to describe sand behaviour for conditions of increasing stress ratio, starting from a hydrostatic state to a peak and ultimate state (Barden and Khayatt (1966)). Negussey and Vaid (1990) gave close examination of stress dilatancy at small stress ratio states. Their experimental results indicate that the stress dilatancy equation would not describe sand behaviour at low stress ratios. Indeed the results produced by these authors showed stress dilatancy plots (see fig4.7) showing a range of stress ratio starting from the isotropic state over which the dilatancy term is constant. This seems to suggest that at small stress ratio, the strain increment ratio is dependent on stress increment, rather than the stress state as is generally assumed in the theory of plasticity. An experimental observation has also been reported by Hettler and Vardoulakis (1984). These research workers performed conventional triaxial tests on large diameter triaxial specimens and measured both the lateral strains and axial strains. Their results indicate that at low stress ratios, starting from an isotropic stress state, the radial strain increments were zero. Assuming that this result is a material response which has been repeatedly observed by these research workers in their tests and in strain controlled true triaxial tests (Goldscheider, 1984) and not the action of end restraint, this property could be understood as a constitutive property of sand.

The present test results fig4.8 do not confirm this constant dilatancy condition at small stress ratios but do indicate clearly that Rowe's stress dilatancy relation is not valid at small stress ratio. The present experimental results could not be relied upon over this range of stress ratio because the instrumentation does not permit accurate measurements of the strains and because of the bedding errors associated with the start of shearing.

φ_{mc} was found corresponding to stress ratio in the range 0.8 – 0.9 for all the

drained compression tests carried out under different confining pressures. It would be worthwhile to note that since the critical state is difficult to reach in the triaxial apparatus especially when testing medium to dense sand, an assumption is generally made about the slope of the critical state line being the same as the characteristic state (see Bardet (1986)). Thus using Rowe's stress dilatancy relation φ_{cv} is assumed to have the same value as φ_{mc} and the resulting stress dilatancy plot as shown in fig 4.8 fits the experimental data reasonably well over the region of high stress ratios. The peak friction angle at failure φ_p was found to be a function of the stress level and relative density which Rowe's stress dilatancy does not attempt to indicate.

In the author's opinion, if use is made of Rowe's stress dilatancy relationship, it is more sensible to use the characteristic state friction angle than the critical state angle of friction, since the latter, when measured using other testing apparatuses gives quite different angles of friction from the one measured at the characteristic state using the triaxial apparatus. Consequently a flow rule needs to be defined taking into account these two distinct states, the characteristic state which is dependent on the stress level and the initial density and the critical state which is independent of the stress level and initial density. Those conclusions apply to a large number of flow rules that have been suggested for sand which assume that those two particular states are the same.

It was also observed in this present experimental result see fig4.8 that the dilatancy term or strain increment ratio changes sign and steadily moves toward the critical state by strain softening before the peak stress ratio is reached. This observation has also been reported by Vardoulakis (1978) (biaxial apparatus), Goldscheider (1975) (true triaxial apparatus) and is contained in Houlsby's data (1981) (see fig4.9).

It has to be noted that during shearing of the specimens, the types of failure

patterns observed (see table 4.1) were slip failure in some cases and bulging in most cases. As a consequence, the final sections of the stress : strain curve cannot be used to derive material constants since the strain measurements are no longer objective. However the shear strain : volumetric strain curve is much more useful in the sense that the magnitude of the strain increments is not correctly measured but the strain increment ratio is not so strongly affected by the localisation into a shear band see Vermeer and Borst (1984). Hence the stress increment ratios or the dilatancy angles are measured with sufficient accuracy despite the non uniformity of deformation. This also indicates that the characteristic state and the critical state should be quite distinct since the stress ratio at which the critical state conditions were reached (that is with the dilatancy rate becoming zero at constant effective stresses) was quite different from the stress ratio at which the dilatancy rate was instantaneously zero.

4– 3 Stress probes

In the tests described above, relatively large stress changes were involved from which certain ingredients of the plasticity theory may be derived (flow rules, hardening law). An alternative is to investigate in detail the response of a material at a particular point, deduce its incremental response and compare it with the prediction of plasticity theory.

In these probing tests, identical samples were subjected to identical stress history, and then subjected to a series of stress probe tests in which the probe was made in a different direction for each test.

The experimental program consisted of applying first an isotropic compression on saturated Lochaline sand samples prepared by air pluviation at the relative density of 70%. All the samples were then sheared under constant cell pressure under

Series	Initial Relative Densities (%)	Effective Confining Pressures (kPa)	Test Path	Failure Type	φ_p (peak Friction angle) (degrees)
1	0.59	100	drained	R.P	37.3
	0.61	100	drained	Bulge	38.0
	0.60	100	drained	Bulge	37.3
	0.58	100	drained	Bulge	37.6
	0.62	100	drained	Bulge	37.9
	0.60	100	drained	Bulge	38.0
	0.80	100	drained	Bulge	39.4
	0.75	100	drained	Bulge	38.1
2	0.69	200	drained	Bulge	38.1
	0.70	200	drained	R.P	38.0
	0.70	200	drained	R.P	39.6
	0.70	200	drained	Bulge	38.6
	0.70	200	drained	Bulge	38.3
	0.70	200	drained	Bulge	38.2
	0.75	200	drained	Bulge	38.7
	0.80	200	drained	R.P	39.2
3	0.69	250	drained	R.P	38.3
	0.70	250	drained	Bulge	38.1
	0.71	250	drained	Bulge	37.9
4	0.69	300	drained	R.P	37.3
	0.69	300	drained	Bulge	36.9

R.P - Rupture plane

TABLE 4.1 (Series of Conventional Drained Tests)

drained conditions until the stress ratio of 0.8 was reached. From this stress state, a probing in different direction for each sample was carried out. Sets of stress probes at a stress ratio of 0.5 were also carried out to investigate the effect of stress state on the stress strain response.

However, this type of tests really requires a computer control system in order to accurately follow the intended stress path which should be applied at constant stress increment ratio. Since these tests involve the simultaneous variation of the cell pressure and the axial pressure, the need for an automated system is vital. Despite this difficulty, a procedure was adopted in order to closely follow the intended stress path, which worked reasonably well for small deformations provided failure states were not approached.

The stress paths for probings starting from a stress ratio of 0.8 are shown in fig4.10. In the paths O−3, O−4, the strain response shows (fig4.11) that dilatancy occurs immmediately after application of the stress increment, whereas path O−2 and O−5 start with further compression and expansion occurs after a certain stress ratio state. For paths O−1 and O−6 only compressive volumetric strains were observed, the shear strains along those paths being almost negligible. These observations then imply a dependency of the resulting strain increment on the applied stress path.

For the other probings starting from the stress state O' at stress ratio 0.5 see fig4.12 and fig4.13, similar patterns of response were observed except that for path O'−3 see fig4.13 the volumetric expansion did not occur immediately after application of stress increment but was delayed until a certain stress ratio state was reached. This then shows some effects of initial stress state on the stress strain response of this fine Lochaline sand. The particular stress ratio 0.95 for which expansion starts occurring is the characteristic state identified from path O−5 fig4.10 which is a conventional drained compression test at constant cell pressure.

This fine Lochaline sand has stress strain response dependent on the stress path applied and the stress state.

Another useful way of interpreting these experimental stress probes is to analyse them in terms of generalised stiffness which takes account of the magnitudes of both the principal strains through the shear strain ϵ_q and the volumetric strain ϵ_p. This will permit comparison of the resulting generalised stiffness corresponding to each direction of stress path for each stress probe. One way of doing this is to define the generalised stiffness as the ratio of the total length of stress path to the total length of strain path. This generalised stiffness is then expressed as:

$$\text{generalised stiffness} = \Sigma\sqrt{(\delta p'^2 + \delta q^2)}/\Sigma\sqrt{(\delta \epsilon_p^2 + \delta \epsilon_q^2)} \quad (4.7)$$

The resulting plots characterising the stress path and strain path lengths as shown in fig4.14 and fig4.15 suggest that the highest stiffness is observed in paths O−8 and O'−4 respectively. As the stress paths are rotated in an anticlockwise manner starting from paths O−8 and O'−4 respectively, the generalised stiffness decreases from its highest value corresponding to the unloading path O−8, O'−4 respectively to the lowest value corresponding to path O−3, O'−3 respectively.

This generalised stiffness approach helps to identify regions of high and low stiffness around the initial stress state in the p − q compression plane. The experimental generalised stiffnesses do not seem to suggest major differences of stiffness (not a sharp change of stiffness) in the case of paths O−5 and O−8 (loading unloading along the same stress path) or O−4 and O−7 (loading unloading along the same stress path). The same apply for paths O'−2 and O'−4 (loading unloading along the same path).

Another approach was also investigated in this research. The strain energy was calculated which takes account of all components of stress changes and the corresponding strains.

This strain energy has been defined in terms of changes of stress from the starting point of the stress probe. This is an objective way of looking at changes of strain energy occurring from this starting point. Working in terms of change of stress rather than actual stress the energy changes on paths in all directions from the starting point can be directly compared.

$$E = \sum_{i=1}^{n} \{[(p_i' + p_{i+1}')/2 - p_0'].\delta\epsilon_p + [(q_i' + q_{i+1}')/2 - q_0)].\delta\epsilon_q\} \quad (4.8)$$

where (p_0', q_0) is the initial anisotropic stress state from which the stress probes start.

The summation ($\sum$) symbol means a numerical integration along a test path.

This quantity E is calculated incrementally since the stress strain relation is non linear. Contours of E can be plotted in the p – q plane, to show the development of strain energy with the applied stress changes. This quantity E combines all components of stress and strain and may be a very useful indicator of stress strain behaviour.

Burland (1989) suggested that contours of constant strain energy could be used as an indicator of the boundary of the region of high stiffness. This strain energy quantity is the sum of the volumetric strain energy and the distortional strain energy. These two components of strain energy occur independently. These contours are shown in fig4.16 and fig4.17. The distance of the initial stress state from a given strain energy contour gives an indication of the stiffness of the soil; the greater the distance, the higher is the stiffness. It follows that the spacing of the strain energy contours is also a quantitative measure of the change of stiffness of the soil along the applied stress path (Burland and Georgiannou (1991)).

These contours show in another way the information that was presented in fig4.14 and fig4.15. Unloading (reduction in stress ratio) is a stiff process. The data are clearly somewhat scattered (the contours in fig4.16 are not very smooth) but it is evident that this starting point is rather close to failure so that strains are large, the stiffness is low and energy is generated rapidly.

The quantity E makes no attempt to separate plastic and elastic strains. A contour of zero plastic strain energy is the same as a yield locus. The evidence for experimental values of elastic stiffness is not sufficiently reliable to be able to deduct elastic from total strain energy values. However, since energy is dissipated rapidly on plastic stress probes, the general shape of the contours could be used (if the stress probing were repeated at various different starting points) to indicate the kinematic translation of the yield locus with different stress histories.

Clusters of stress probes have been applied in the past by Lewin and Burland (1970) to samples of clay. Their findings are shown in fig4.18. The strain increment ratio (ratio of volumetric to distortional strain increment) is partly dependent on the stress path. The region of high stiffness around a point is associated with stress paths involving unloading. These findings are in agreement with the present experimental findings. The experimental results of Lewin and Burland (1970) show (fig4.18 (a) and fig4.18 (b)) that the region delimited by the stress probes corresponding to $\theta = 180^0$ and $\theta = 270^0$ corresponding to increase of q with decrease of p' is the region where the deformations are largest for a given length of stress probe.

Burland and Georgiannou (1991) show experimental results on clayey sands (fig4.19, fig4.20) for which again stress probes with increasing q and decreasing p' give the softest response when presented in terms of strain energy contours (see fig4.20). The probings shown in fig4.19 were carried out by applying series of stress paths: paths OABC and ODE are for undrained compression and extension tests respectively, paths OF and OG are for conventional drained compression and extension tests respectively, path OH is a test in which the shear stress is held constant while the mean effective stress was incresed, and path OI is one in which the mean effective stress was held constant while the shear stress was decreased.

The strain energy contours give an indication of the anisotropic stiffness response of the soil to the applied stress path.

4- 4 Shear box tests

Three series of tests were performed each at different normal vertical stress, in order to check both the peak strength and the residual strength.

The tests were conducted on 60x60 mm samples of dry Lochaline sand, prepared using the air pluviation technique developed in this study. The density of the samples was the same and is expressed in terms of relative density, which is 80%.

The normal vertical stresses applied were respectively 80, 145, and 266 kPa.

Each test was carried out three times in order to control the reproducibility and of the results under the same conditions.

The results are shown in fig4.21, fig4.22 and fig4.23 and when compared with the results obtained in the triaxial apparatus in terms of mobilised angle of friction at the peak show a very good agreement.

The angle of friction obtained in the shear box apparatus after reaching a large horizontal displacement which was about 30 degrees was considered to be the angle of friction corresponding to the estimated critical state conditions reached in the triaxial apparatus which as mentioned before was difficult to achieve due to the loss of uniform deformation at this large strain level.

The main observations were that the peak strength is dependent on the stress level while the residual strength or critical state is not. The end of strain softening for this fine Lochaline sand occurs at a horizontal displacement of about 4mm.

However, the test conducted under a normal vertical stress of 266 kPa showed some anomalies: the critical stress ratio was slightly higher than in the other tests in repeated tests. The reason for this is not clear.

The vertical displacement vs the horizontal displacement shows a compression followed by an expansion at all the stress levels (fig4.23).

With normal load P, shear load Q and vertical and horizontal displacement y and x, a stress dilatancy plot for these tests can be presented in terms of the ratios Q/P which is directly related to the angle of mobilised friction and $\delta y/\delta x$ which is related to the dilatancy angle and is simply the slope of the displacement curve x:y.

The stress dilatancy equation of Taylor (1948) links the work done by the applied loads P and Q on the soil sample during incremental displacements δy and δx to the applied normal load through a frictional constant μ.

Taylor's equation is expressed as:

$$\delta W = \mu.P.\delta x \quad (4.10)$$

$$\text{where } \delta W = P.\delta y + Q.\delta x \quad (4.11)$$

rearranging this equation gives:

$$Q/P + \delta y/\delta x = \mu \quad (4.12)$$

This equation has some analogy with some of the different flow rules that have been proposed for interpretation of triaxial tests on sand. However interpretation of quantities P, Q, δy, δx in terms of stresses and strains is not feasible because the soil in the shear box apparatus is clearly not deforming homogeneously (Wood (1990)).

Data from some of Taylor's own tests on Ottawa sand are shown by Wood (1990) (fig4.24) to match rather well with this stress dilatancy equation, with some discrepancies in the early stages of shearing which might result from considering

total rather than plastic deformations.

However, the Lochaline sand results shown in fig4.25 seem to show no correspondence at all with Taylor's flow rule. The drop in friction after the peak is much more rapid than can be attributed to increase in volume of the sand. This might be attributed to the effect of tilting which was quite significant after the peak strength was reached.

CHAPTER V

A CONSTITUTIVE MODEL FOR SAND IN TRIAXIAL COMPRESSION

5– 1 Introduction

The stress strain behaviour of soil is in general stress path dependent, because during virgin loading, soil deformations are largely irrecoverable. The magnitudes of these deformations depend on the stress level which makes the response of soil to any change of stress dependent on the maximum stresses previously experienced by the soil.

It is also widely accepted that soil deforms plastically immediately after the application of stress; medium – dense to dense sand dilates when it is sheared; the stress : strain curve shows a decrease in stress ratio with further straining after a peak strength has been reached. Elasticity theory alone cannot account properly for these features. Attempts to use non linear elastic models have been tried in the past, for example Duncan and Chang (1970); these show that such models can be used to predict soil behaviour but only in situations which involve a relatively small stress change. The same could be said about rigid plastic models where a possible application could be seen in the case where the stress changes are very large.

In this chapter the sand will be modelled as an elasto plastic material. It is believed that such a model can take account of the main features which are observed in tests which can be performed in triaxial compression.

During the development of the model, the number of internal variables and material constants necessary for the description of the material response has been kept as small as possible without sacrificing the salient features of the observed soil response. Complex models necessitate a large number of parameters, of which some may be derived from laboratory tests and others by curve fitting which renders the model empirical; a large number of parameters makes also the physical feel for the predicted response of soil very difficult.

Some of the fundamental concepts of modelling that have been introduced by the Cam– clay models through the work of Roscoe et al (1958,1968) have been retained in the present model.

5– 2 Elastic properties

The starting point of the elastic properties for sand is the Hertzian contact theory, which deals with two linear elastic bodies in contact and asssumes that the deformation is mainly local to the contact points.

Angular bodies behave slightly differently from rounded particles. Janbu (1963) suggested that moduli could be expressed as a power law of pressure. The bulk modulus of sand could be expressed as:

$$K = p_a.A.(p'/p_a)^n \qquad (5.1)$$

where p_a is the atmospheric pressure

A is a dimensionless constant

n is an exponent which depend on the angularity and grading of particles and is usually between 1/3 and 1/2

This approach is generally an accepted way for fitting sand behaviour.

Sand would also be expected to have its shear modulus a function of a power law of pressure, which could be expressed in similar way to the bulk modulus:

$$G = p_a.B.(p'/p_a)^m \qquad (5.2)$$

where m varies in the same way as n

Taking m = n would be equivalent to assuming a constant Poisson's ratio.

Assuming that the shear modulus is also a function of the pressure leads to a non conservative behaviour as small amount of dissipation or creation of energy can accompany certain cycles of stress change.

Another approach is often taken by assuming that the volumetric strain on unloading under isotropic compression is purely elastic and hence can be expressed as:

$$d\epsilon_p^e = \kappa.dp'/(p'.v) \qquad (5.3)$$

where κ is the slope of the swelling line in the v:lnp' plane

Hence bulk modulus $K = v.p'/\kappa$ (5.4)

It might be assumed that Poisson's ratio μ is constant and has the value of 0.2 (Duncan and Chang (1970), Lade (1977)). Therefore the shear modulus can be derived by linking it to the bulk modulus through the relation:

$$G' = (3/2).([1-2\mu]/[1+\mu]).K \qquad (5.5)$$

and then the elastic shear strain could be expressed as:

$$d\epsilon_q^e = dq/(3.G') \qquad (5.6)$$

However all the reported results (Lee and Seed (1967), Vesic and Clough (1968)) show that unlike clay, the slope of the compression curve of sand in the v:lnp' plane varies with the confining pressure. It is then more appropriate since there is a non linear relationship between the specific volume v and lnp' to use a power law relationship of specific volume and pressure to accurately express this non linearity. Nakai (1989) suggested a power law expressed as:

$$d\epsilon_p^e = C_e.m.(p'^{[m-1]}/p_a^m).dp' \qquad (5.7)$$

where C_e: slope of unloading curve in $v:p'^m/p_a^m$ plane as shown in figs.1

m: material constant related to the angularity of the sand

p_a: atmospheric pressure

The bulk modulus is then:

$$K = (p_a^m/p'^{[m-1]})/(C_e.m) = p_a^m/(p'^{[m-1]}.C_e.m) \qquad (5.8)$$

Assuming a constant Poisson's ratio of 0.2, the shear modulus G is then expressed as:

$$G = (3/2).([1-2\mu]/[1+\mu]).K \qquad (5.9)$$

The discussion here has been restricted to the case of isotropic elasticity. Real soil may not correspond to this simple idealisation. Many materials, however, show more limited forms of anisotropy. A cross – anisotropic material, also known as a transversely isotropic material, possesses an axis of symmetry for its mechanical properties.

A soil deposited vertically and then subjected to equal horizontal stresses will be

expected to exhibit a vertical axis of symmetry and be transversely isotropic. The behaviour of transversely isotropic material may be described by five elastic constants. For the case of triaxial stress conditions Graham and Houlsby (1983) suggested a form of anisotropy using only three parameters which can be measured in triaxial tests. Convenient parameters are identified such as an equivalent bulk modulus K^*, equivalent shear modulus G^*, and a coupling modulus J which expresses the relationships in transversely isotropic soil between mean stress and shear strain and between shear stress and volumetric strain. The resulting stiffness equation is expressed as:

$$\begin{bmatrix} \delta p' \\ \delta q \end{bmatrix} = \begin{bmatrix} K^* & J \\ J & 3G^* \end{bmatrix} \begin{bmatrix} \delta \epsilon_p^e \\ \delta \epsilon_q^e \end{bmatrix}$$

Inside the yield locus the response is elastic, so stress paths heading inside this yield locus on paths identified as unloading paths from the experimental studies, were used in the present research work to derive these three parameters.

The result was that no value could be determined for the parameter J, since the two stress paths used for its determination led to two very different values. Thus this approach although more realistic has not been pursued further and elastic parameters have been defined using the assumed isotropic response as defined previously in this section using two parameters $C_e = 0.60$ and $m = 0.3$ (these values have been derived from the results of isotropic compression tests shown by Nakai (1989) relative to Toyoura sand which has almost similar grading curve and roundness as Lochaline sand).

5–3 Yield with its corresponding plastic potential functions

In the present study, two separate yield mechanisms are assumed for volumetric

and shear yielding. This concept is not novel in the incremental theory of plasticity. and was probably first employed by Prevost and Hoeg (1975). This concept of double hardening has been adopted in the past by Lade (1977), Ohmaki (1979), and Vermeer (1978) see fig 5.2 among others.

In the double hardening models proposed by Prevost and Hoeg (1975), Vermeer (1978), two different types of yield locus are used to describe the yielding properties of soil:

- Shear yielding which is used to describe the development of irrecoverable shear strains with accompanying dilatancy (volume change).

- Volumetric yielding which is used to describe the development of irrecoverable volumetric strains due to compression at low stress ratios.

It is assumed that these two types of yielding take place independently; there is no coupling between shear deformation with accompanying dilatancy and volumetric deformation due to isotropic compression.

Koiter (1953) generalised plasticity theory from a single yield mechanism to include a family of yield mechanisms.

According to Koiter, if the family of yield mechanisms is associated with sets of yield and plastic potential functions expressed, respectively, as

$$F_k(\sigma_{ij}) \text{ and } G_k(\sigma_{ij})$$

where k= 1, 2....n denotes the numbers of yield mechanisms, then the plastic strain increments can be written as:

$$d\epsilon_{ij} = \sum_{k=1}^{n} C_k H_k (\partial G_k / \partial \sigma_{ij}) dF_k \quad (5.10)$$

where $C_k = 0$ if $F_k < 0$ or $dF_k < 0$

$C_k = 1$ if $F_k = 0$ and $dF_k > 0$

and H_k = a non negative scalar function of stress, plastic strain and strain history.

This idea of describing the plastic strains as the sum of two independents parts was introduced into soil mechanics by Roscoe and Burland (1968). They defined each part by means of a yield surface, a yield condition and an associated flow rule.

This present model uses then two different sets of yield and potential functions and combines the resulting strain components according to Koiter's generalised theory.

In the following it is assumed that the material is isotropic and the change of size of the yield locus for the two mechanisms is linked through an isotropic hardening rule which will be defined.

5-3-1 Shear yield with its corresponding plastic potential functions

5-3-1-1 Shear yield function

The shear yield function has been selected on the basis of the reported work mentioned in chapter 2. The shear yield function was chosen to be of the form:

$$F_q = \eta = \eta_o \quad (5.11)$$

where $$\eta = q/p' \quad (5.12)$$

η_o is a parameter indicating the current size of the yield locus.

This type of yield function simply indicates that the family of yield loci could be described by a series of constant stress ratio lines. This is in accordance with the behaviour of soil under primary loading, as soil deformations are dependent on the maximum stress level previously experienced. On unloading and reloading at low stress levels, the response is purely elastic. If the previous maximum stress ratio is reached upon reloading, and the magnitude of stress increases to values larger than this maximum stress ratio, the stress strain response continues as for the primary loading, almost unaffected by the previous cycle of loading and unloading. It is to be noted that at higher stress levels this is not true, and a curved yield locus should be used at higher stress levels.

5–3–1–2 Plastic potential function

During the past three decades, many flow rules have been proposed for sand. Some have been based on plastic dissipation of energy like for instance the original Cam–Clay; others have been derived from fundamental considerations of inter–particulate mechanics like for instance Rowe's flow rule. Those flow rules have been tested by a number of investigators but primarily only under monotonic loading with increasing stresses under axisymmetric stress and plane strain conditions. It has been concluded that Rowe's stress dilatancy rule can broadly describe the stress dilatancy relationship for sand. Confirmations of the validity of this particular flow rule have had a great impact on the numerical modelling of granular materials.
A study of Rowe's stress dilatancy rule leads to the following conclusions:

– The stress ratio at which soil changes from contraction to dilation is independent of the stress level and initial density. This particular stress ratio is assumed to be the same as the critical state stress ratio.

– The maximum strain increment rate or dilatancy is linked to the peak stress ratio through the famous equation:

$$R = K \,.\, D \quad (5.13)$$

where K = constant = $\tan^2(\pi/4 + \varphi_{cv}/2)$ (5.14)

$$D = -2.\delta\epsilon_3/\delta\epsilon_1 \quad (5.15)$$

$$R = \sigma_1'/\sigma_3' \quad (5.16)$$

– When the rates of change of the effective stresses and volumetric strain become zero, the soil reaches a critical state by strain softening from the peak stress ratio.

– Rowe's stress dilatancy is not stress path dependent under monotonic loading with increasing stresses.

The original Cam–Clay flow rule which is considered to fit the behaviour of sand quite well is also adopted as a flow rule for this type of shear yielding. This flow rule is based on considerations of the dissipation of energy by plastic work. It has the form:

$$dW_p = M_c.p'.d\epsilon_q^p \quad (5.17)$$

where $$dW_p = q.d\epsilon_q^p + p'.d\epsilon_p^p \quad (5.18)$$

Rewriting this equation using (5.17) and (5.18) we get

$$d\epsilon_p^p/d\epsilon_q^p = M_c - \eta \quad (5.19)$$

where M_c is the critical state stress ratio and $\eta = q/p'$.

This flow rule is similar to Rowe's stress dilatancy, although the latter predicts a curved line at high stress ratios in the η:$d\epsilon_p^p/d\epsilon_q^p$ plane.

The original Cam-Clay flow rule when integrated to obtain the plastic potential function gives a rather simple mathematical expression. We know that the projection of the plastic potential onto the p'-q plane is such that the plastic strain increment direction coincides with the outward normal of the plastic potential:

$$dq/dp' = - d\epsilon_p^p/d\epsilon_p^q \quad (5.20)$$

Hence after integration the plastic potential is expressed as:

$$G_q \text{ (plastic potential)} = \eta + M_c.Ln(p/p_o) \quad (5.21)$$

where p_o indicates the parameter which controls the size of the potential curve.

Having deduced the main characteristics of these flow rules, it is possible to relate them to experimental evidence which has been produced both from conventional triaxial stress paths and from non-conventional triaxial stress paths such as constant mean effective stress paths and proportional loading (including isotropic compression paths which represent proportional loading for $\eta = 0$).

Another aspect of these flow rules that needs to be investigated is the validity of these relations at small stress ratios or at small strains, preferably including proportional loading paths.

5-3-1-3 Experimental findings

In this section, it is intended to produce the Author's data together with other data available in the literature.

From the experiments conducted in this research work, particularly those following conventional triaxial stress paths, the following results have been obtained:

- The characteristic state stress ratio was found to depend on the initial density and the stress level. This particular stress ratio appeared to increase with the stress level and at higher stress level appears to approximate the critical state ratio; this latter result could not be verified on an experimental basis because of the low stress level used in the present tests but Negussey et al (1987) among others have produced such experimental evidence. The initial density has the opposite effect: the characteristic stress ratio decreases with an increase in relative density.

- The experimental evidence also suggests that the peak stress ratio cannot be associated with the maximum dilatancy; on the contrary there seems to be a change in the sign of the rate of dilatancy before the peak stress ratio is reached, and the critical state stress ratio is very different from the characteristic state stress ratio. This experimental evidence is contained in the author's data. Houlsby (1981), Vardoulakis (1978) (biaxial apparatus), Goldscheider (1984) (this latter used true triaxial apparatus under strain control) produced excellent quality data which points to the existence of this constitutive property of sand which is the inversion of dilatancy rate near the peak stress ratio region

- At small stress ratios, the strains measured in this research project are not reliable because bedding errors were not prevented at the start of the test and more sophisticated transducers are needed to measure the initial axial and lateral deformations. However, as has been mentioned before, Hettler and Vardoulakis (1984) reported very accurate measurements of axial and lateral strains which indicate that at low stress states, the radial strain increment was zero. The range of stress ratio over which this radial strain increment was zero was dependent on the initial density.

If it is assumed that this is not the effect of end restraints, then this experimental observation could be considered as a constitutive property of granular material. Negussey and Vaid (1990) investigated the response of their particular sand to small stress ratios in the same manner and concluded that at small stress ratios the strain increment ratio was constant and dependent on the density. The range of stress ratio over which this holds is dependent on the density and was found to be between 0 and 0.5. Nova and Wood (1979) also raised this issue of stress dilatancy at small stress ratios and suggested another form of flow rule for small stress ratios on the basis of conceptual arguments.

– For proportional loading, El Sohby (1969) and Lade (1977) among others produced a series of tests at constant stress ratio (recalculated in terms of η) with values between 0 and 1.6 (El Sohby) and between 0 and 1.13 (Lade). The results all indicate that increase of stress level is associated with decrease of volume for stress ratio up to 1.5. At stress ratios higher than 1.5 volumetric expansion occurs and Rowe's stress dilatancy might be applied. It may be concluded that for proportional loading paths at constant stress ratios lower than around 1.5 Rowe's stress dilatancy rule does not apply but for high stress ratios greater than around 1.5, the stress dilatancy rule might be applied.

For compression at constant stress ratio below 1.5 volumetric strain hardening can be described by means of a power law of mean effective stress.

Developing from the evidence presented above, an attempt is made here to present a new flow rule for sand.

5–3–1–4 SHEAR HARDENING LAW AND FLOW RULE FOR SAND

5–3–1–4–1 Shear Hardening law

A hardening law has to be defined in order to predict the magnitude of strains.

One approach is taken by Lade (1977). He suggested that the position of the yield surface is a function only of the plastic work. The constant f_p for the yield locus is indirectly expressed as a function of plastic work W_p.

$$W_p = F_p(f_p) \quad (5.22)$$

F_p is a monotonically increasing or decreasing positive function.

In this equation, it is assumed that there exists a unique relationship between the total plastic work W_p and the amount of hardening or softening expressed by the value f_p which is given by a relation developed in terms of the first and third invariant:

$$f_p = ([I_1{}^3/I_3] - 27).\ (I_1/p_a)^m = \text{constant} \quad (5.23)$$

Where $I_1 = \sigma_1 + \sigma_2 + \sigma_3$

$$I_3 = \sigma_1.\sigma_2.\sigma_3$$

p_a being the atmospheric pressure and m a material constant representing the curvature of the yield curve.

The constant f_p for the yield envelope is indirectly expressed as a function of the plastic work W_p which is calculated using the expression

$$W_p = \Sigma\ \sigma_{ij}\ .\ d\epsilon_{ij}^p \quad (5.24)$$

Lade establishes the function F_p empirically, involving powers and exponentials to give f_p in terms of W_p.

Prevost and Hoeg (1975) suggested a continuous mathematical function as a fit for the shear stress : plastic shear strain curve which allows for hardening and softening.

They expressed their hardening function as follows:

$$H(\epsilon_p^p, \epsilon_q^p) = A.[B.(\epsilon_q^p)^2 + \epsilon_q^p] / [1 + (\epsilon_q^p)^2] \quad (5.25)$$

with

$$\delta H/\delta \epsilon_q^p = \delta q/\delta \epsilon_q^p \quad (5.26)$$

$$\delta q/\delta \epsilon_q^p = A.[1 + 2.B.\epsilon_q^p - (\epsilon_q^p)^2] / [1 + (\epsilon_q^p)^2]^2 \quad (5.27)$$

The parameter A is related to the plastic volume change. For this it is assumed that the residual shear resistance, q_{res}, corresponds to the shear resistance at the critical state conditions.

$$q_{res} = M_{cs}.p_c' \quad (5.28)$$

where p_c' gives a measure of the size of the current yield surface. The following relationship has been suggested for p_c':

$$p_c' = p_{c1}'.\exp.[\beta.\epsilon_p^p - \delta.(\epsilon_q^p - \epsilon_{q(peak)}^p)] + p_{co}' - p_{c1}' \quad (5.29)$$

with p_{c1}' is an experimental constant

β is an experimental constant

δ has the value: 0 if $\epsilon_q^p \prec \epsilon_{q(peak)}^p$

and 1 if $\epsilon_q^p \succ \epsilon_{q(peak)}^p$

p_{co}' is the initial value of p_c' before any stress change is apllied.

This type of hardening has been used in the present research work, but using the stress ratio instead of the shear stress.

Their hardening function when formulated in terms of stress ratio can be expressed as:

$$H(\epsilon_q^p) = A.[B.(\epsilon_q^p)^2 + \epsilon_q^p] / [1 + (\epsilon_q^p)^2] \qquad (5.30)$$

This hardening function is supposed to depend on the plastic shear strain so that

$$\delta H/\delta\epsilon_q^p = \delta\eta/\delta\epsilon_q^p \qquad (5.31)$$

so that :

$$\delta\eta/\delta\epsilon_q^p = A.\ [1 + 2.B.\epsilon_q^p - (\epsilon_q^p)^2] / [\ 1 + (\epsilon_q^p)^2]^2 \qquad (5.32)$$

where the parameter A is either related to the initial slope of the stress : strain curve or related to plastic volumetric strains or related to the critical state conditions. Three possible choices can then be given for the parameter A. It might be appropriate to relate the parameter A to the critical state conditions by assuming that the residual stress ratio corresponds to critical state conditions.

The peak stress ratio is determined by setting $\epsilon_q^p = \epsilon_q^p$ (at peak) in which

$$\epsilon_q^p \text{ (peak)} = B + \sqrt{(1 + B^2)} \qquad (5.33)$$

The critical state ratio is determined by setting

$$\eta_{cs} = A.B \qquad (5.34)$$

However it was found that this type of hardening although simulating the hardening and softening of the material, does not seem to represent the critical state conditions and the effect of stress level on the stress strain response. Furthermore as can be seen from equation (5.32) at low strain levels e.g. for $\epsilon_q^p \approx 0$, the incremental

stiffness increases in that range which is not an observed material response. It is believed that if a suitable expression can be found for the parameter A, then this hardening function could be quite attractive.

A rather different approach was suggested by Zytynski (private communication to Wroth, 1976). He plotted the stress ratio η for a triaxial test against the volumetric strain ϵ_p. Zytynski fitted this curve by the simple expression:

$$d\epsilon_p^p = A.\eta.[(M_{co} - \eta)/(N - \eta)].d\eta \quad (5.35)$$

where A is a constant determining the magnitude of strain

M_{co} is the characteristic state stress ratio

N is the maximum stress ratio

Use of Eqn (5.35) has been explored in the present research work. However, it is found that using this equation it is not possible to predict any strain softening from the peak stress ratio.

It is then useful to define a new shear hardening law that is able to simulate softening.

5–3–1–4–1–1 <u>New Shear Hardening law</u>

The existing soil models fail to describe the strain softening behaviour of soil. Banerjee et al (1992) suggested that the hardening moduli are controlled by the evolution of the peak stress ratio and the current stress ratio. They further assumed that a variable peak stress ratio M_p was a function of the strain history, and is given by an evolutionary function of the form:

$$dM_p = \eta.(M_c - \eta).(M_p^2 - \eta^2).d\epsilon_q^p \quad (5.36)$$

where M_c = critical state stress ratio

This evolutionary function for peak stress ratio, does not appear to allow any softening to occur. Indeed, the peak stress ratio is reached when η reaches M_p after which M_p remains constant and consequently η will not drop from its peak value. For this reason, another formulation of this equation seemed appropriate and led to a better simulation of the softening of the material, accounting for the main features observed in the triaxial compression plane.

This modified function is expressed as:

$$dM_p = \eta.(M_{co} - \eta).(M_p - M_c)d\epsilon_q^p \quad (5.37)$$

where M_{co} is the characteristic state stress ratio corresponding to the maximum volumetric compression where the dilatancy term is instantaneously zero.

M_{c0} and the intial value of $M_p = M_{p0}$ are controlled by a state parameter ψ (this parameter is defined in section 5-6).

When softening occurs this means $d\eta$ becomes negative and beyond this stage $d\eta$ and dM_p are forced to be equal.

The hardening law for the shear yielding can be expressed as:

$$H_q = d\eta_0/d\epsilon_q \quad (5.38)$$

Where η_0 is a parameter controlling the size of the yield locus which is assumed to depend on the shear strain.

$$H_q = \eta.M_p/(M_p - \eta) \quad (5.39)$$

5-3-1-4-2 A New Flow Rule For Sand

From what has been said in previous sections, it seems logical to try to define another flow rule which could describe the experimental behaviour of sand observed in experiments conducted in such a manner that homogeneous deformation occurs and accurate measurements have been made. Use of internal measurement devices with high resolution may be desirable as it has been observed that apparatus deformations may sometimes be of the same order as sand deformations.

The hardening rule for shear yielding has already been defined in the previous section. A function is suggested linking the plastic strain increment ratio to the stress ratio:

$$d\epsilon_p^p / d\epsilon_q^p = d \quad (5.40)$$

$$d = (M_{co} - \eta).(M_p - M_c) \quad (5.41)$$

This equation is equivalent to writing $d\epsilon_p^p = dM_p/\eta$ (5.42).

This flow rule clearly differentiates between the critical state and the characteristic state and shows dependency of the stress dilatancy relationship on stress level and density by including the state parameter ψ which controls the parameters M_{c0} and M_{p0}. Stress path dependency is also demonstrated using the double hardening model that is being defined, which incorporates the plastic volumetric strain due to the isotropic compression.

This flow rule has also the capability of predicting the inversion of the rate of dilatancy near the peak region. As noted this feature has been observed experimentally and appears to be a constitutive property of sand.

Nova and Wood (1979) proposed an expression:

$$\eta.d = c \qquad (5.43)$$

where c = constant

This expression simply means that at low stress ratios the dilatancy is very high. However, according to the experimental evidence reported by Hettler and Vardoulakis (1984) and Negussey and Vaid (1990) it appears that at low stress ratio the dilatancy term is constant. This implies that at low stress ratio the stress dilatancy relationship does not hold.

A relation between stress increment ratio and strain increment ratio then seems more appropriate. Hettler and Vardoulakis (1984) suggested a relation between stress increment and shear strain increment of the form:

$$\delta\epsilon_q = (2/3).C.\alpha.(q/p_0)^{[\alpha-1]}.(\delta q/p_0) \qquad (5.44)$$

where α is a number greater than 1

C depends on the initial density and the stress path

p_0 is the initial isotropic pressure

q is the shear stress

At initial stages of shearing, up to a certain stress ratio level

$$\delta\epsilon_r = 0 \text{ so that } \delta\epsilon_p = \delta\epsilon_a + 2.\delta\epsilon_r = \delta\epsilon_a \qquad (5.45)$$

$$\delta\epsilon_q = 2/3.(\delta\epsilon_a - \delta\epsilon_r) = 2/3.\delta\epsilon_a \qquad (5.46)$$

$$\delta\epsilon_p/\delta\epsilon_q = 3/2 \qquad (5.47)$$

Having then established the shear hardening function and the flow rule we can get the magnitude of the strain increments.

$$d\epsilon_q^p = H_q.(\partial G_q/\partial q).dF_q \quad (5.48)$$

$$d\epsilon_p^p = H_q.(\partial G_q/\partial p').dF_q \quad (5.49)$$

which in explicit form can be expressed as:

$$d\epsilon_q^p = \eta.(M_p/[M_p - \eta]).d\eta \quad (5.50)$$

$$d\epsilon_p^p = \eta.(M_p/[M_p - \eta]).(M_{c0} - \eta).(M_p - M_c).d\eta \quad (5.51)$$
$$= d\epsilon_q^p.(M_{c0} - \eta).(M_p - M_c) = dM_p/\eta$$

The strain increments have then been fully defined for the shear yield mechanism.

5-3-2 Volumetric yield with its corresponding plastic potential functions

5-3-2-1 Volumetric yield surface

As has already been mentioned, the shear yield which is quite well defined for sand, fails to predict the volumetric strain that occurs under isotropic compression. For this reason although not very well defined for sand, a volumetric yield surface is chosen on the basis of the previous work carried out by Vermeer (1978), Prevost et al (1975) among others. Although the modified Cam-Clay ellipse could be chosen as yield surface for isotropic compression (Wroth and Houlsby (1985)), for reason of simplicity and convenience a surface perpendicular to the mean effective stress axes is chosen and is expressed as

$$F_p = p' = p_o \quad (5.52)$$

where p_o represents the current size of the yield locus.

The introduction of a non-associative flow rule might seem to be justified even under low stress ratios (Miura et al (1984)). However, an associative flow rule will give sufficient accuracy, since in most cases strains developed during low stress ratio compression are quite small.

5-3-2-2 Volumetric Hardening law

As has been mentioned in the previous section, a volumetric hardening of the Cam-Clay type is not appropriate for modelling the isotropic compression of sand since all the reported results (Lee and Seed (1967), Vesic and Clough (1968)) show that unlike clay, the slope of the compression curve in the v: lnp' plane varies with the confining pressure. However if the range of change of confining pressure is relatively small as is the case in this present study, the average slope could be worked out and volumetric hardening using the Cam Clay expression becomes applicable and gives acceptable accuracy in predicting the volumetric strain.

Nova and Wood (1979) refered to some test results (Frydman (1972)) shown in fig 5.3 for sand on loading and unloading under isotropic compression and assumed that the volumetric strains are purely elastic upon unloading and then derived the slopes of normal compression line and unloading reloading line, λ and κ respectively in the v:lnp' plane. Tatsuoka (1972) also produced similar results on Fuji River sand shown in fig 5.4.

This volumetric hardening function is expressed as:

$$H_p = \delta\epsilon_p^p / \delta p' = (\lambda - \kappa)/(v.p') \quad (5.53)$$

where v is the specific volume

The strain increments are then fully defined for the volumetric yielding and can be expressed as follows:

$$d\epsilon_q^p = 0 \qquad (5.54)$$

$$d\epsilon_p^q = ([\lambda - \kappa]/[v.p']).dp' \qquad (5.55)$$

Although it has been suggested that the Cam Clay expression can describe volumetric hardening when the change of confining pressure is small, it is noted that the volumetric strains produced by isotropic compression are more exactly expressed by a power law of mean effective stress. This provides a better way of differentiating between clay and sand since the latter is known for its relatively low compressibility. Nakai (1989) suggested an expression for the volumetric hardening using a power law expression of mean effective stress. This expression is:

$$H_p = d\epsilon_p^{ic}/dp' = m.(C_p - C_e).\ (p'^{[m-1]}/p_a^m) \qquad (5.56)$$

where m = material constant dependent on the angularity of particles

C_p = slope of the normal compression line in ϵ_p:$(p'/p_a)^m$ plane

C_e = slope of the unloading reloading line in ϵ_p:$(p'/p_a)^m$ plane

In this present reseach work, this power law of mean effective stress has been chosen to describe volumetric hardening.

This volumetric hardening that is associated with isotropic compression may also be applied to the case of proportional loadings since for constant stress ratios below 1.5

only compressive volumetric strains have been observed experimentally.

In addition to values of the elastic parameter C_e and material constant m that have been derived from isotropic unloading compression curve, C_p, the plastic parameter has been given the value of 0.80.

5-3-3 Total plastic response

The total plastic response can be obtained by combining the two yielding mechanisms using Koiter's (1953) formulation assuming that these two yield mechanisms are activated independently (although in reality coupling may occur between the two mechanisms).

The total plastic strains can be obtained by summing the strain components of each yield mechanism respectively. The explicit expression of the total plastic strain components, the total shear strain and the total volumetric strain respectively are:

$$d\epsilon_q^p = \eta.([M_p]/[M_p - \eta]).d\eta \qquad (5.57)$$

$$d\epsilon_p^p = m.(C_p - C_e).(p'^{[m-1]}/p_a^m).dp + d\epsilon_q^p.(Mc - \eta) \qquad (5.58)$$

The families of the resulting yield locus are shown in fig5.5. Plastic deformations take place when yielding of the material occur. Yielding or plastic deformations occur when either the stress ratio increases or the mean effective stress increases or when both quantities increase. For each mechanism a corresponding hardening rule has been defined, each one is assumed to follow an isotropic hardening rule which involves only a change of size of the yield locus (expansion/contraction).

A non associative flow rule has been adopted for the shear yielding of sand on the basis of experimental evidence which is available in the literature (see Vermeer and

Borst (1984) for example).

For the case of volumetric hardening which corresponds to isotropic compression, an associative flow rule has been assumed for simplicity and practicality.

5– 4 Control of Parameters

It is often a common practice in geotechnical engineering to characterise the mechanical behaviour of granular materials by a single parameter that is the relative density and some indication about the particle shape and size of particles. However the use of the relative density on its own is not sufficient since it does not accommodate the influence of the stress level.

Experimental evidence of Lee and Seed (1967) and Vesic and Clough (1968) shows that at high stress levels both initially dense and initially loose sand behave similarly which is probably due to crushing of the material and hence change of the grading curve. Thus correlation between strengths obtained at low stress levels and high stress levels is virtually meaningless since the material tested before application of a high stress level is different from the material obtained at the end of the test.

Been and Jefferies (1985,1986) suggested the use of a parameter that they called a state parameter ψ which combines the influence of initial void ratio and stress level. These authors calculated values of $\psi = (v_{\lambda i} - \Gamma)$ in v: lnp' plane, where $v_{\lambda i}$ is the intercept on normal compression line and Γ the location of critical state line in the compression plane v: lnp' at p' = 1 (see fig5.6). The value of $v_{\lambda i}$ has been calculated from the volume and mean stress obtaining when the sand is about to be sheared in a triaxial test. Thus they include the effect of the volume change that has occurred as the sample is originally compressed but not the effect of volume change during a shear test (Wood (1990)). The state parameter was measured against a reference state. This reference state has been defined as the steady state line which

represents the locus of all the points in v:lnp' plane at which a soil deforms under conditions of constant effective stress and void ratio; this seems to correspond to the critical state line which is defined similarly. This reference state will be referred to here as the critical state. These authors have managed to determine the critical state line experimentally as a straight line in the v:lnp' plane. An implicit assumption was made by Been and Jefferies that critical state line and normal compression lines are staight and parallel in a semi– logarithmic compression plane v:lnp'.

Knowledge of this state parameter can give information about the strength and dilatancy rate that are expected in triaxial compression tests.

In the following, a state parameter will be defined which includes the effect of volume change that has occurred both as the sample is compressed and as a result of dilatancy during a shear test in other words allows the variation of v_λ throughout the test.

The critical state line is very difficult to measure experimentally, especially for dense sand as shear bands occur for post peak shear stress which produce non uniform deformations at large strains. The critical state line is very difficult to locate in the v:lnp' plane. An approximate location for a curved critical state line in the compression plane is suggested in this research work.. The experimental evidence that is available in the literature (see the data of Lee and Seed (1967) for example) suggest that for sand the isotropic compression lines have a smaller slope than the critical state line at the same stress level. At very high stress level, when particle crushing becomes a major feature of the response (major volume changes), the isotropic compression and critical state lines may be considered parallel.

The approach taken here will then be to estimate the stress ratio at the critical state conditions, the critical state stress ratio M_c, together with the measured characteristic state M_{c0} and the initial value of the parameter M_{p0}. This is determined by trial and error until the experimental peak stress ratio is matched. Both the specific volume v throughout the test and the specific volume v_{cs} at the critical state

conditions can then be determined. Hence values of $(v - v_{cs})$ which is the state parameter ψ can be calculated at any stage of the test.

The estimated critical state line will be the locus of all points in the v:lnp' plane at which a soil deforms in a condition of constant effective stresses and specific volume. The specific volume has been calculated from the following expression:

$$v = (1 + e_0).(1 - \epsilon_p) \quad (5.59)$$

where e_0 is the initial void ratio

ϵ_p is the total volumetric strain calculated using (5.56) in the case of isotropic compression or (5.58) in the case of shear.

The specific volume at the critical state conditions can be expressed as:

where $$v_{cs} = (1 + e_{cs}).(1 - \epsilon_{pcs}) \quad (5.60)$$

e_{cs} is the critical state void ratio

ϵ_{pcs} is the volumetric strain at the the critical state conditions

Using (5.59) and (5.60) it can be seen that the isotropic compression and critical state lines are curved and not parallel in the v:lnp'compression plane.

The experimental results as shown in figs. 7(a) show a non linear relationship between the parameter M_p and state parameter ψ when results of triaxial tests on samples prepared at different initial densities and different stress levels are compared. In the same manner M_{c0} can be related to the state parameter ψ as shown in figs. 7(b).

The two plots shown in figs. 7(a) and in figs. 7(b) show that when the results of triaxial samples prepared at different initial densities and subjected to different stress levels respectively are compared using the state parameter ψ, the variation of M_{c0} is rather small compared to the variation of M_p with ψ. It may be sensible to relate the state parameter ψ to the parameter M_p only since the latter already includes the parameter M_{c0}.

It is also interesting to relate the state parameter to the stress ratio which gives a physical feel about the response of soil in terms of strength and dilatancy rate as seen in fig 5.8.

In order to bring together results of sands of different mineralogy, grading curves and angularity, the state parameter should be normalised so that the data of these sands can be brought together. Hird and Hassona (1986) used the specific volume range ($v_{max} - v_{min}$) as the quantity by which the initial state parameter could be normalised. However, they concluded that this quantity was not suitable for bringing together the data of different sands.

An attempt is undertaken here by suggesting a normalising parameter other than the one used by Hird and Hassona (1986). Their parameter gives an indication of the range of packings available at low stress levels but does not appear to relate directly either to the slope of the critical state line at low stress levels or to the slope of isotropic compression curves at higher stress levels, where crushing starts to become important (Wood (1990)).

The normalising parameter that might take into account these factors could be ($v_{cs} - v_{min}$) which may produce a composite state variable that brings together data of different sands. Dividing the state parameter ψ by this quantity ($v_{cs} - v_{min}$) will produce the normalising parameter as shown in fig 5.9. Data of other sands are not available to test the usefulness of this parameter.

5- 5 Performance and predictions of the model

This model, apart from its simplicity and the fact that it uses only six parameters to predict the stress strain behaviour of sand under monotonic loading and stress probes, is believed able to describe the most important features for sand.
In the case of monotonic loading this model is able to predict the main features that are observed experimentally in the triaxial apparatus which are summarised as follows:

- Distinction between the characteristic state and critical state.

- Decrease of strength with further straining after the peak strength is reached, thus allowing for softening to occur. This characteristic is associated with medium to very dense sand tested at low stress level, loose sand does not show a decrease in strength after the peak is reached (see fig 5.10).

- Effect of stress level on volumetric strain- shear strain (suppression of dilatancy at high stress level regardless of the initial density, see fig 5.11).

- Effect of stress level on the parameter M_p the value of which is linked to the peak stress ratio (see fig 5.12).

- Dependency of dilatancy on stress level and density as shown in fig 5.13. This plot also shows inversion of dilatancy rate before the peak strength is reached for the case of medium to dense sand tested at low stress level.

These are predictions of the behaviour of sand subjected to simple paths as for instance conventional drained triaxial tests conducted at constant confining cell pressures and constant mean effective stress paths.

Predictions of the response of sand to stress probes using this double hardening model gives the following results:

- dependency of dilatancy on the applied stress path.

The stress probes carried out around a stress state corresponding to a stress ratio of 0.8 are shown in fig5.14.

Stress path O-1 is a constant shear stress path for which only compressive volumetric strains occur, the shear strains associated with this path are assumed to be zero. According to this model, the mechanism of yielding on this path is purely volumetric yielding. Similarly this model predicts only plastic compressive volumetric strain for stress path O-6.

The predicted deformations on stress path O-2 are calculated assuming that there are two mechanisms of yielding occurring simultaneously leading to two types of plastic deformations, the plastic deformations due to a volumetric yielding and plastic deformations due to shear yielding. The magnitudes of volumetric strains are important for the shear yielding due to dilatancy while the volumetric strains due to volumetric yielding are less important; the plastic shear strains are entirely due to shear yielding. For stress path O-4 which is a constant mean effective stress path only shear yielding is assumed to occur, leading to volumetric strains which are relatively important due to the effect of dilatancy; the deformations occurring on stress path O-3 are also due to shear yielding and are similar to those associated to path O-4. The results for stress paths O-3 and O-4 suggest that dilatancy occurs immediately upon application of stress increments on these paths, while there appear to be a greater rate of dilatancy for path O-3 than for path O-4.

The predicted results are shown in fig5.15 and fig5.16 (elastic assumptions about shear and volumetric strains are included in all results shown in this dissertation).

The predictions for the other series of stress probes carried out around an initial

stress state representing 0.5 have also been studied. The results for this initial stress state are shown in fig5.17, fig5.18 and fig5.19.

The difference in response for these two initial states arises principally because the initial stress ratio of 0.8 in fig5.14 corresponds to the assumed characteristic state so that samples 0–3 and 0–4 start to dilate immediately, whereas sample 0'–3 compresses.

The stress probe calculations have been shown for paths similar to the experimental stress probes. A complete set of probes at two initial stress ratio 0.8 and 0.5 respectively which shows trends of response more systematically is shown in fig5.20, fig5.21 and fig5.24 for an initial stress ratio of 0.8 and fig5.22, fig5.23, and fig5.25. As can be seen in fig5.24 and fig5.25 the predictions are presented in the form of generalised stiffness : strain length path. This model predicts an increase of stiffness at both initial stress ratio (0.8 and 0.5) for stress paths OA, OH and O'A', O'H'. For stress paths involving shear loading, a drop of this generalised stiffness is predicted.

This model successfully predicts the general characteristics of the behaviour of sand subjected to simple paths and stress probes at different initial states. It can be used to predict the response of sand to more complex stress paths in the triaxial compression plane. However, the success of its predictions to complex stress paths is not guaranteed unless experimental evidence is produced to support it.

5– 6 Limitation of the model

This model has some limitations as does every model. It assumes that a purely elastic region exists. This comes from the isotropic hardening that has been chosen. In isotropic strain hardening the yield surface expands to accommodate the stress states that are beyond the current yield surface, and as this surface expands the elastic region increases in size. On unloading the yield surface is not allowed to shrink and the response of soil to unloading stress changes is purely elastic. Real soil on loading, unloading and reloading shows hysteretic response with dissipation of energy, and plasticity. The model predicts a sharp change of stiffness from high to low values when soil passes from elastic to plastic response. Experimental evidence as presented in Chapter 4 (see fig4.14 and fig4.15) for paths O– 2 and O– 8, which are paths corresponding respectively to loading and unloading at the same constant stress increment ratio, suggest that the transition of response from loading to unloading is rather smooth. Experiments in which sand is loaded, unloaded then reloaded indicate that the elastic range is rather small, which means that after a small unloading there occur plastic deformations which are not recovered on reloading. For the case of stress reversals where there is a sudden change of direction of stress path, the model predicts a rather sharp transition from initial high stiffness (elastic) to low stiffness (plastic) which is not supported by the experimental evidence presented here and that published elsewhere. This model is unable to reproduce these features since both unloading and reloading are assumed to develop a purely elastic response, thus recoverable strains are obtained on cycles of unloading – reloading. The intention here in this research work has been confined to the case of monotonically increasing stresses and stress probes for which the model performs reasonably well. For stress reversals or cyclic loading, which this model was not intended to predict, another framework within the theory of plasticity needs to be developed so that mechanisms of dissipation of energy on unloading– reloading

cycles can be implemented and smoothing out of the sudden change in stiffness as the yield locus is passed can be incorporated.

Other approaches to modelling soils are described below where an attempt is made to link these effects mentioned above specifically to plasticity.

Bounding surface plasticity which has been described by Dafalias and Herrmann (1980) and used by Bardet (1986) offers a possibility of extension of conventional elastic– plastic models in order both to smooth out the changes in stiffness that are associated with passage through an assumed yield point and also to generate a hysteretic response on cycles of unloading and reloading (Wood (1991)).

A simplified way of presenting the concepts of this model will be given here.

In this model a bounding surface is defined which is no longer the boundary between elastic and plastic response of soil to stress changes. As shown in figs.26, for every stress point A a yield locus through this stress point may be imagined which for simplicity is taken similar to the bounding surface and an image point B on a bounding surface can be determined. When the stress point is on the bounding surface and $\delta = 0$ conventional plastic behaviour is given; inside this surface $\delta > 0$ and a reduced plastic behaviour is obtained provided p'_e (the size of the current yield locus in the p': q effective stress plane is characterised by a reference pressure p'_e) is increasing while when p'_e is decreasing, for stress changes directed towards the interior of the yield surface, only elastic deformations are produced. This models hysteretic response and is able to smooth out the transition from elastic to plastic behaviour.

Kinematic hardening models introduce an inner yield surface which bounds a small region of truly elastic response. This region translates according to a kinematic hardening rule. Models such as the " bubble" model of Al– Tabbaa and Wood (1989) which is a two surface kinematic extension of the Modified Cam– Clay model combine the features of kinematic hardening, isotropic hardening and bounding surface plasticity models.

Another alternative has also been produced involving the use of multiple yield loci in what are usually termed kinematic hardening models which assume that a series of nested surfaces translate independently in stress space according to a kinematic rule, but are never allowed to intersect. A number of yield loci of progressively larger sizes, all similar in shape to the Modified Cam– Clay, are nested together in stress space. When a stress path is applied, it meets successive yield loci and drags them with it as it traverses them, with the current incremental stiffness inversely proportional to the number of loci being dragged. The yield loci are each caused to translate by the stress path and each one is associated with a simple kinematic hardening rule with which the overall plastic strains are determined. This concept also models the hysteretic effect but requires a large number of material constants especially when the number of yield loci is large as in the model of Prevost and Griffiths (1988).

The models reviewed above give some indication of how plasticity theory can be modified to accommodate different aspects of soil behaviour. It might be worthwhile to say that although these models use different concepts in order to match the experimental results they do not provide a fundamental understanding of the complex behaviour of soil which is the main factor by which a model should be judged to be useful or not. Usefulness might not necessarily be attributed to a model which closely fits the stress strain curve or field tests but to the one which embodies some explanation of the mechanisms underlying the observed behaviour. Indeed soil is a very complex material, and any model which achieves a high degree of accuracy is likely to be complex, thus involving functions and parameters which may be of unknown significance if conditions in real problems depart in any way from those for which the model was derived. For these reasons a simpler model is preferred which places more emphasis on providing understanding of soil behaviour than on high precision in fitting the experimental data.

CHAPTER VI

CONCLUSION

6– 1 Introduction

It is time now to draw some conclusions concerning the work carried out in this reseach project.

This work involved both experimental and theoretical studies of the stress strain relationships for sand. The experimental part involved simple triaxial tests following conventional triaxial compression stress paths as well as more complex stress paths involving stress probes. In addition a group of shear box tests was performed.

The theoretical part involved the construction of an elasto – plastic model based on the theory of incremental plasticity and incorporating predictions of critical states. The constitutive equations were formulated for conditions of axisymmetric stresses.

The model uses two set of yield surfaces (see figs. s, Chapter 5) which correspond to two assumed mechanisms of yielding: shear yielding and volumetric yielding. Inside these two yield surfaces the response of soil to any stress increment is purely elastic, in other words the response to cycles of loading and unloading is assumed to be elastic. The elastic response was assumed to follow a power law of mean effective stress. Thus the two elastic parameters expressed in term of bulk modulus K and shear modulus G are both power law functions of mean effective stresses; the shear modulus has been obtained by assuming a constant Poisson's ratio. This assumed elastic response fits the stress level dependent behaviour of sand that has been shown in the literature.

For the shear yielding mechanism, experimental evidence for a curved yield surface in the p': q plane is available in the literature but for the sake of simplicity a constant stress ratio line has been selected as a yield locus because the curvature of experimental yield loci appears to be small. The experimental work involved mainly monotonic changes of stresses so a curved or straight yield locus would not much affect the predicted stress strain response since such paths only cross the yield locus once. The choice of this form of yield locus can also be supported by the fact that all tests have been conducted at fairly low stress levels so that the curvature of the yield locus is not particularly important.

The flow rule that has been defined for shear yielding has many advantages. Firstly it is based exclusively on experimental evidence, secondly it distinguishes between the characteristic state and the critical state, and thirdly it includes the effects of stress level and initial density on the resulting stress dilatancy plots. Many flow rules that have been established for sand bypass these effects and suggest that the characteristic state and critical state occur at the same stress ratio and do not include the stress level dependency of the resulting stress dilatancy relationships.

The hardening rule for this type of yielding has been derived from conventional drained compression tests.

The volumetric yielding has been included in order to account for volumetric strains that

occur under isotropic compression. A surface orthogonal to the isotropic stress axis has been assumed as a yield surface. An associated flow rule has also been assumed since the plastic strains developed under this mechanism of yielding have in general been reported to be small (Miura et al, 1984). The hardening rule for this type of yielding is similar to that used in the Cam Clay models but differs in detail since it uses a power law of mean effective stress.

For the case of shear yielding, three parameters are required to describe the plastic behaviour. The characteric state stress ratio is an observed value or can be linked with the state parameter ψ. The critical state stress ratio can be determined by observing the trend of stress : strain response at large strain. Finally a parameter M_{p0} (initial value of M_p) is found by trial and error method until the observed peak stress ratio is calculated. In this type of yielding the softening of the material is included and it is at this stage where the concept of critical state has been introduced in the constitutive equations.

In the case of volumetric hardening the three parameters are derived from isotropic compression tests involving loading and unloading. The parameters have been defined as C_e, C_p and m, respectively the slope of swelling line, compression line and m; a constant exponent related to the angularity of sand.

This model has been shown to give good general agreement with the experiments.

However, this model has some limitations. it assumes that during cycles of unloading and reloading the response is purely elastic, implying that there is an expected sharp transition of stiffness from elastic response (high value) to plastic response (low). This is clearly not the observed material reponse. In order to remedy this deficiency which arises because of the elastic plastic framework in which the model has been formulated, other approaches are required such as bounding surface plasticity or kinematic hardening plasticity with nested yield surfaces.

In spite of this shortcoming, if the model is applied for conditions of monotonic change of stresses it will perform rather well.

6- 2 Extension to general stress states

Axisymmetric stress conditions are rarely encountered in civil engineering practice except for one dimensional compression of soil or under the centre of the foundation of a circular load. Application of the model is straightforward for these simple problems. For more general situations the constitutive relations must be incorporated into a finite element program and the constitutive equations need to be transformed from stress and strain variables p' and q into general stresses and strains.
This could be done in terms of principal stresses and strains by using the general stress and strain invariants as described by Wood (1984).

$$p'^{*} = (1/3).(\sigma_1 + \sigma_2 + \sigma_3) \qquad (6.1)$$

$$q^{*} = (1/\sqrt{2}).[(\sigma_1 - \sigma_2)^2 + (\sigma_1 - \sigma_3)^2 + (\sigma_2 - \sigma_3)^2] \qquad (6.2)$$

$$d\epsilon_q^{*} = (\sqrt{2}/3).\ [(d\epsilon_1 - d\epsilon_2)^2 + (d\epsilon_1 - d\epsilon_3)^2 + (d\epsilon_2 - d\epsilon_3)^2] \qquad (6.3)$$

$$d\epsilon_p^{*} = d\epsilon_1 + d\epsilon_2 + d\epsilon_3 \qquad (6.4)$$

For plane strain situations it is generally assumed that there is no deformation in the direction orthogonal to the plane of deformation so that $d\epsilon_2 = 0$.

$$d\epsilon_q^{*} = \eta^{*}.(M_p/(M_p - \eta^{*})).\ d\eta^{*} \qquad (6.5)$$

$$d\epsilon_p^{*} = m.(C_p - C_e).\ (p'^{*(m-1)}/p_a^{m}).\ dp'^{*} + d\epsilon_q^{*}.(M_c - \eta^{*}) \qquad (6.7)$$

with $d\epsilon_2 = 0$ (6.8)

where $\eta^* = q^*/p'^*$ (6.9)

The superscript p which indicates plastic strain has been deliberaltely omitted for clarity.

No guarantee can be given whether this simple model will perform well under general stress conditions. This model was derived from the results of element tests under a limited stress conditions.

Implicit assumption has been made in trying to extend this model to general stress conditions that the rotation of the direction of principal stresses without change in their magnitudes results in no additional plastic strains. In reality the influence of anisotropy on the rotation of the direction of principal stresses can result in additional plastic strains (Wroth and Houlsby (1985)).

These effects will influence the constitutive relations of soil, but how much deviation from the actual behaviour is predicted is not certain.

Another assumption that has been made here when generalising this model from triaxial to more general stress states is that a section of the yield surface is circular in the π plane. This is a simple assumption to make, however experimental evidence shows that this grossly overestimates the strength in triaxial extension for many soils and does not seem to take into account the effect of the intermediate stress which in the case of plane strain will not be correctly predicted.

Alternatives to this circular section of yield surface in the octahedral plane are the Mohr–Coulomb criterion (an irregular hexagon) or the shapes suggested by Lade (1972) or Matsuoka and Nakai (1974) (see fig 6.1). These may lead to a better estimation of the strength in triaxial extension and a better estimation of the value of the intermediate principal stress in plane strain.

Using any of these deviatoric shapes of yield surfaces implies that q^* as used in the incremental stress : strain equations should be redefined from expression (6.2) to be

dependent on Lode's angle θ as defined in fig 6.2.

This angle varies between -30^0 and 30^0 with these limiting values corresponding respectively to triaxial extension and triaxial compression. For plane strains conditions the angle θ would be between these two limits. The angle θ is given by:

$$-30^0 < \theta = (1/3).\sin^{-1}[\ (3.\sqrt{3}/2).(J'_3/J'^{(1/2)}_2)\ ] < 30^0 \quad (6.10)$$

where $J'_1 = (1/3).\sigma'_{ij}.\delta_{ij} = p'^*$

$$J_2' = (1/2).S_{ij}.S_{ij} = (q^{*2})/3$$

$$J'_3 = (1/3).S_{ij}S_{jk}.S_{ki}$$

$$S_{ij} = \sigma_{ij} - \delta_{ij}.I'_1$$

δ_{ij} is the kronecker delta, it has the value:

1 if i = j

and 0 if i ≠ j

If the section of the yield surface is assumed to be non circular then the general deviatoric stress q* is replaced by $q^*.\ f(\theta)$

This function $f(\theta)$ has different forms depending on the yield criterion used. Zienkiewicz and Pande (1977) suggested a form which is a smoothed version of the Mohr–Coulomb criterion and passes through the corners of the Mohr–Coulomb hexagon for triaxial compression and extension.

Then $$f(\theta) = 6/[\ 6 + (q^*/p).\ (\ 1 - \sin 3\theta\ )\ ] \quad (6.11)$$

6- 3 Suggestions for future work

Three suggestions can be recommended as future work:

-1- Suggestions have been made concerning factors that will influence the way in which the constitutive model should be extended to general states of stress. The model should be incorporated in a finite element program and its ability to predict the response of typical geotechnical structures involving the loading of sand should be explored.

-2- The experimental work has been very limited. Considerably more testing is required to explore the stiffness variations of Lochaline sand under a greater range of stress histories and stress probe directions in the conventional triaxial apparatus. Performance of similar tests under conditions of triaxial extension will be important. The development of computer feedback control of the triaxial apparatus would improve the accuracy with which such stress probes could be applied.

-3- Axially symmetric stress paths represent a very limited proportion of the stress changes to which real soils are subjected. True triaxial apparatus are available in which the stress probing work could be extended under conditions of three different principal stresses.

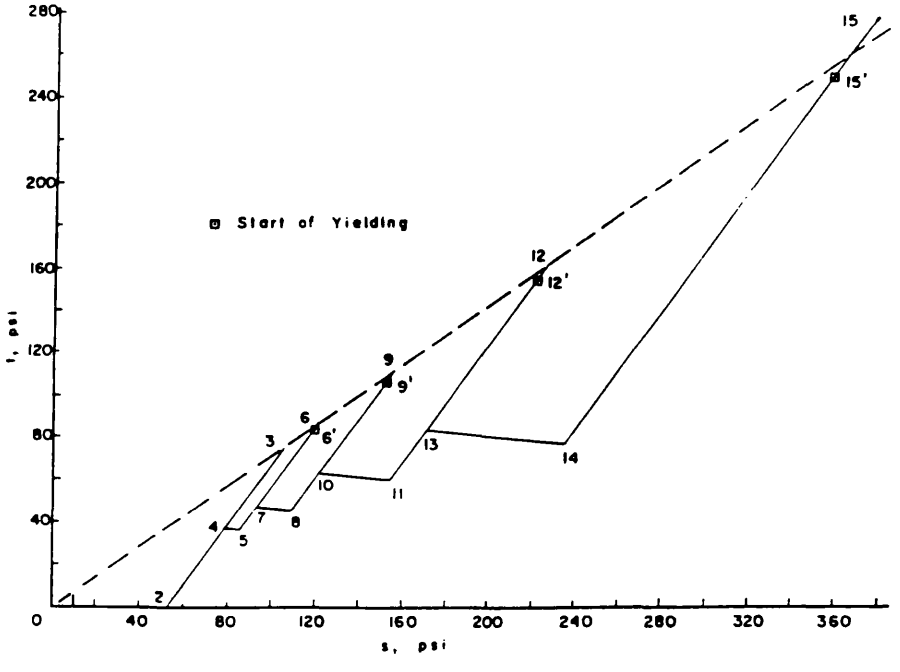

Fig 2.1 Multi– stage stress path

(after Poorooshasb et al, 1966, 1967)

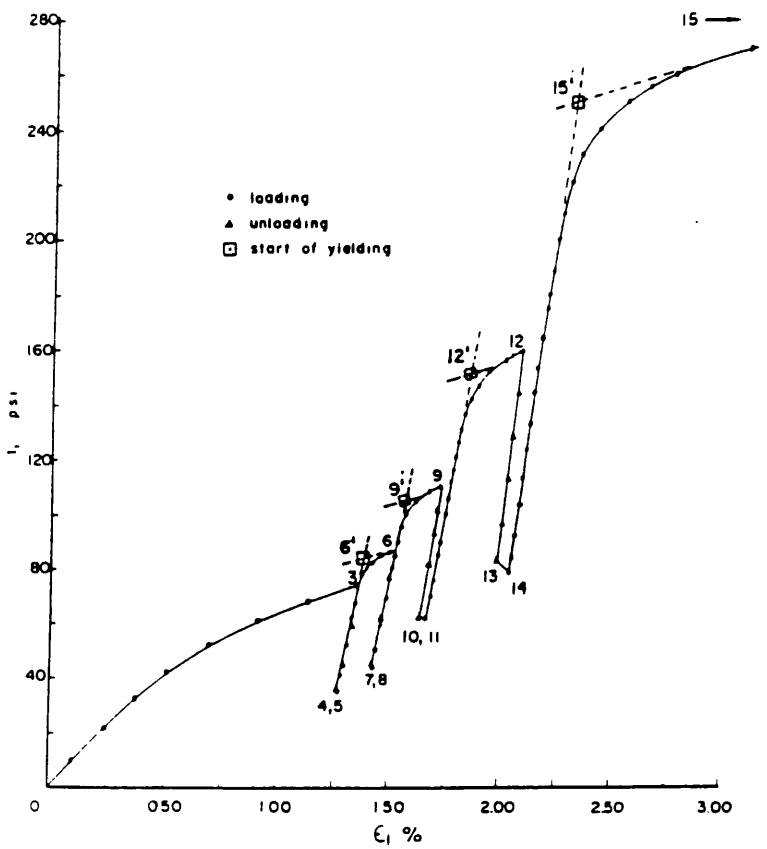

Fig 2.2 Stress strain curve with yield points

(after Poorooshasb et al, 1966, 1967)

Fig 2.3

Yield loci (—) and plastic potentials (- -) for dense Ottawa sand (after Poorooshasb, Holubec, and Sherbourne, 1966, 1967).

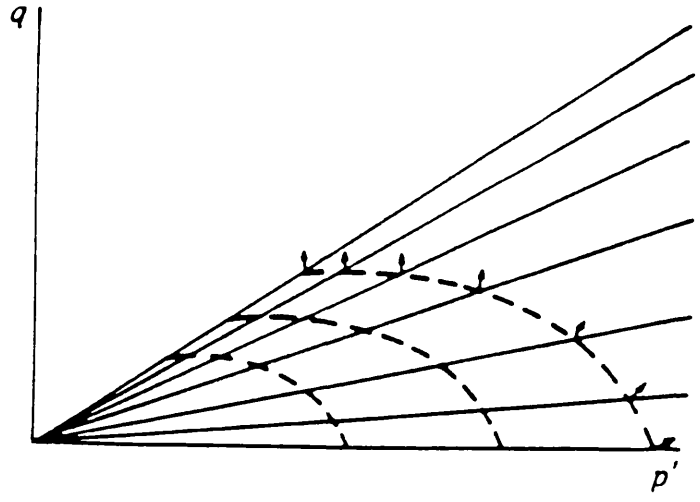

Fig 2.4

Yielding in triaxial probing tests on dense Fuji River sand: (a) stress path in p' q plane used to examine yielding (●); (b) yielding observed in plot of stress ratio q/p' and volumetric strain ε_v; (c) yielding observed in plot of stress ratio q/p' and triaxial shear strain ε_q; (d) segments of yield curves in p' q plane (after Tatsuoka, 1972).

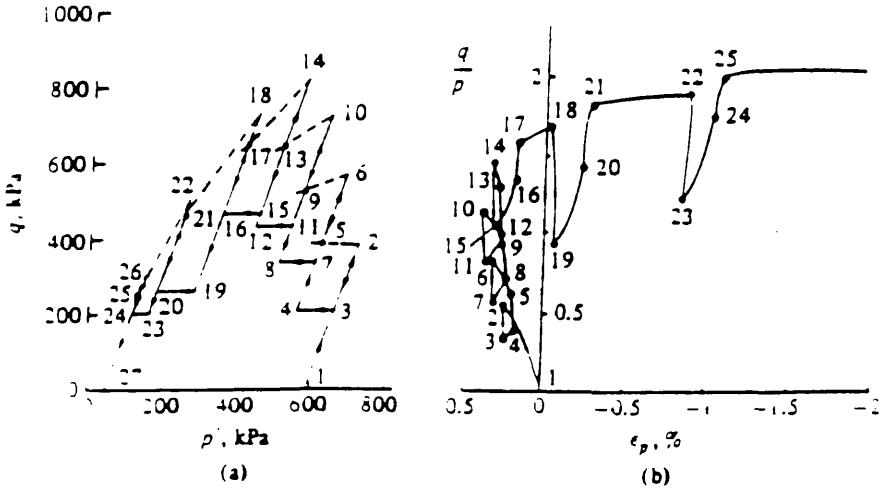

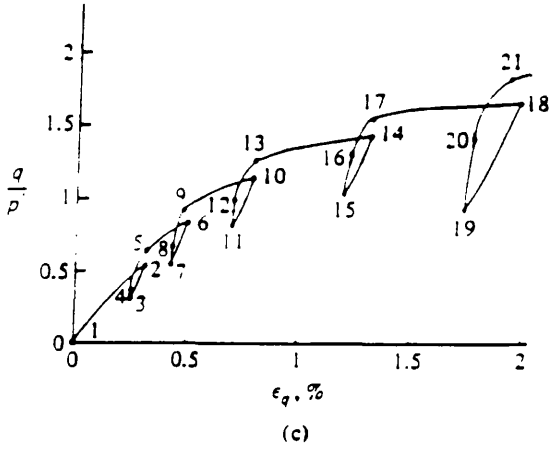

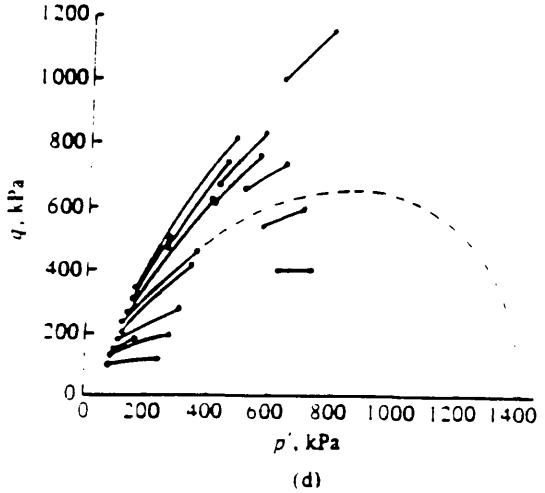

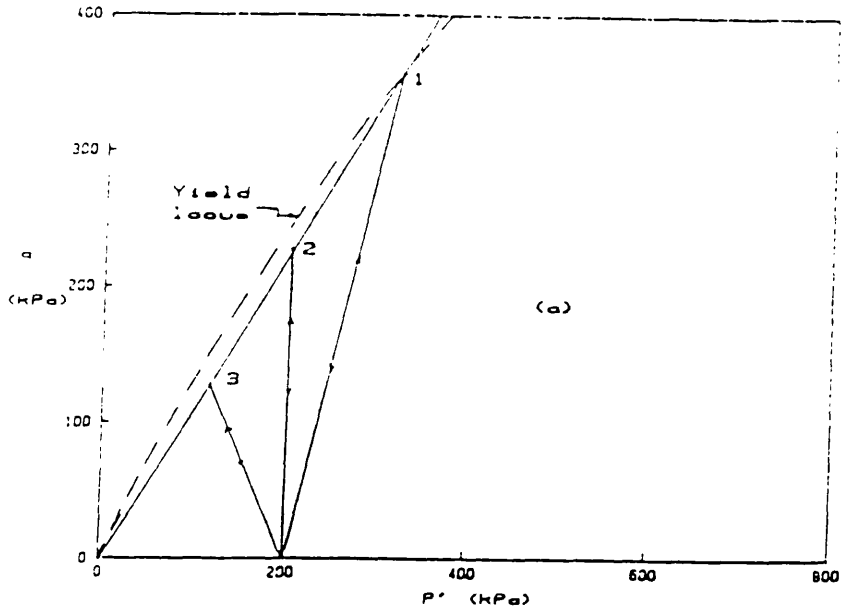

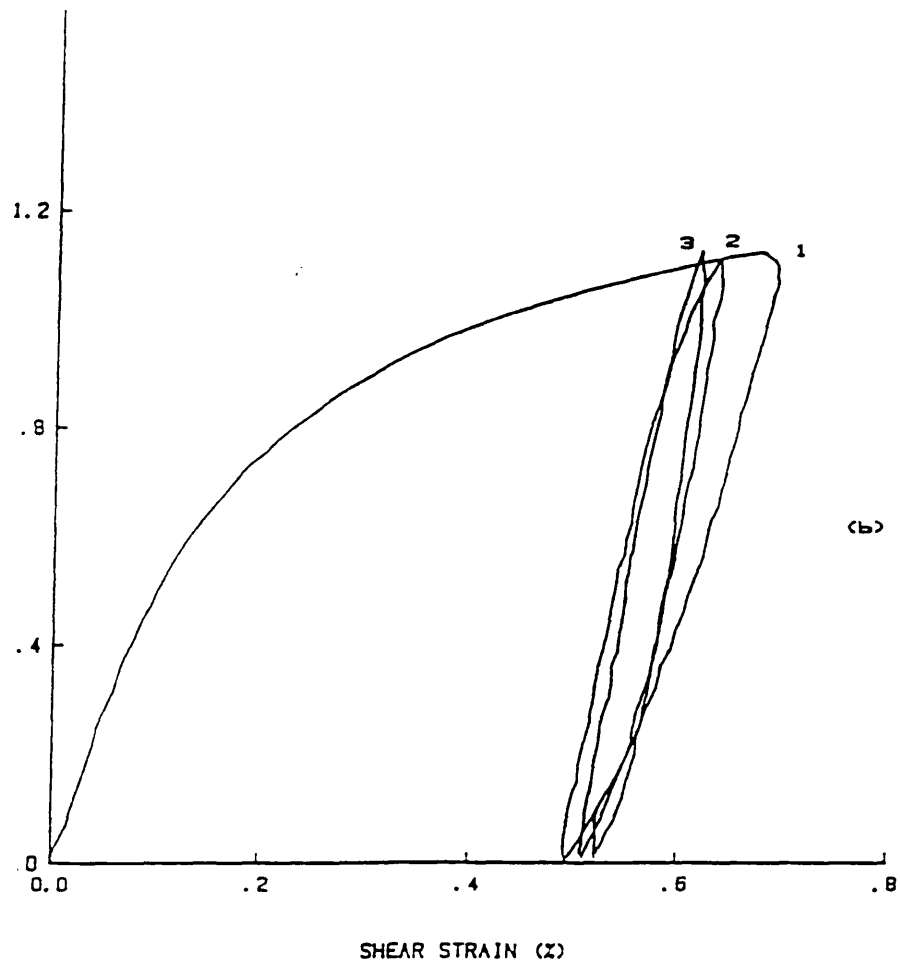

Fig 2.5 Examination of the proposed yield loci (after Khatrush, 1987)

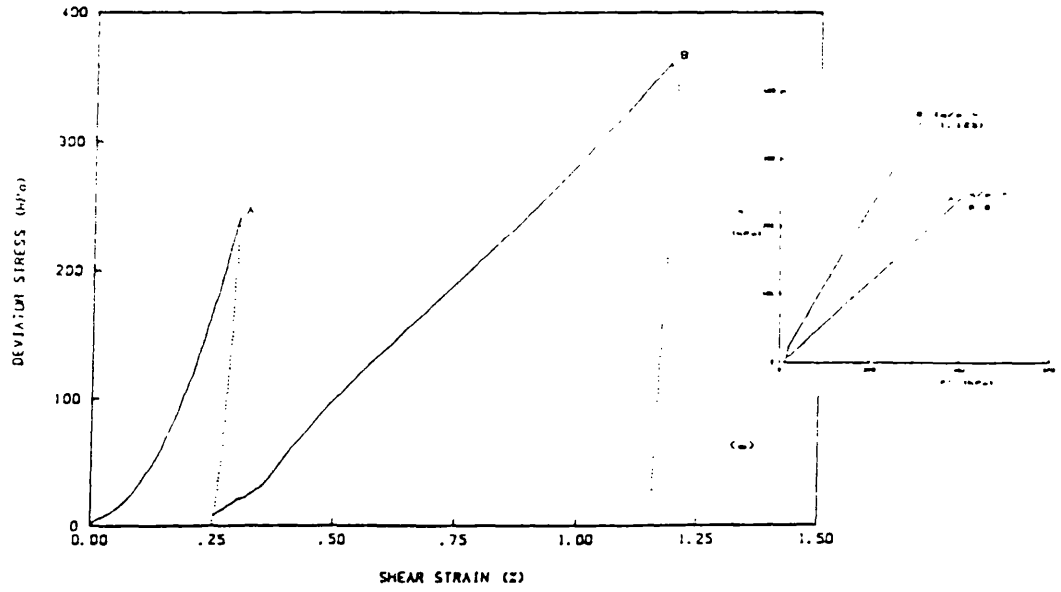

a

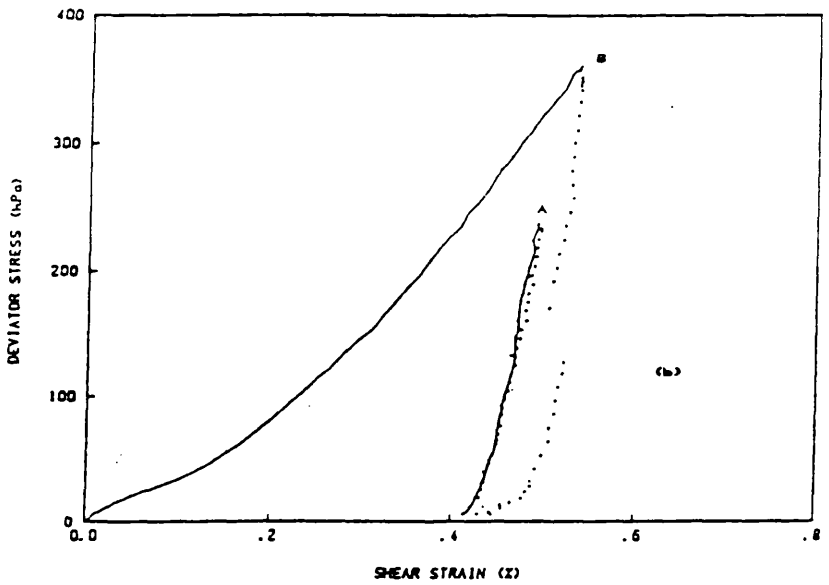

b

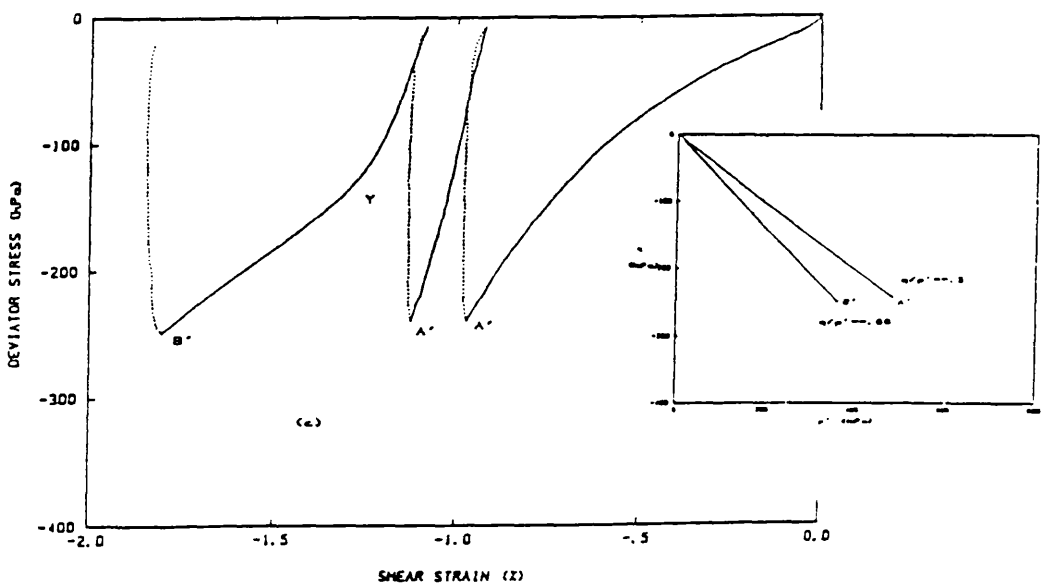

(c)

Fig 2.6 Resulting stress–strain data from cyclic stress paths during various constant stress ratios (after Khatrush, 1987)

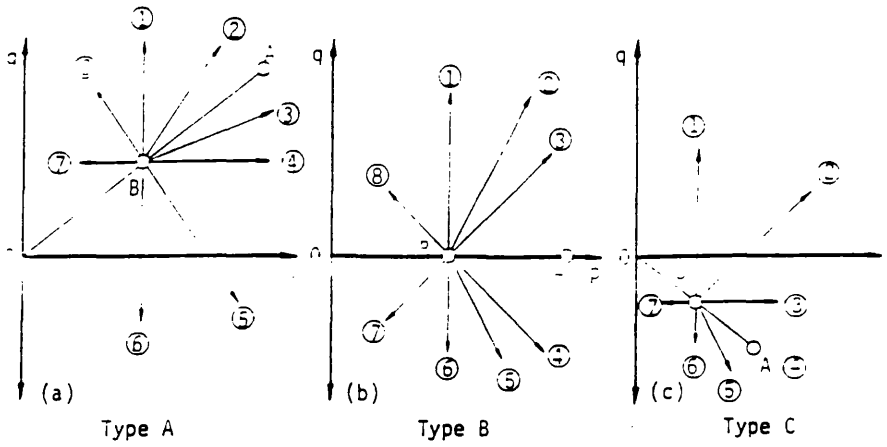

Stress paths for detemination of yield points corresponding to Point "A"

Fig 2.7 (after Yusufuku et al, 1991)

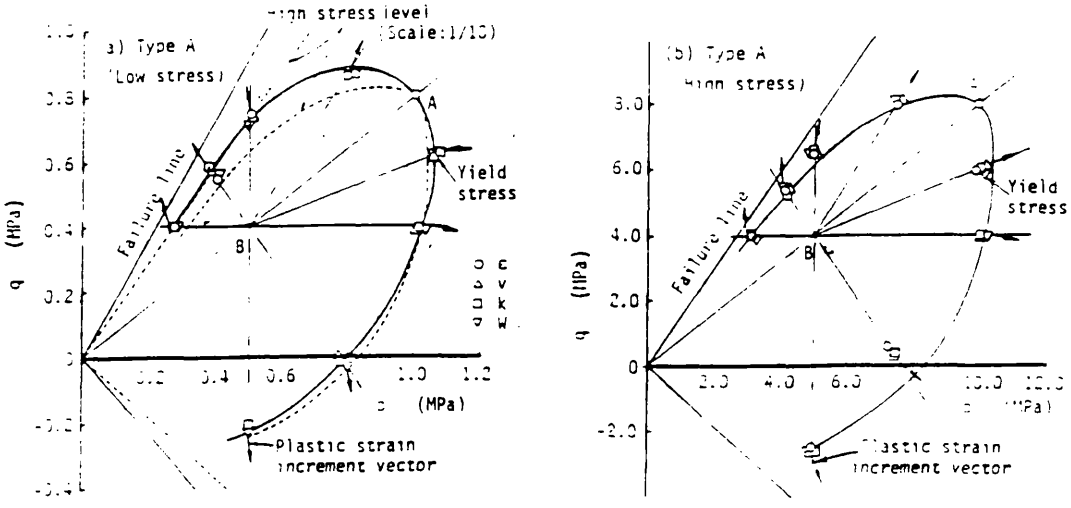

Experimental yield curves obtained from tests of Type A in the : (a) low stress level ; (b) high stress level

Fig 2.8 (after Yusufuku et al, 1991)

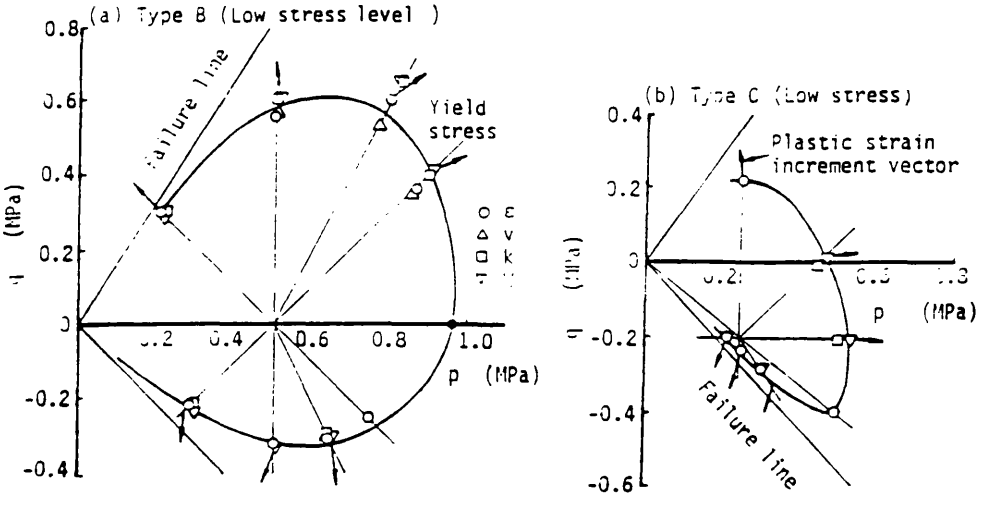

Experimental yield curves in the low stress level for :
(a) results of Type B ; (b) results of Type C

Fig 2.9 (after Yusufuku et al, 1991)

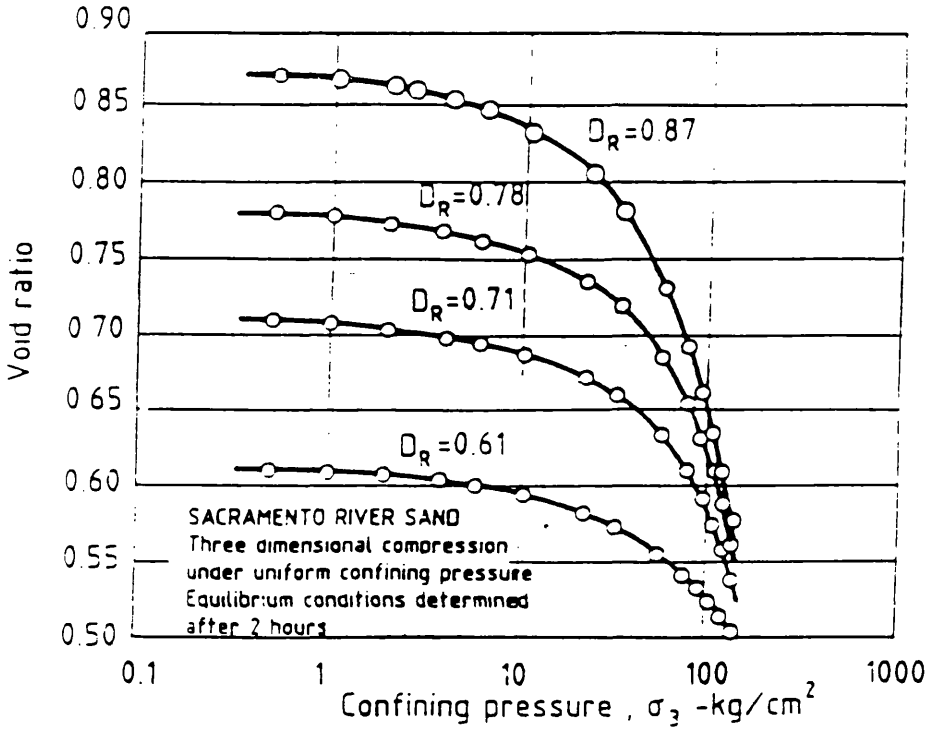

Fig 2.10 PRESSURE-VOID RATIO CURVES FOR SAND AT FOUR INITIAL DENSITIES (AFTER LEE AND SEED)

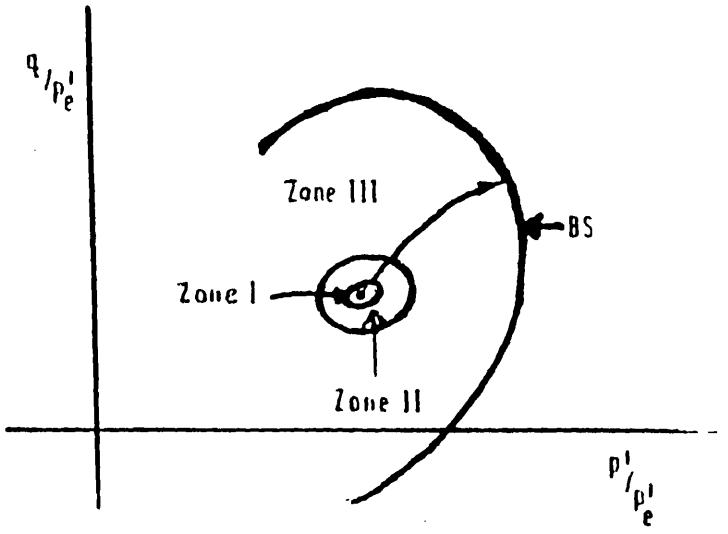

Fig 2.11 Identification of Zones I, II and III in triaxial stress space (after Jardine, 1992).

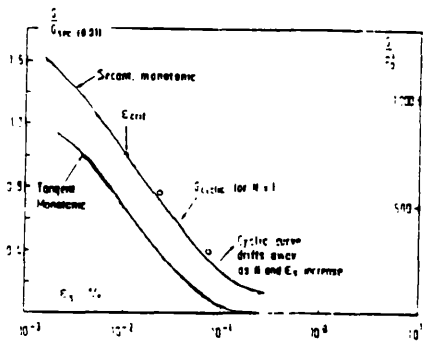

Fig 2.12 Shear stiffness– ϵ_s relationships for Magnus till (after Jardine, 1992)

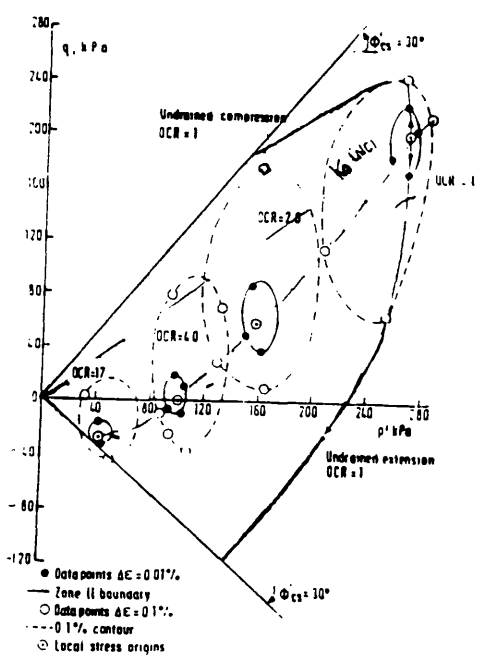

Fig 2.13 Movement and evolution of small strain regions due to K_0 swelling: Magnus till. (Note $\Delta\epsilon = 0.01\%$ contour is approximate Zone II boundary) (after Jardine, 1992)

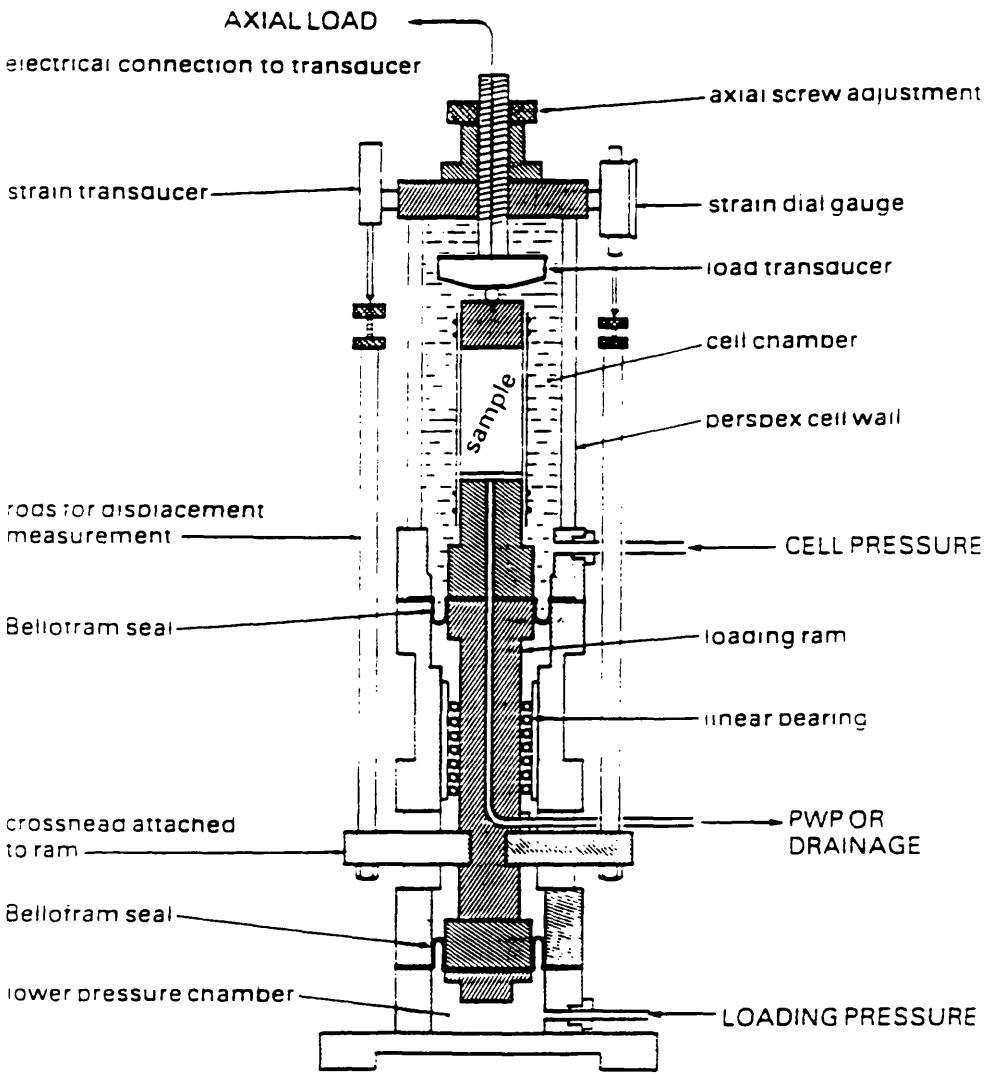

Fig 3.1 Simplified diagram showing principal features of the Bishop – Wesley cell (after K.H.Head, 1984)

Fig 3.2 New configuration of pressure and drainage lines

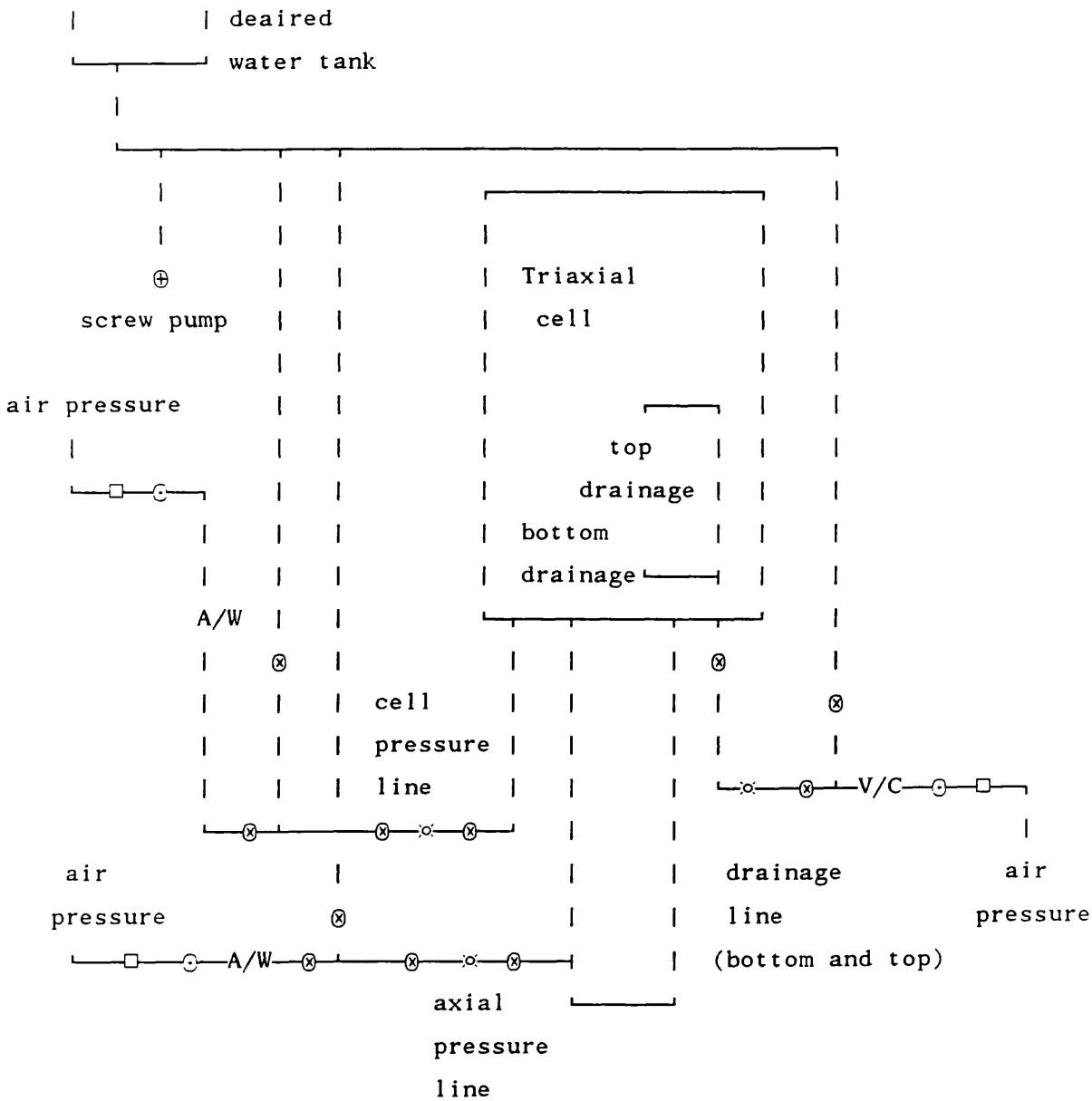

A/W air water interface

V/C volume change device

pore pressure transducer

screw pump

pressure regulator

pressure gauge

valve of pressure

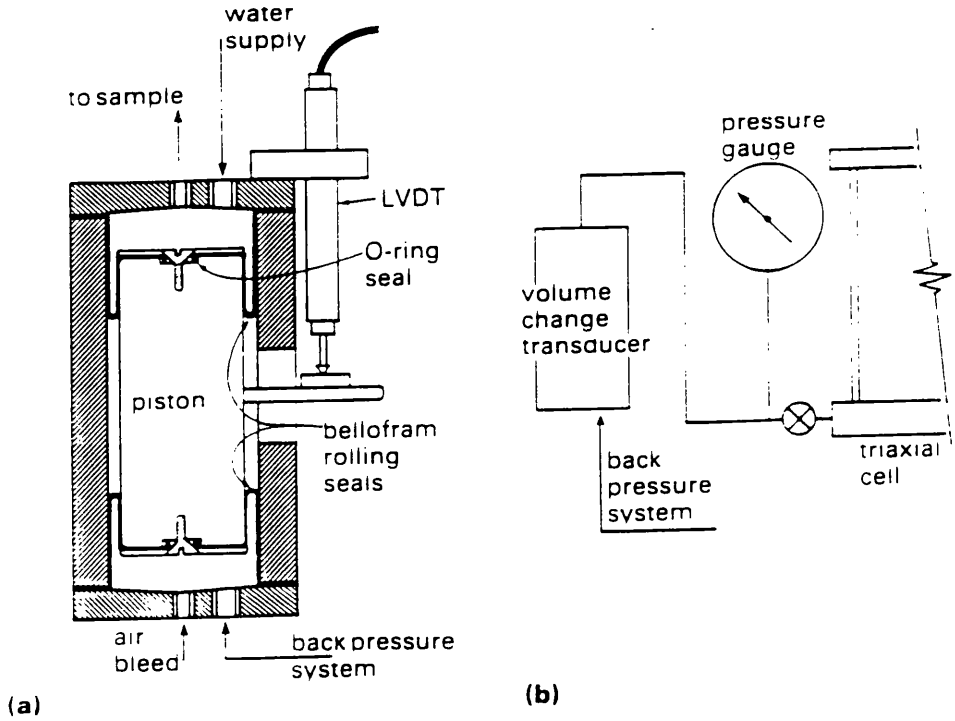

Fig 3.3 Volume–change transducer. Imperial College

(a) principle

(b) Layout of connection to triaxial cell

(after K.H.Head, 1984)

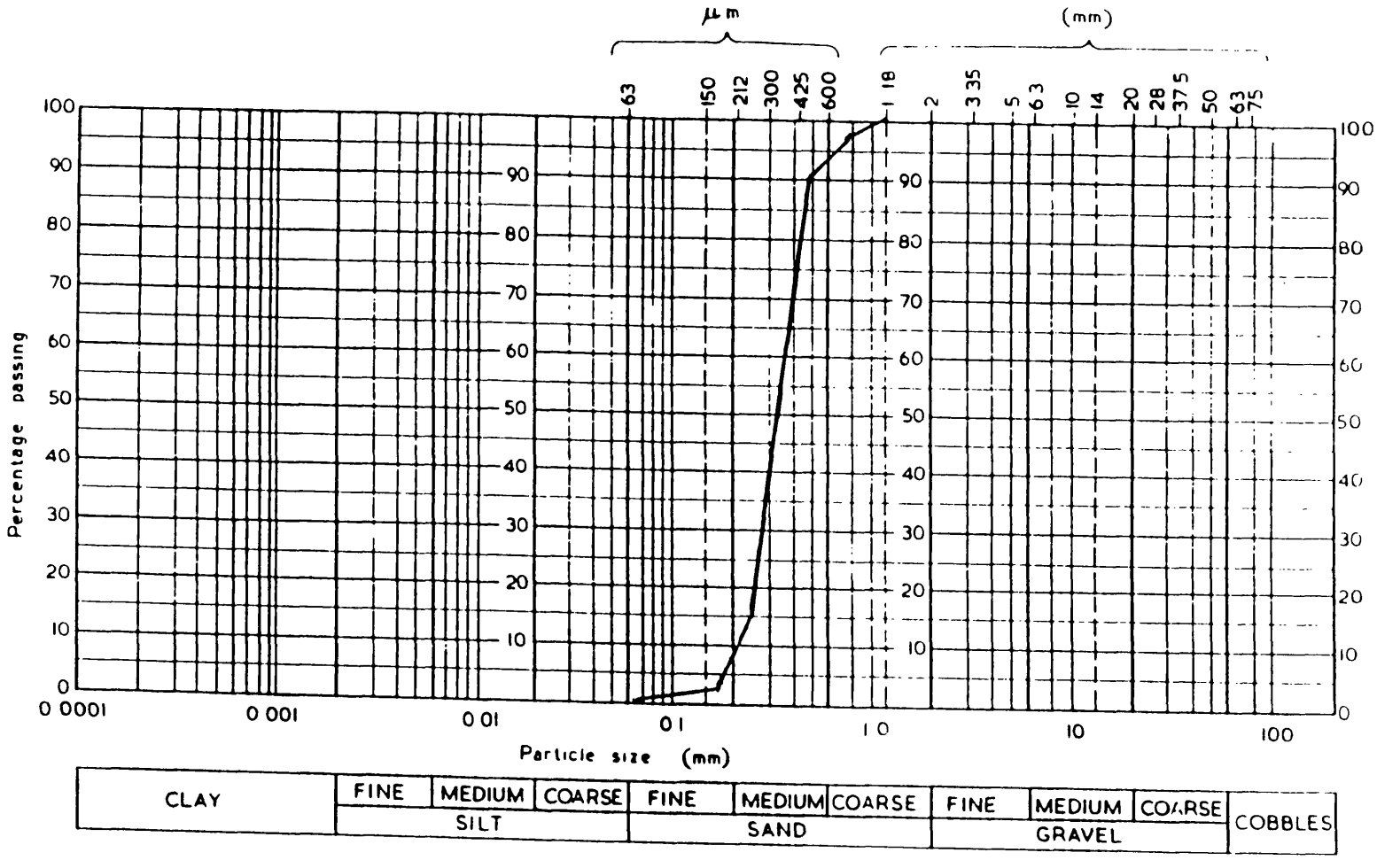

Fig 3.4 Particle size distribution

of Lochaline sand

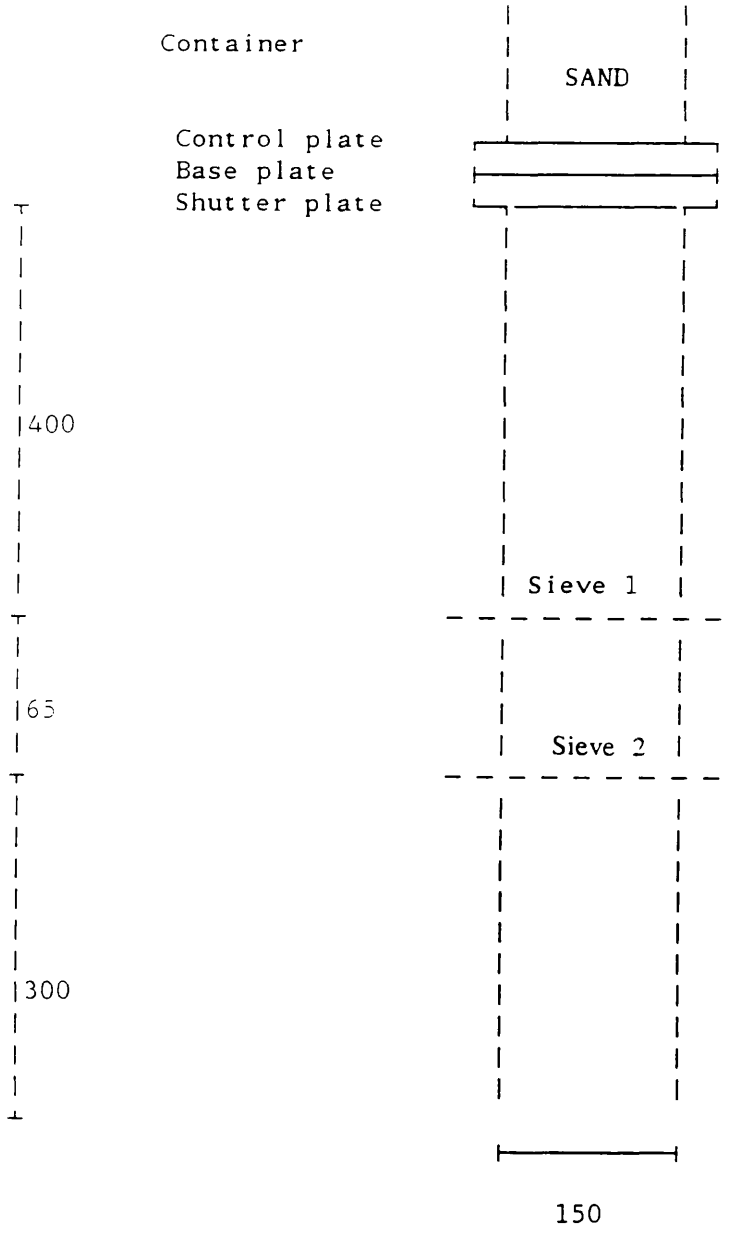

Tower for pluviation of sand through air

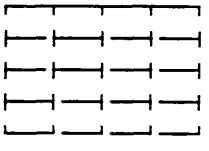

Sieve mesh (square opening 3.35 mm (B.S))

Plate (square) with apertures

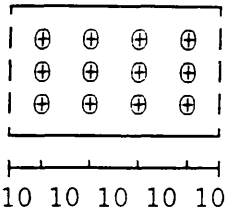

⊕
D = 10
aperture size (mm)

10 10 10 10 10 (spacing in mm)

Fig 3.5 Variable aperture hopper

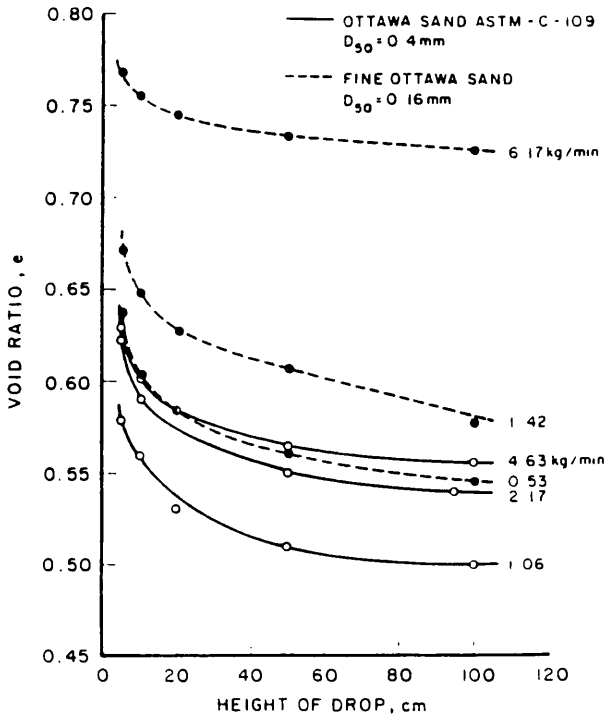

Fig 3.6 Height of drop, mass pouring rate and particle size effects on void ratio (after Vaid et al, 1988)

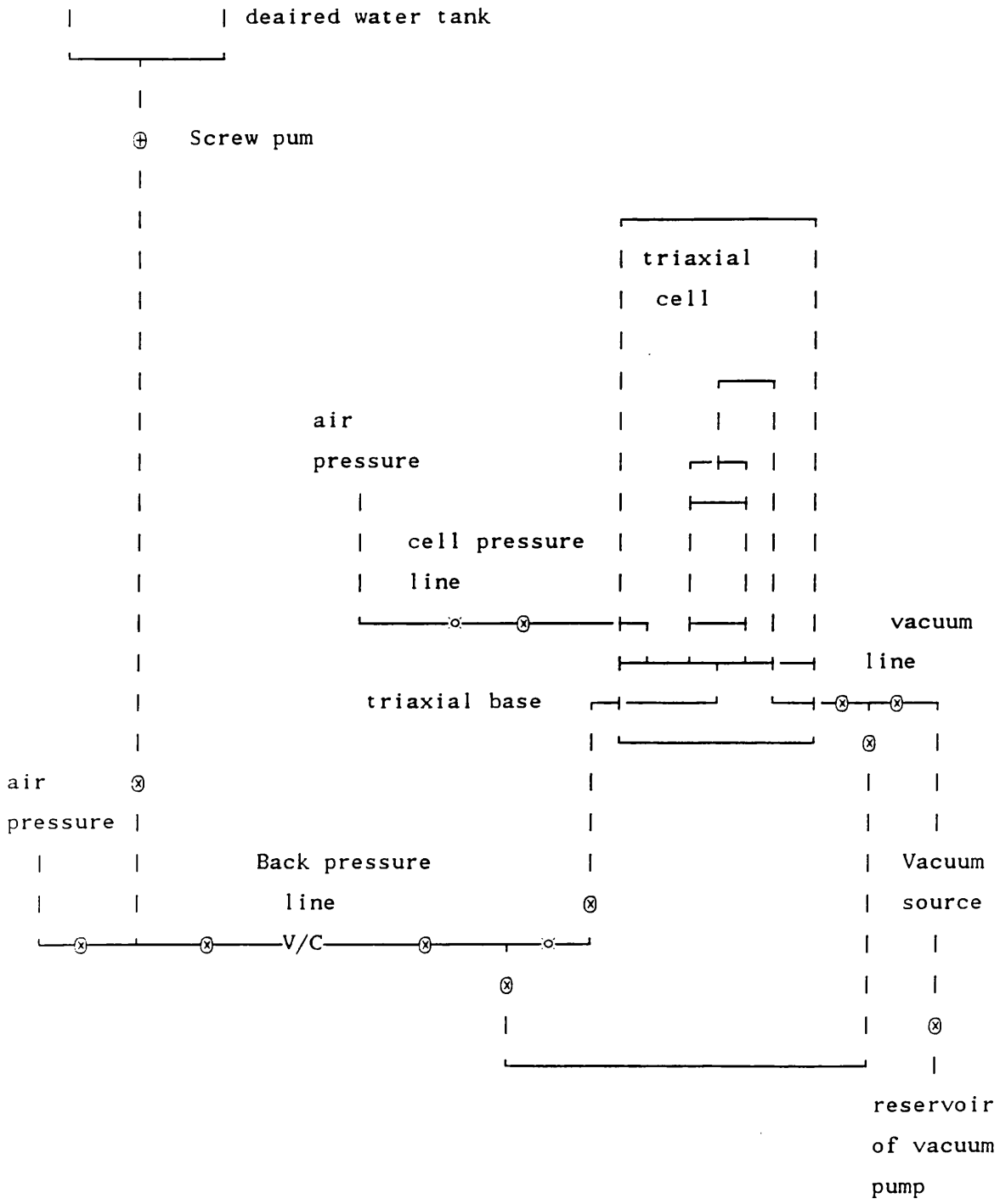

V/C volume change device

srew pump

valve of pressure

pore pressure transducer

Fig 3.7 Experimental arrangement for saturating soil specimen using initial vacuum technique

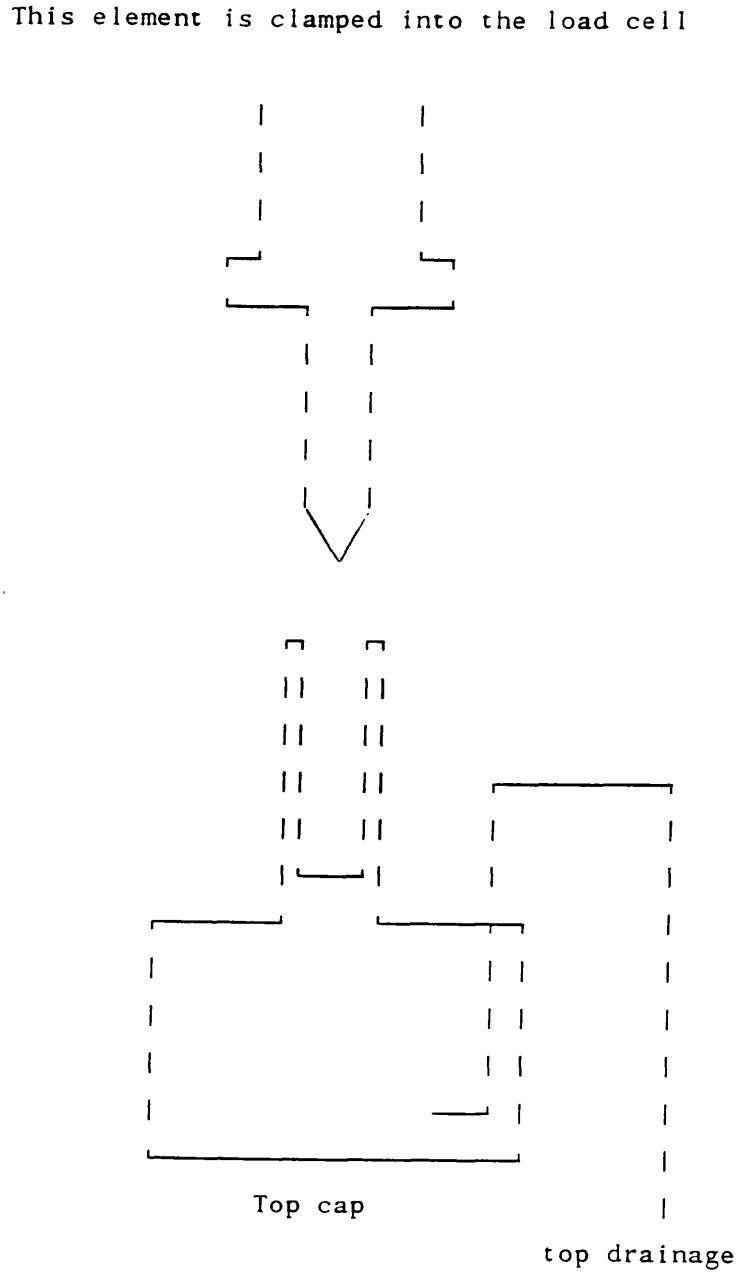

Fig 3.8 Experimental arrangement for eliminating tilting of top cap at large strains

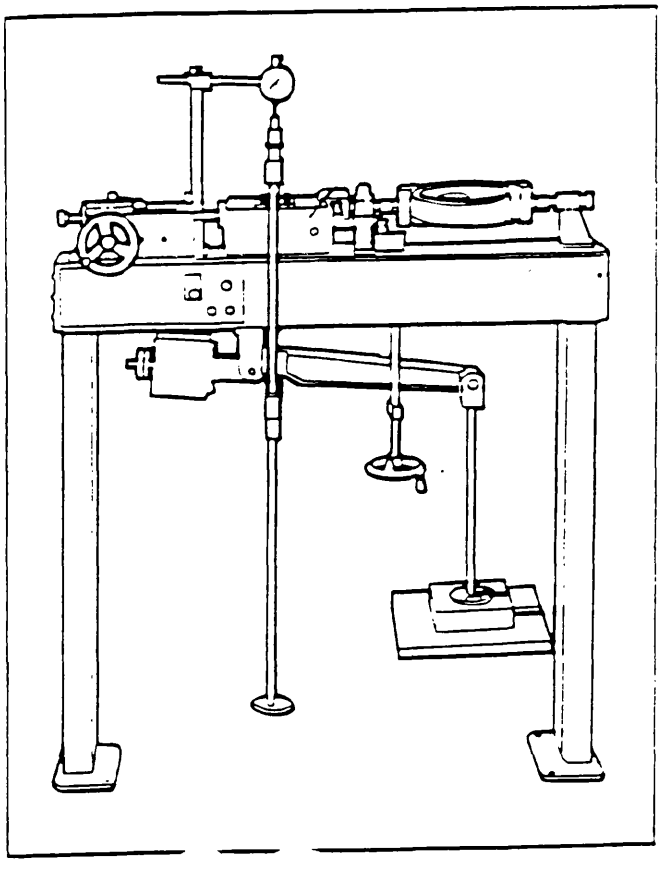

Fig 3.9 General arrangement of shear box assembly (ELE manual)

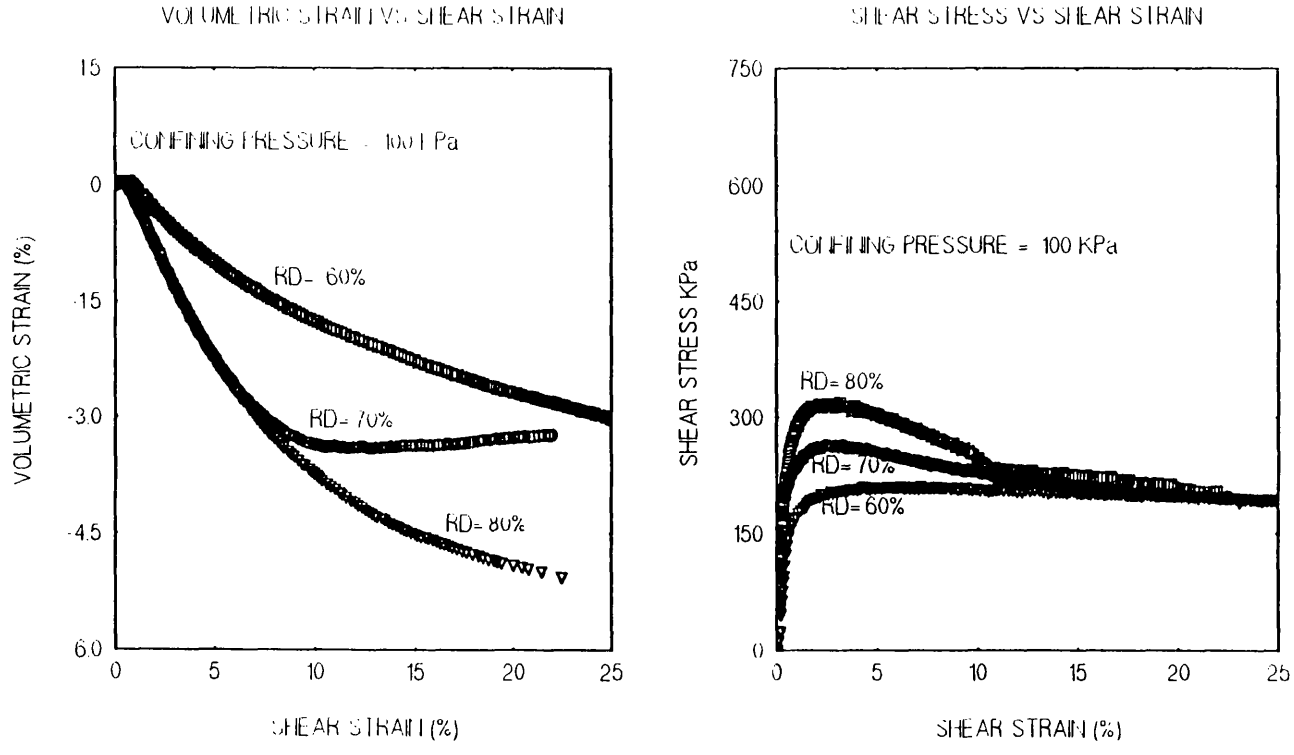
VOLUMETRIC STRAIN VS SHEAR STRAIN
CONFINING PRESSURE = 100 KPa
RD= 60%
RD= 70%
RD= 80%
VOLUMETRIC STRAIN (%)
SHEAR STRAIN (%)
15
0
-15
-3.0
-4.5
-6.0
0
5
10
15
20
25
SHEAR STRESS VS SHEAR STRAIN
CONFINING PRESSURE = 100 KPa
RD= 80%
RD= 70%
RD= 60%
SHEAR STRESS KPa
SHEAR STRAIN (%)
750
600
450
300
150
0
0
5
10
15
20
25

Fig 4.1

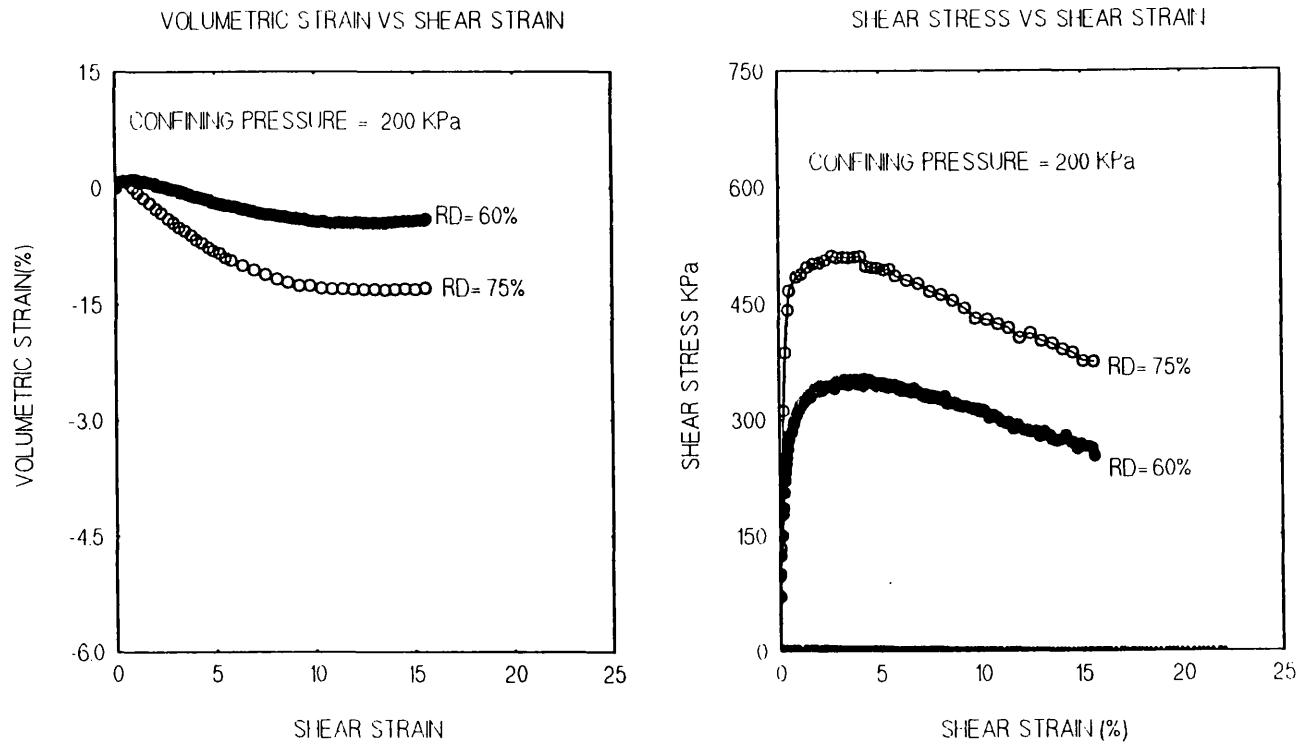
VOLUMETRIC STRAIN VS SHEAR STRAIN
CONFINING PRESSURE = 200 KPa
RD= 60%
RD= 75%
VOLUMETRIC STRAIN(%)
SHEAR STRAIN
15
0
-15
-3.0
-4.5
-6.0
0
5
10
15
20
25
SHEAR STRESS VS SHEAR STRAIN
CONFINING PRESSURE = 200 KPa
RD= 75%
RD= 60%
SHEAR STRESS KPa
SHEAR STRAIN (%)
750
600
450
300
150
0

Fig 4.2

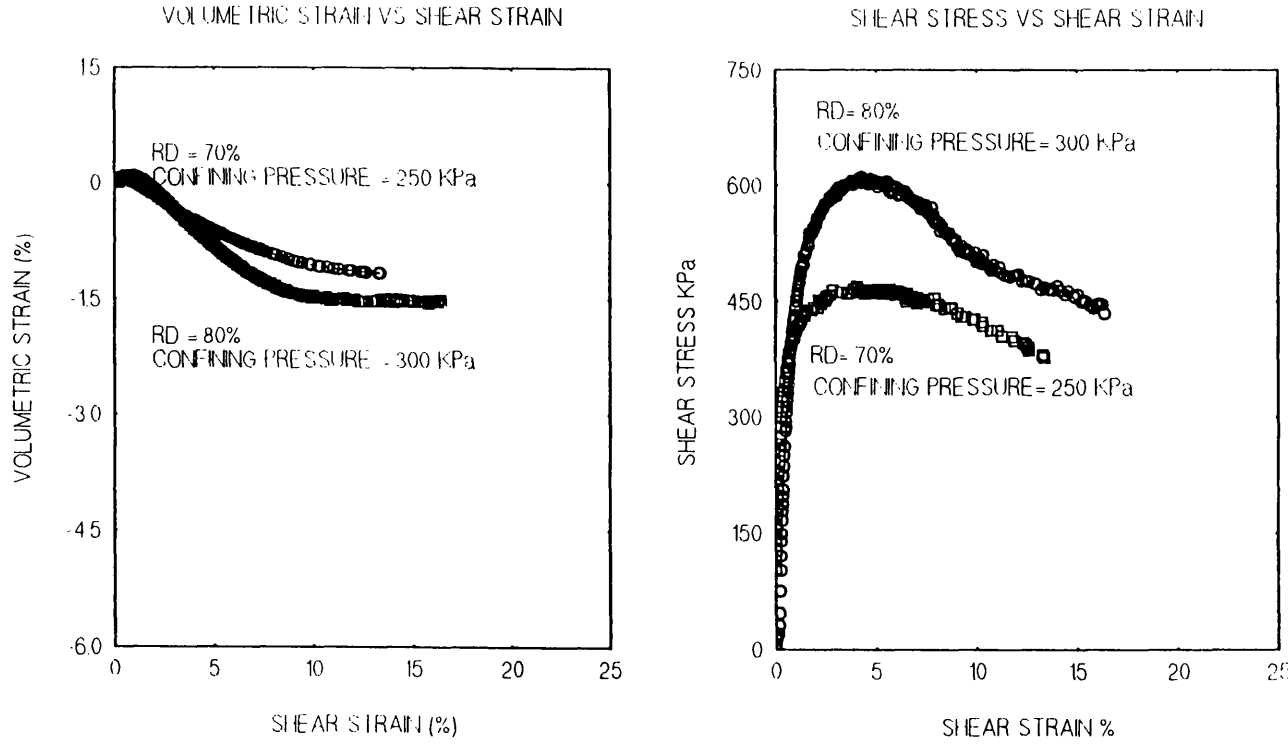
VOLUMETRIC STRAIN VS SHEAR STRAIN
VOLUMETRIC STRAIN (%)
15
0
-1.5
-3.0
-4.5
-6.0
0
5
10
15
20
25
SHEAR STRAIN (%)
RD = 70%
CONFINING PRESSURE = 250 KPa
RD = 80%
CONFINING PRESSURE = 300 KPa
SHEAR STRESS VS SHEAR STRAIN
SHEAR STRESS KPa
750
600
450
300
150
0
SHEAR STRAIN %
RD= 80%
CONFINING PRESSURE= 300 KPa
RD= 70%
CONFINING PRESSURE= 250 KPa

Fig 4.3

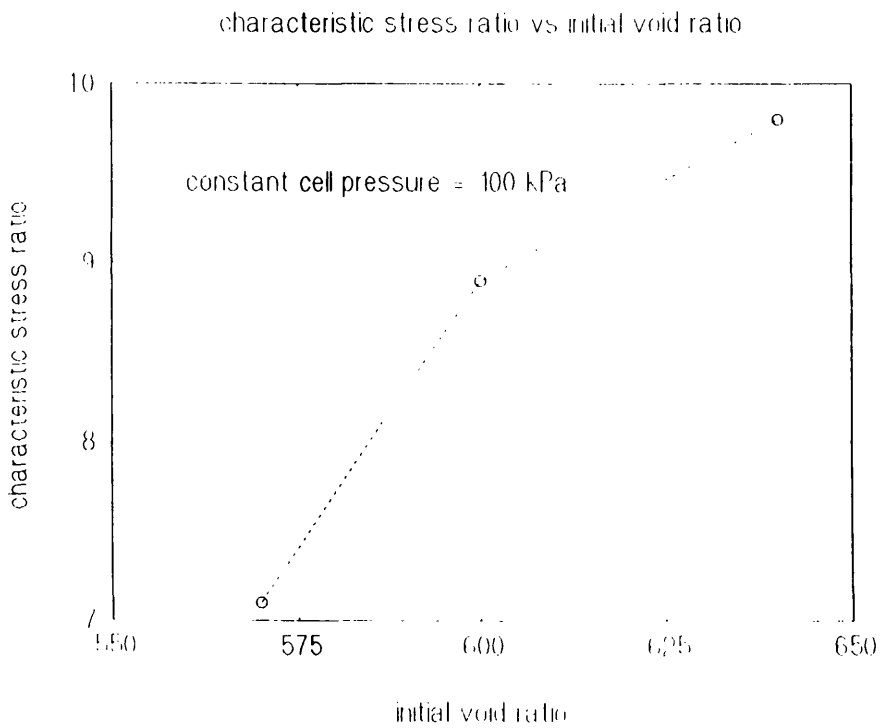
characteristic stress ratio vs initial void ratio
10
9
8
7
constant cell pressure = 100 kPa
characteristic stress ratio
550
575
600
625
650
initial void ratio

Fig 4.4 (a)

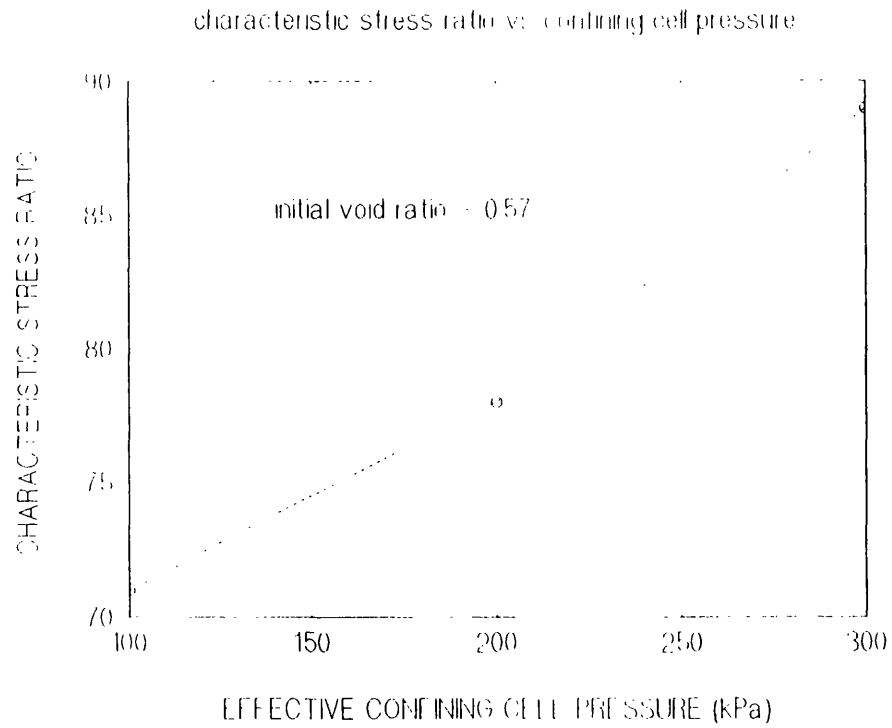
characteristic stress ratio vs confining cell pressure
CHARACTERISTIC STRESS RATIO
90
85
80
75
70
initial void ratio = 0.57
100
150
200
250
300
EFFECTIVE CONFINING CELL PRESSURE (kPa)

Fig 4.4 (b)

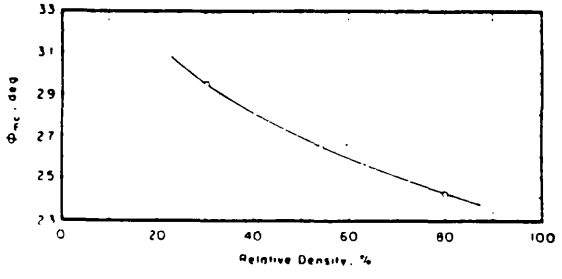

Mobilized friction angle at maximum contraction versus initial relative density—medium Ottawa sand.

a

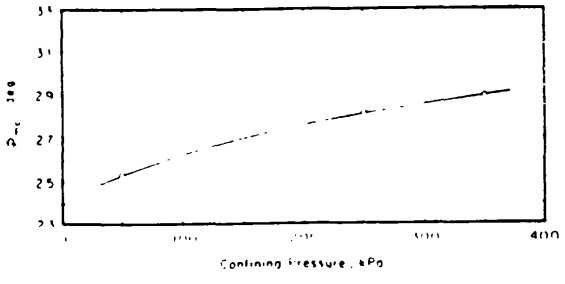

Mobilized friction angle at maximum contraction versus confining pressure—medium Ottawa sand. $D_r = 50\%$

b

Fig 4.5 (after Negussey et al, 1987)

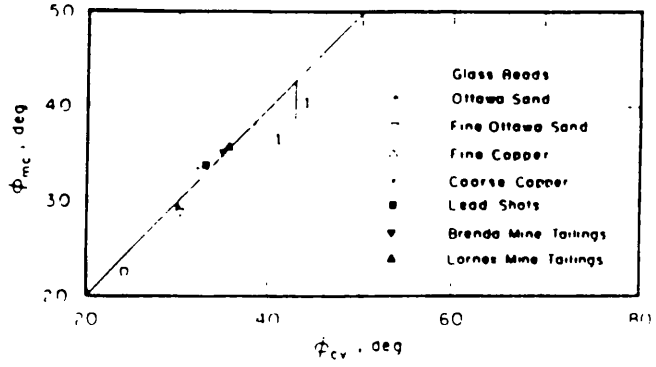

Mobilized friction angle at maximum contraction in triaxial tests versus constant-volume friction angle in ring shear; effective confining pressure = 200 kPa

Fig 4.6 (after Negussey et al, 1987)

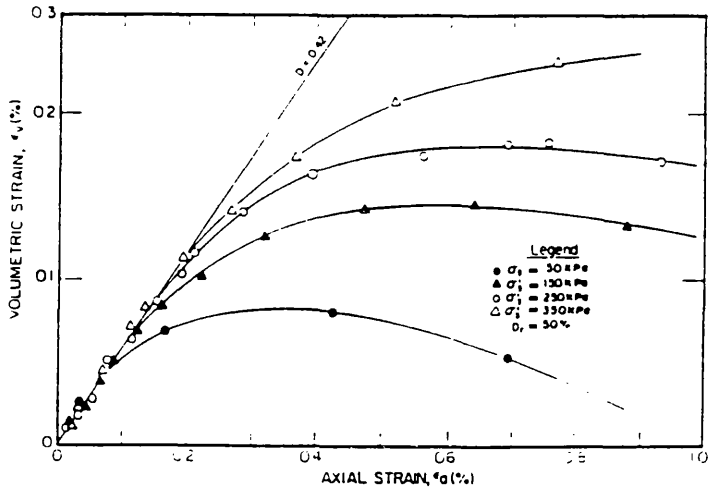

Strain paths for conventional triaxial stress paths

a

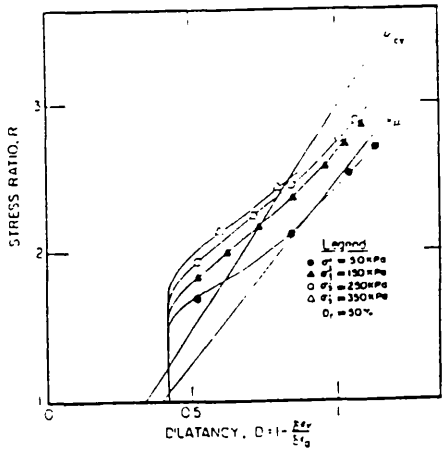

Stress dilatancy plot of conventional triaxial test results

b

Fig 4.7 (after Negussey et al, 1990)

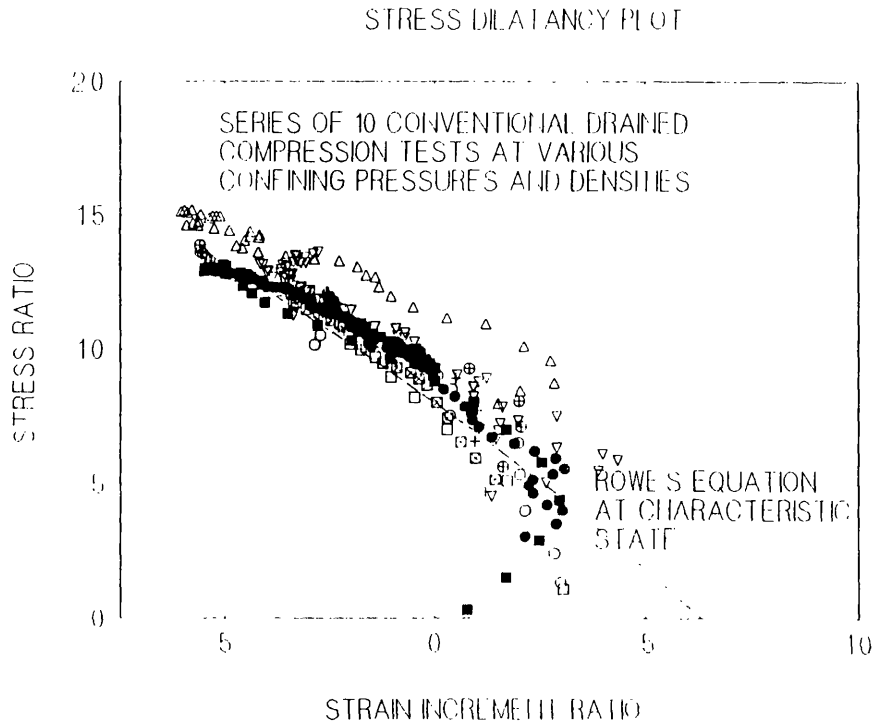
STRESS DILATANCY PLOT
SERIES OF 10 CONVENTIONAL DRAINED
COMPRESSION TESTS AT VARIOUS
CONFINING PRESSURES AND DENSITIES
ROWE S EQUATION
AT CHARACTERISTIC
STATE
STRESS RATIO
STRAIN INCREMENTAL RATIO
20
15
10
5
0
5
0
5
10

Fig 4.8

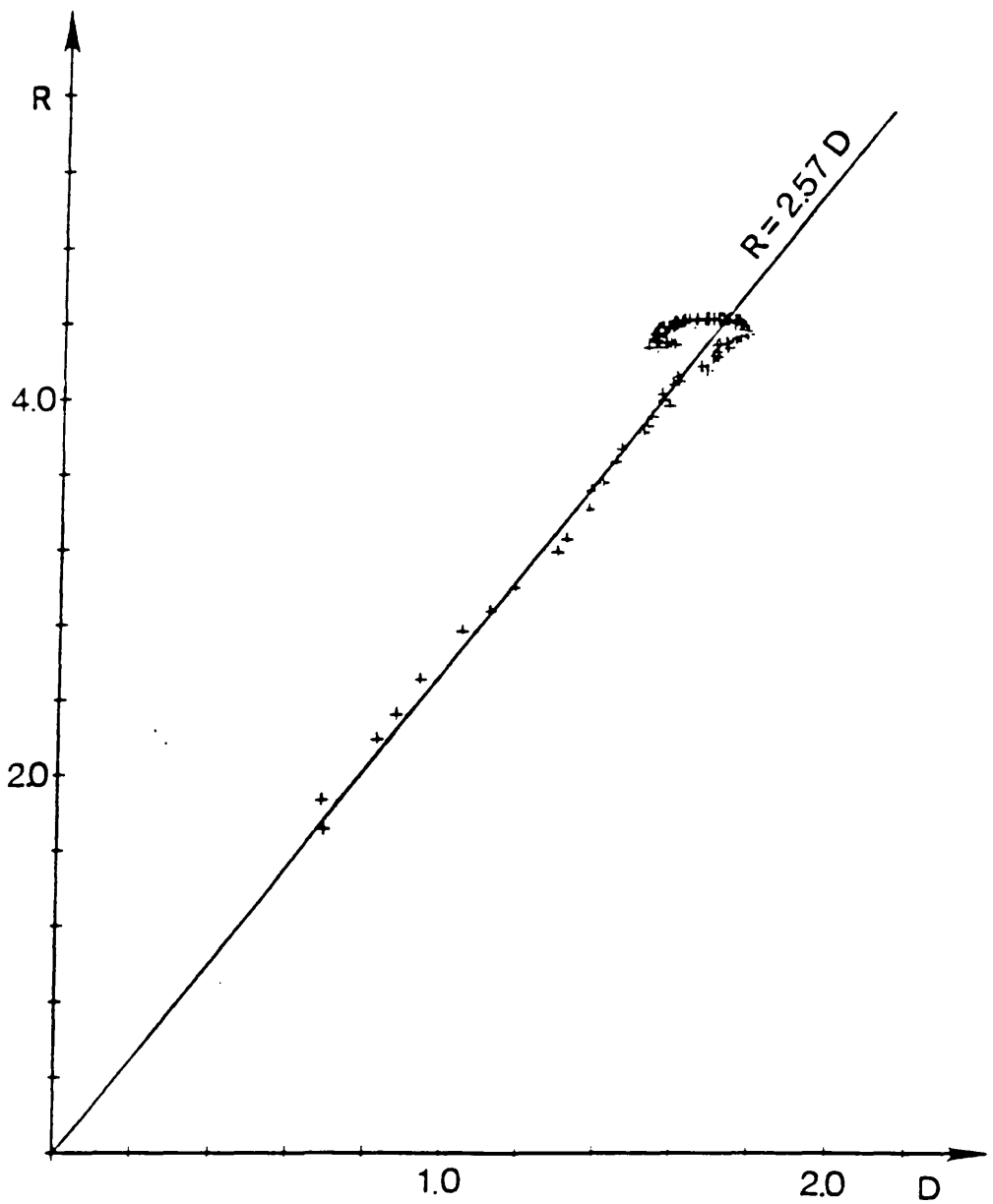

Fig 4.9 (after Houlsby, 1981)

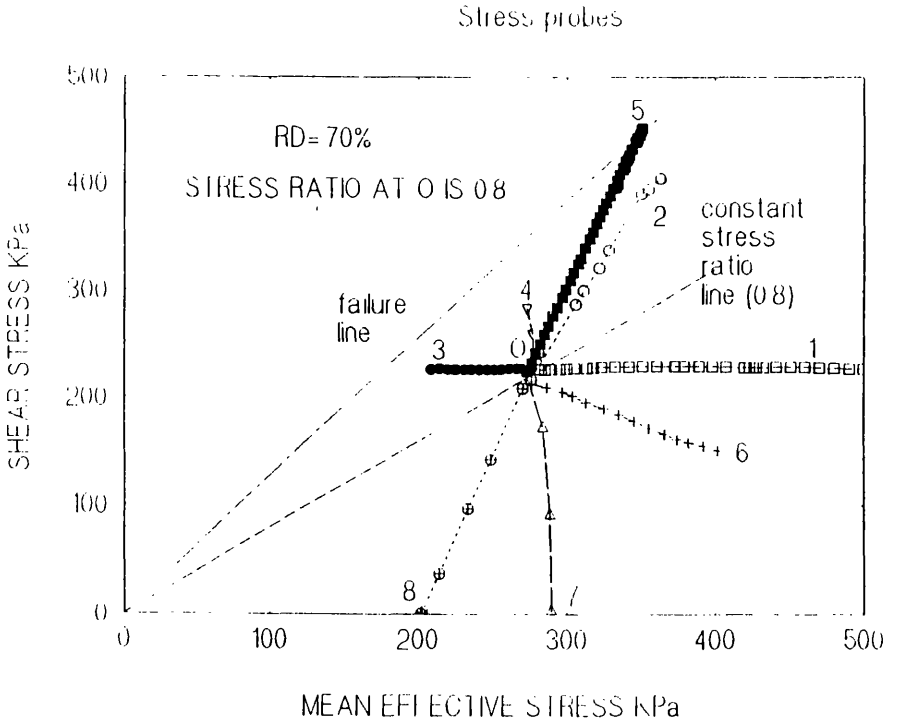
Stress probes
RD= 70%
STRESS RATIO AT O IS 08
failure line
constant stress ratio line (08)
0
1
2
3
4
5
6
7
8
SHEAR STRESS KPa
MEAN EFFECTIVE STRESS KPa
0
100
200
300
400
500

Fig 4.10

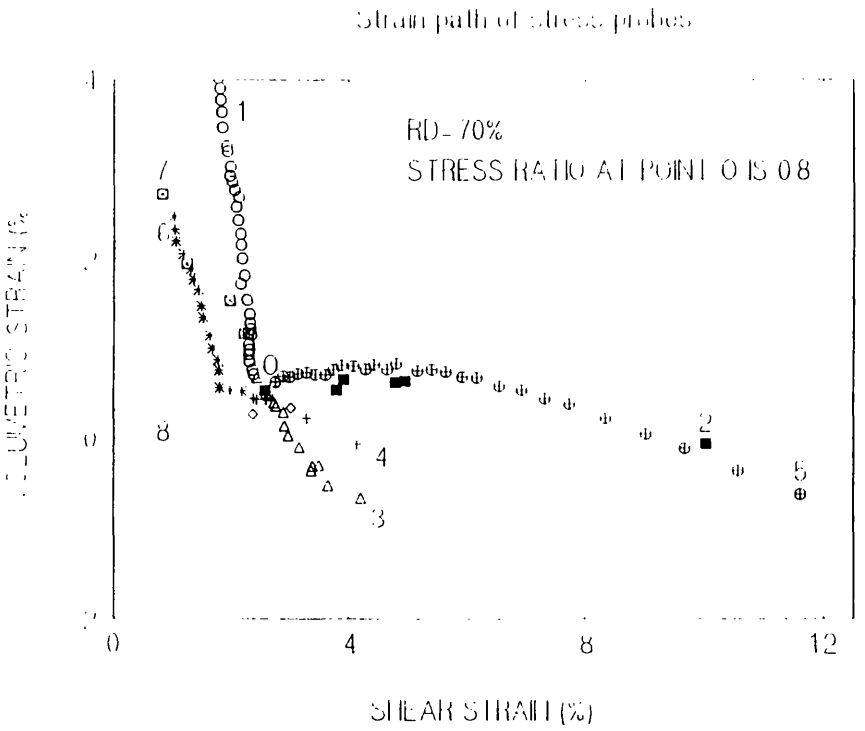
Strain path of stress probes
RD= 70%
STRESS RATIO AT POINT 0 IS 0.8
0
4
8
12
SHEAR STRAIN (%)

Fig 4.11

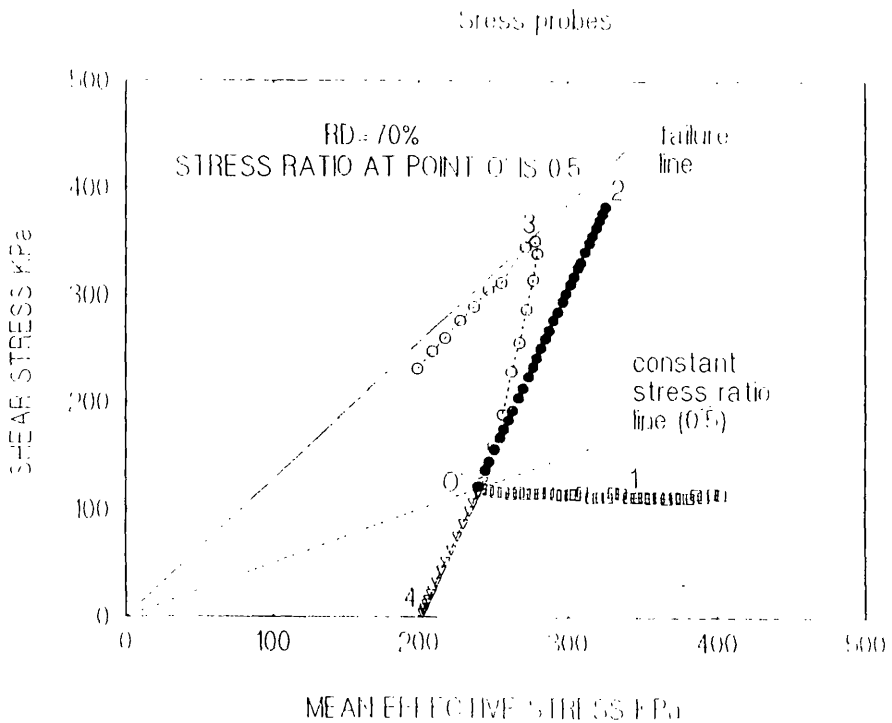
Stress probes
RD = 70%
STRESS RATIO AT POINT O IS 0.5
failure line
constant stress ratio line (0.5)
SHEAR STRESS kPa
MEAN EFFECTIVE STRESS kPa
0
100
200
300
400
500
1
2
3
4
O

Fig 4.12

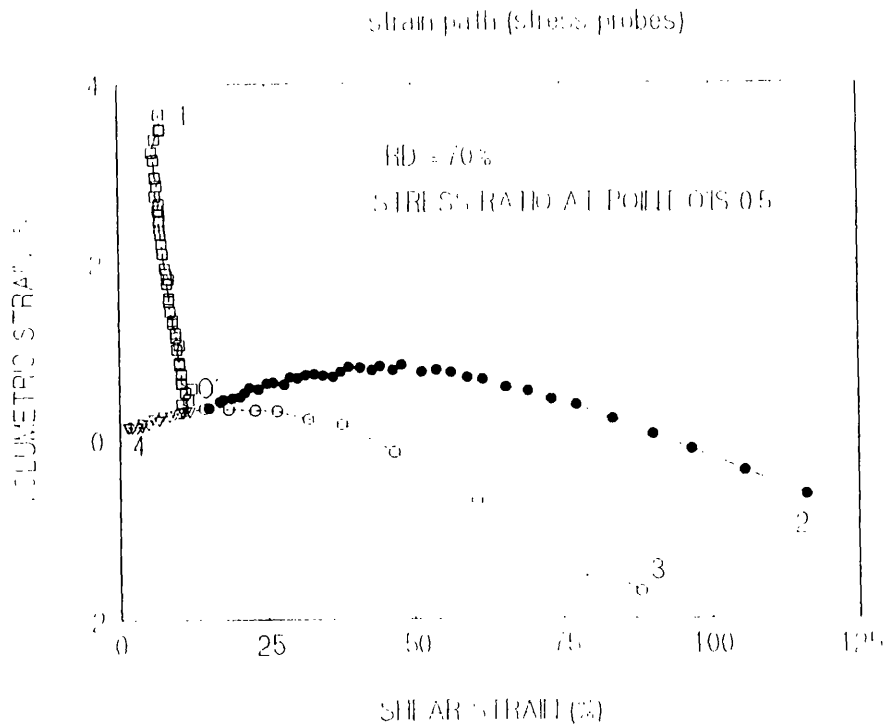
Strain path (stress probes)
RD = 70%
STRESS RATIO AT POINT OTS 0.5
0
25
50
100
SHEAR STRAIN (%)

Fig 4.13

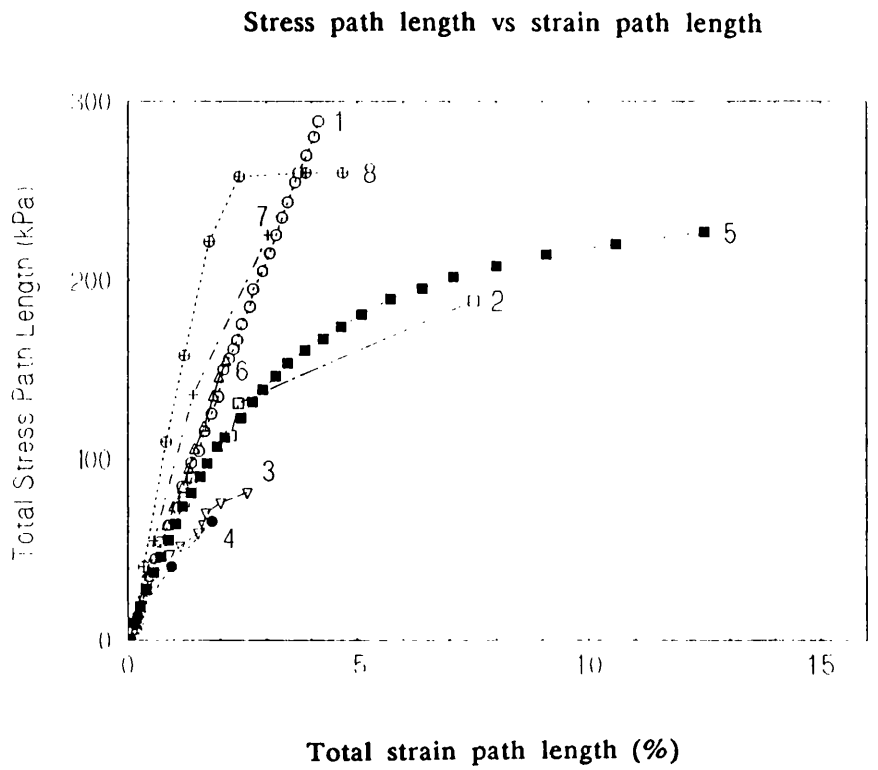
Stress path length vs strain path length
Total Stress Path Length (kPa)
300
200
100
0
0
5
10
15
1
2
3
4
5
6
7
8
Total strain path length (%)

Fig 4.14

Stress path length vs strain path length

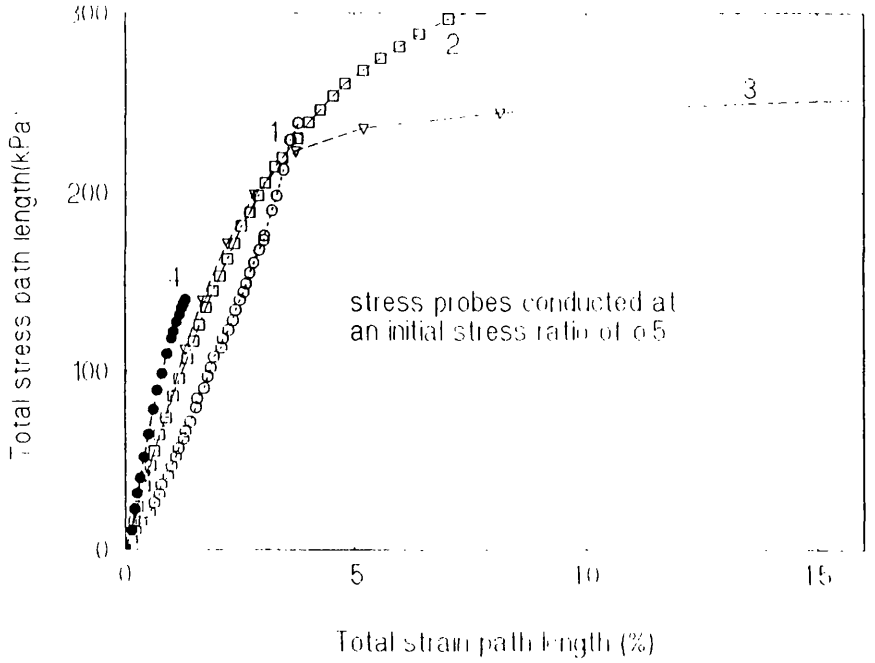

Fig 4.15

Fig 4.16

Total strain energy contour

(kJ/m³)

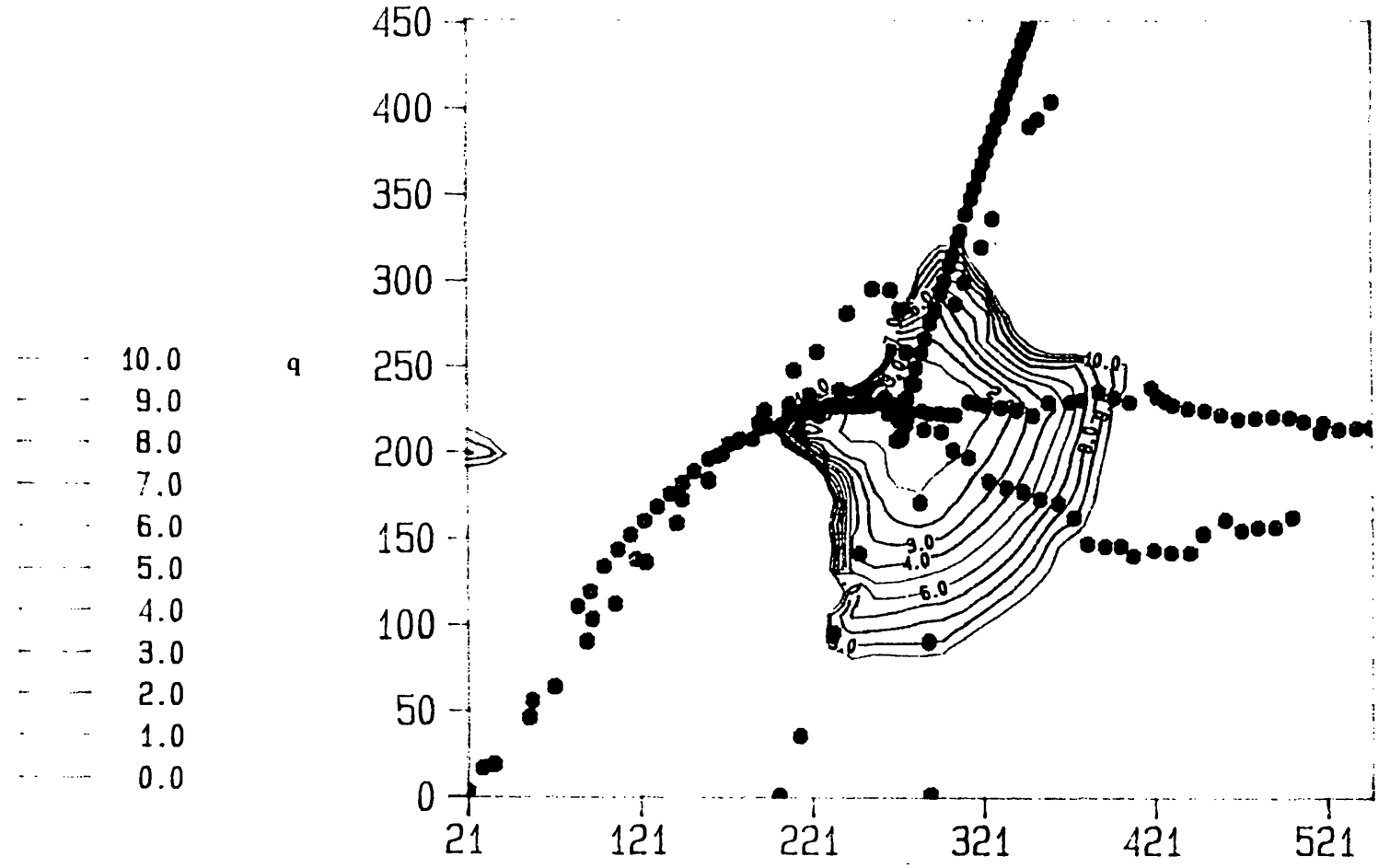

Fig 4.17

Total strain energy contours

(kJ/m^3)

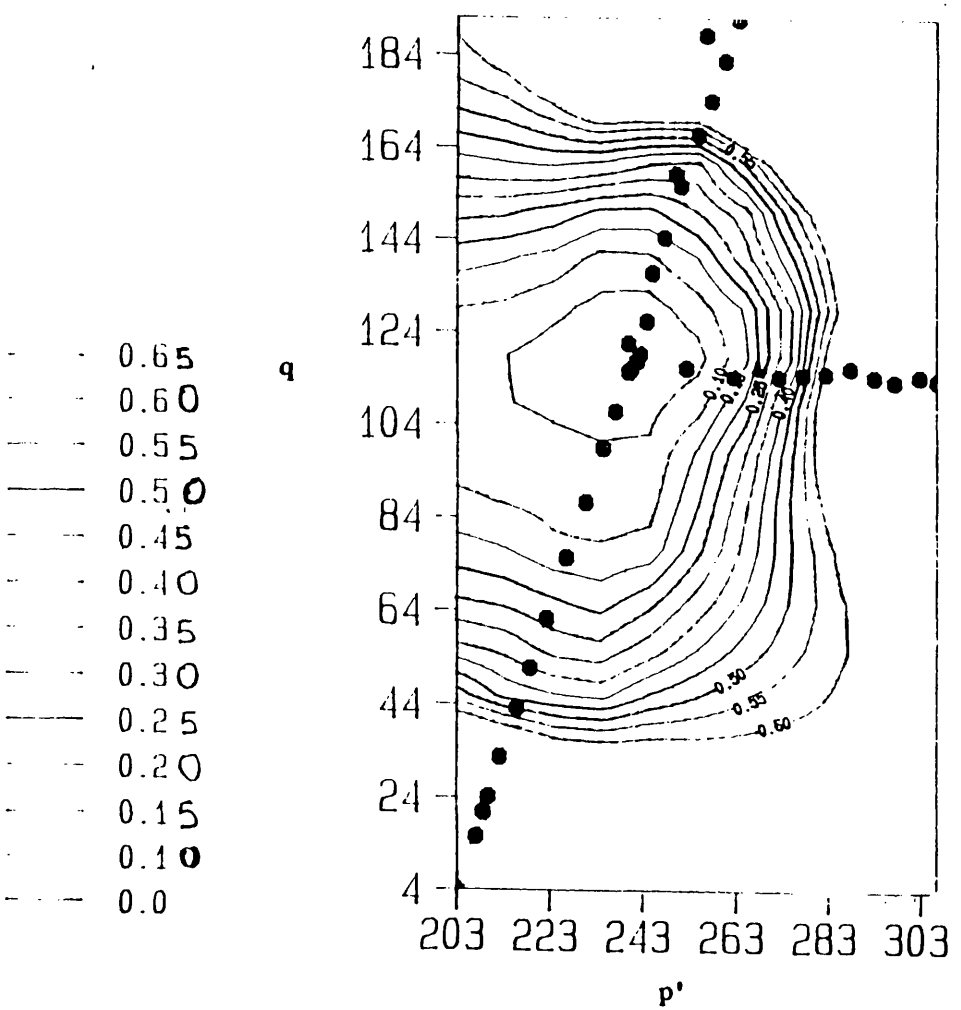

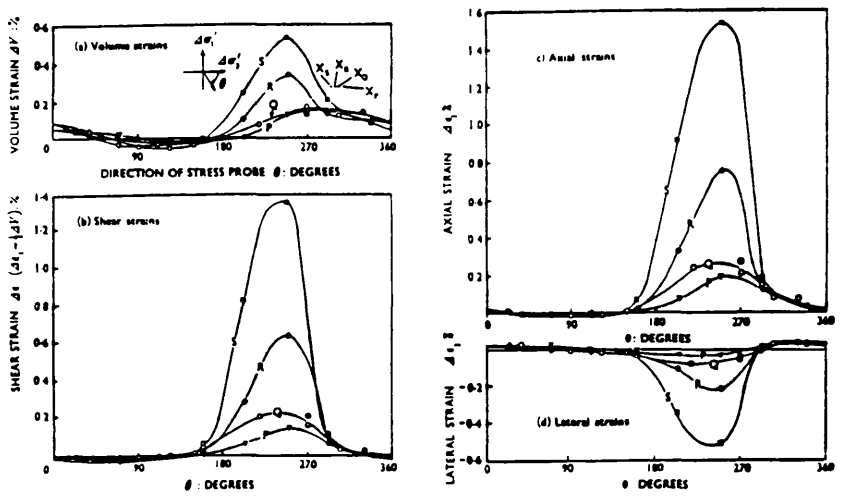

(a) (b)

Fig 4.18 (after Lewin and Burland, 1970)

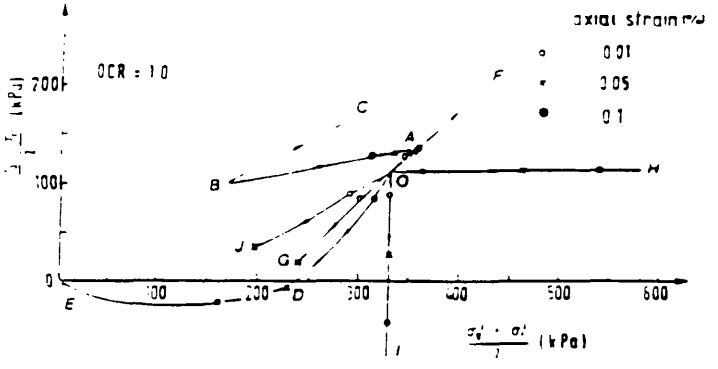

Fig 4.19 (after Burland and Georgiannou, 1990)

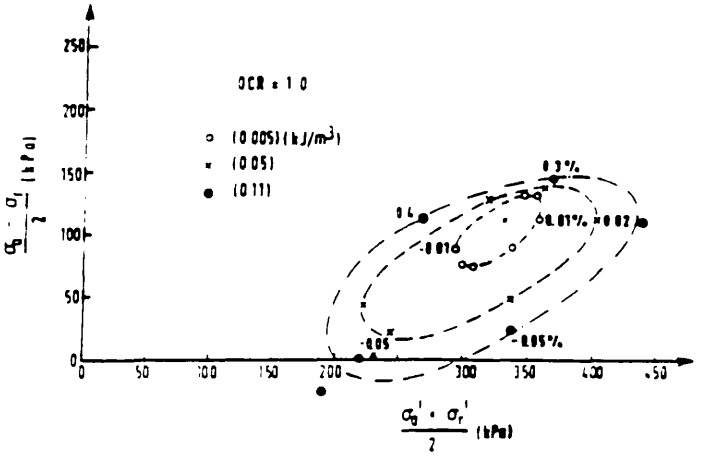

Fig 4.20 (after Burland and Georgiannou, 1990)

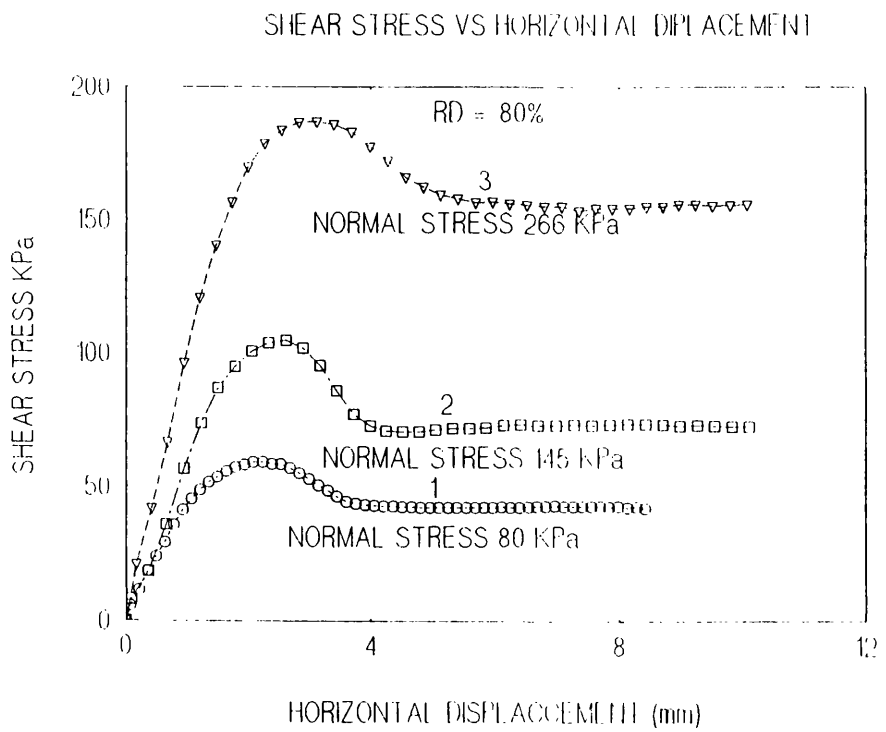
SHEAR STRESS VS HORIZONTAL DISPLACEMENT
RD = 80%
3
NORMAL STRESS 266 KPa
2
NORMAL STRESS 145 KPa
1
NORMAL STRESS 80 KPa
SHEAR STRESS KPa
200
150
100
50
0
0
4
8
12
HORIZONTAL DISPLACEMENT (mm)

Fig 4.21

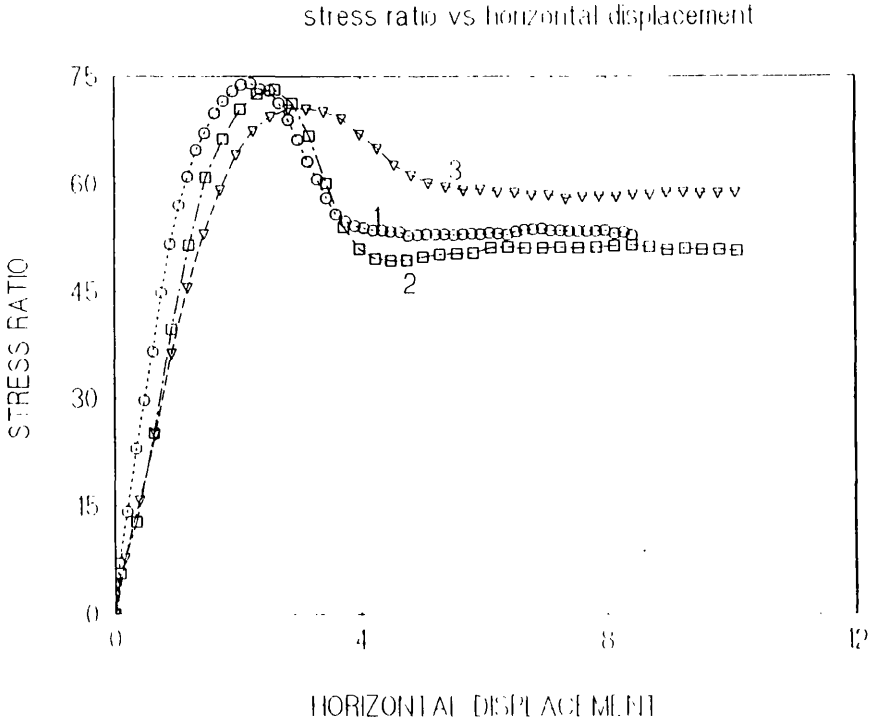
stress ratio vs horizontal displacement
75
60
45
30
15
0
STRESS RATIO
0
4
8
12
HORIZONTAL DISPLACEMENT
1
2
3

Fig 4.22

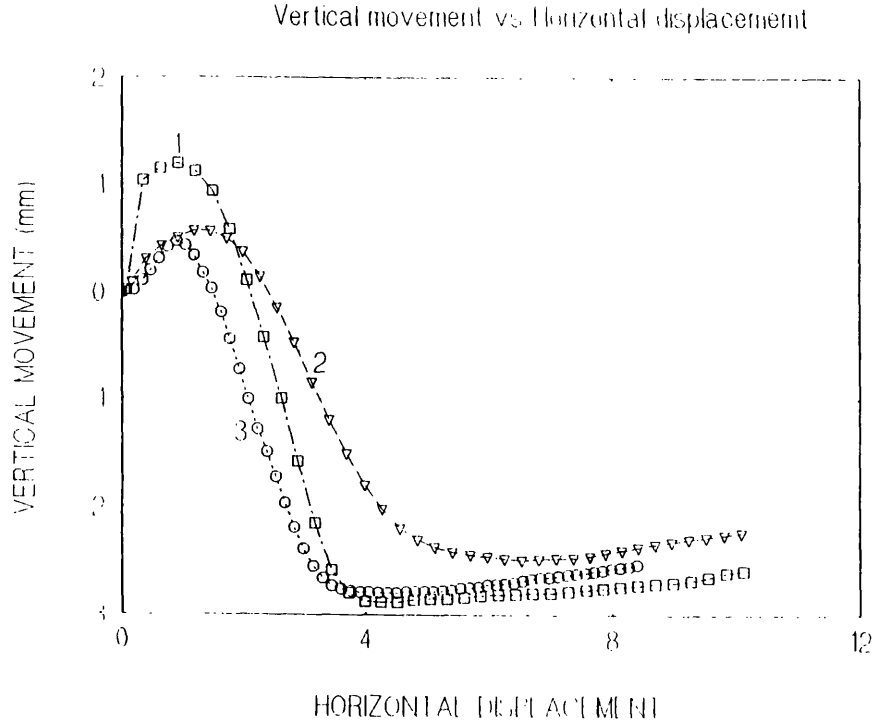
Vertical movement vs Horizontal displacement
VERTICAL MOVEMENT (mm)
1
0
1
0
4
8
12
1
2
3
HORIZONTAL DISPLACEMENT

Fig 4.23

Stress ratio and dilatancy in direct shear tests on Ottawa sand with expression ↦ ↺superimposed (× , dense; •, loose): (a) friction Q/P and dilatancy $\delta v/\delta x$; (b) $Q/P + \delta v/\delta x$ and shear displacement x (data from Taylor, 1948).

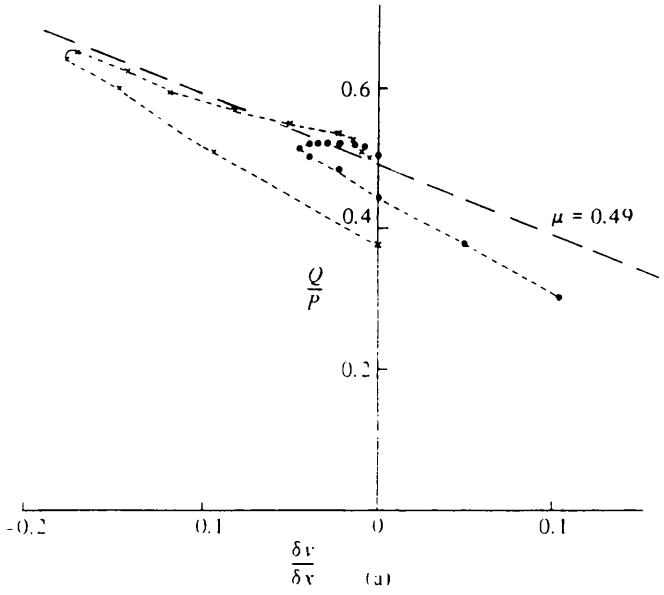

Fig 4.24

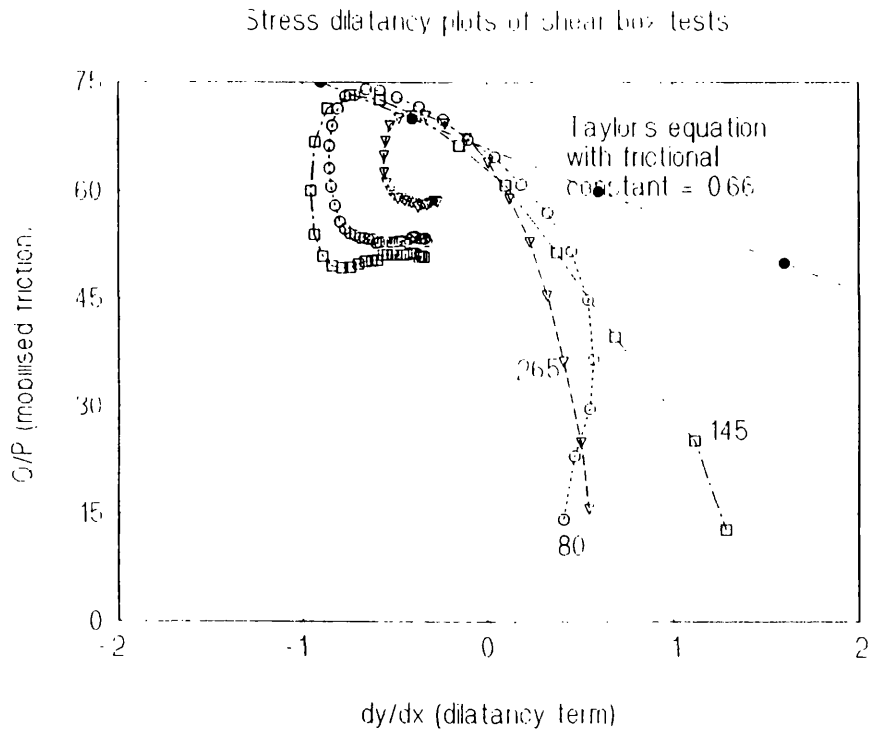
Stress dilatancy plots of shear box tests
Taylor's equation
with frictional
constant = 0.66
80
145
265
75
60
45
30
15
0
-2
-1
0
1
2
O/P (mobilised friction,
dy/dx (dilatancy term)

Fig 4.25

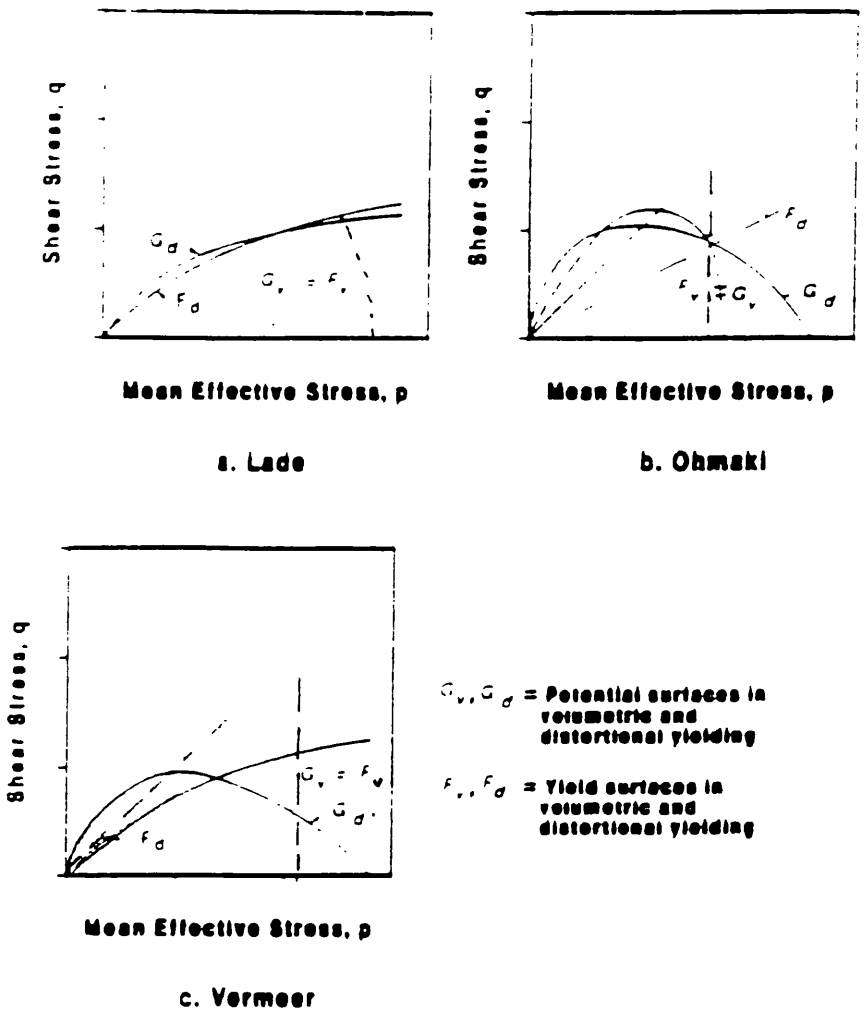

Fig 5.2 **Potential and Yield Surfaces in Selected Existing Models**

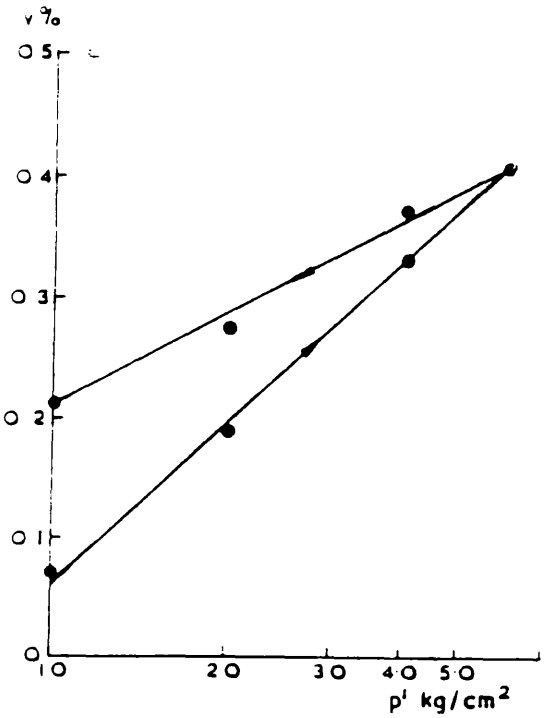

Volumetric strain *versus* mean normal stress for hydrostatic loading and unloading of sand (after Frydman, 1972)

Fig 5.3

Isotropic compression and unloading of loose and dense Fuji River sand (after Tatsuoka, 1972)

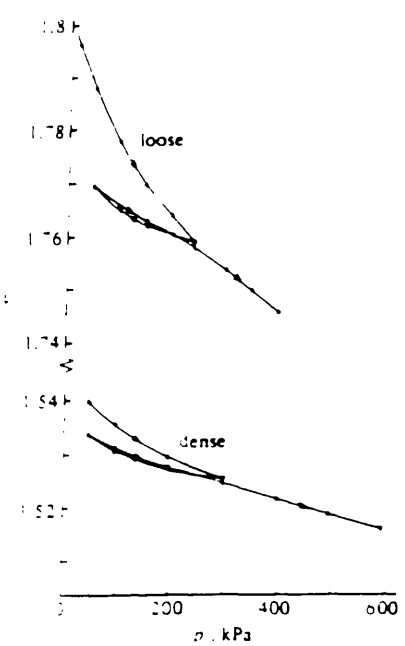

Fig 5.4

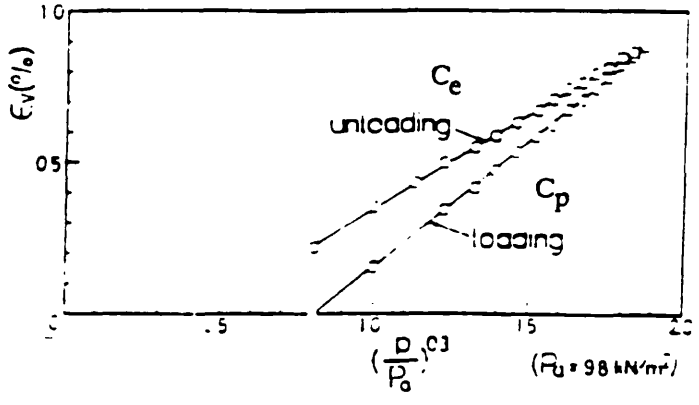

Results of loading and unloading isotropic consolidation tests

Fig 5.1 (after Nakai, 1989)

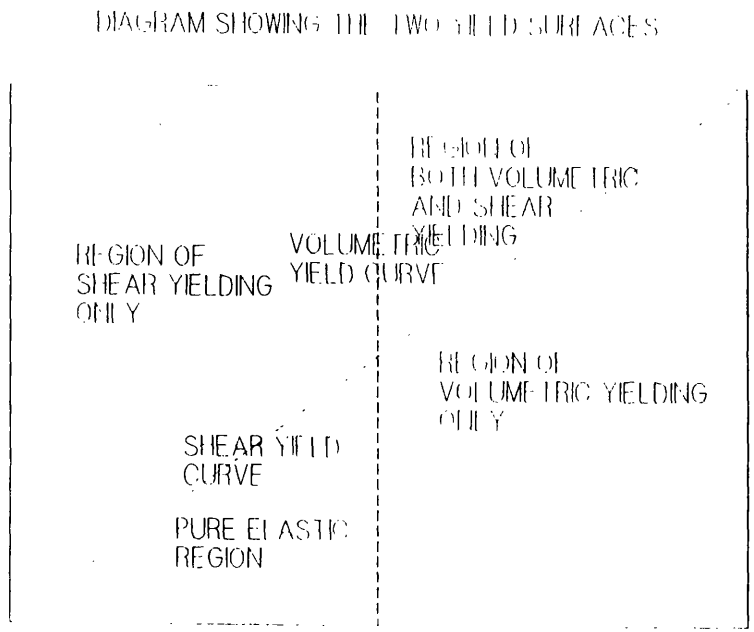
DIAGRAM SHOWING THE TWO YIELD SURFACES
REGION OF
SHEAR YIELDING
ONLY
VOLUME TRIC
YIELD CURVE
REGION OF
BOTH VOLUMETRIC
AND SHEAR
YIELDING
REGION OF
VOLUMETRIC YIELDING
ONLY
SHEAR YIELD
CURVE
PURE ELASTIC
REGION

Fig 5.5

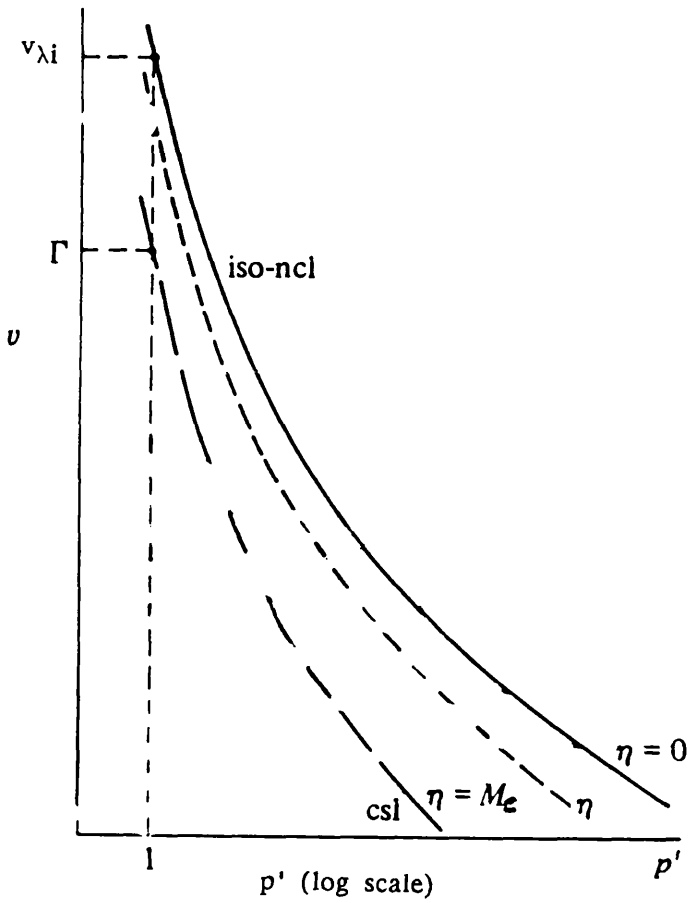

Fig 5.6 Critical state line (csl) and isotopic compression line (iso— ncl) in the compression plane p':v.

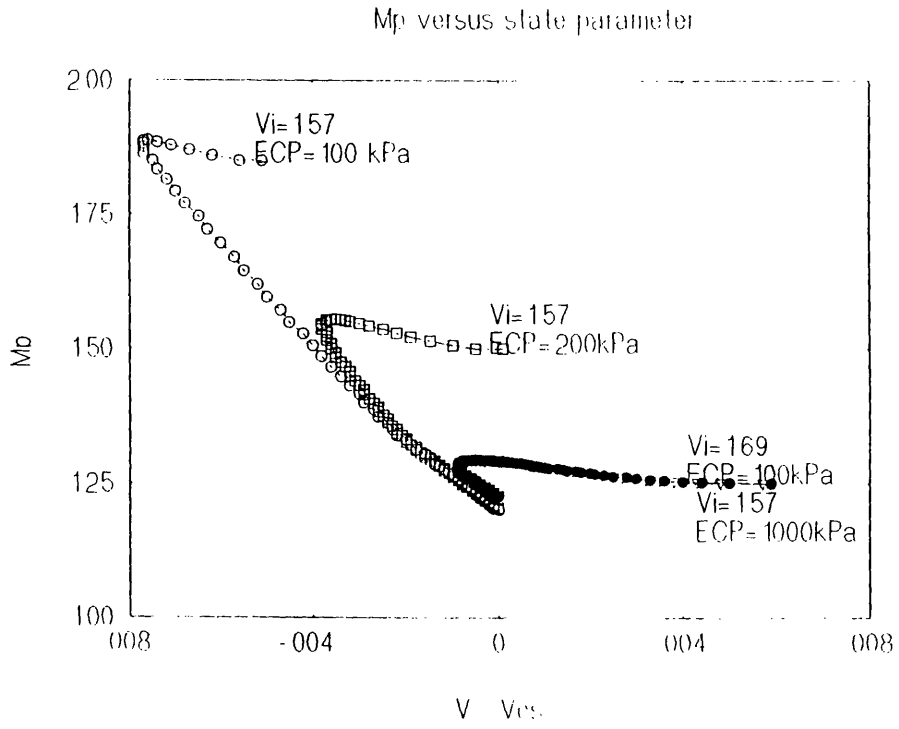
Mp versus state parameter
200
175
150
125
100
Mp
Vi=157
ECP=100 kPa
Vi=157
ECP=200kPa
Vi=169
ECP=100kPa
Vi=157
ECP=1000kPa
008
-004
0
004
008
V Ves

Fig 5.7 (a)

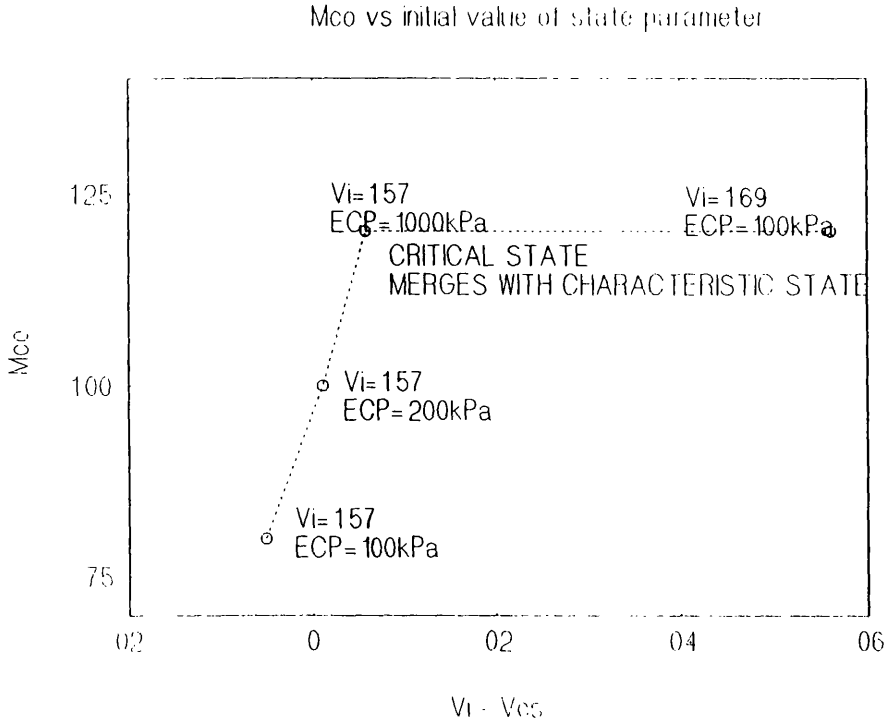
Mco vs initial value of state parameter
125
100
75
Mco
Vi=157
ECP=1000kPa
Vi=169
ECP=100kPa
CRITICAL STATE
MERGES WITH CHARACTERISTIC STATE
Vi=157
ECP=200kPa
Vi=157
ECP=100kPa
02
0
02
04
06
Vi - Ves

Fig 5.7 (b)

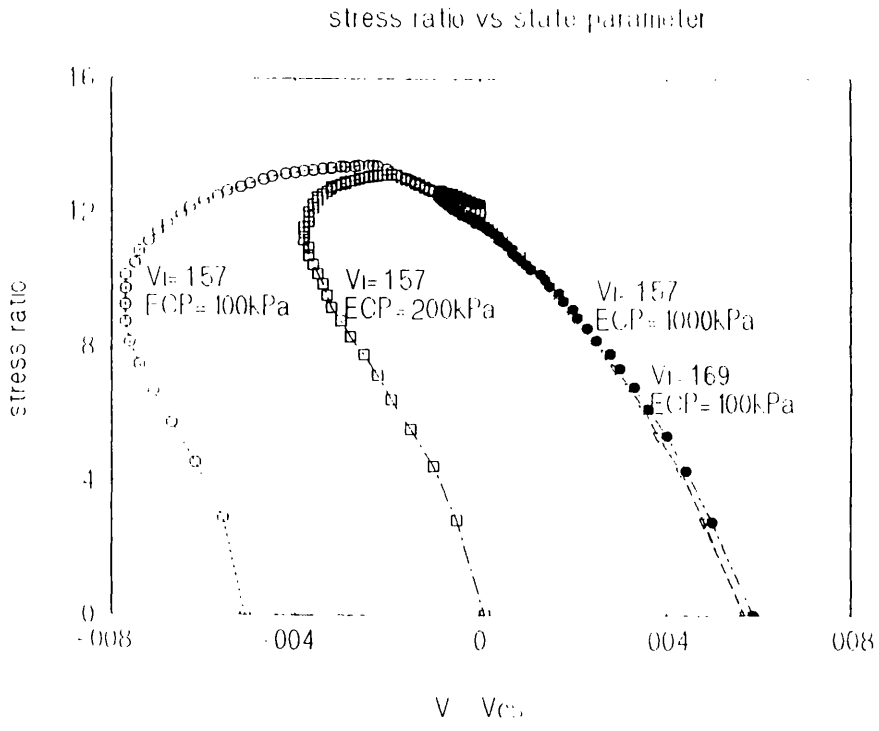
stress ratio vs state parameter
stress ratio
16
12
8
4
0
-.008
-.004
0
.004
.008
V Vcs
VI= 157
ECP= 100kPa
VI= 157
ECP= 200kPa
VI= 157
ECP= 1000kPa
VI= 169
ECP= 100kPa

Fig 5.8

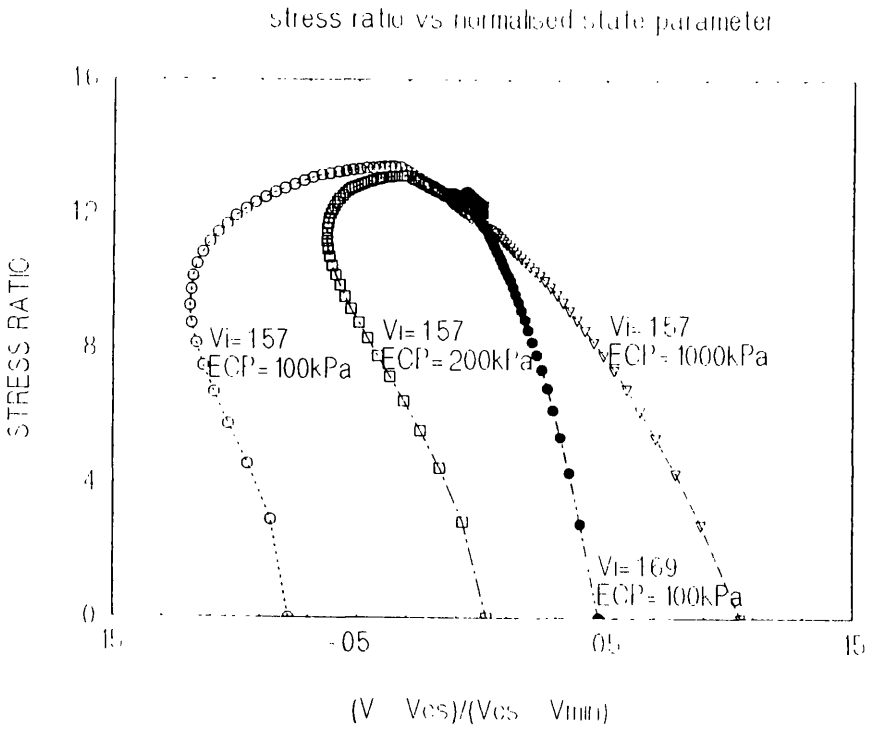
Stress ratio vs normalised state parameter
STRESS RATIO
16
12
8
4
0
-.15
-.05
.05
.15
(V Vcs)/(Vcs Vmin)
Vi= 157
ECP= 100kPa
Vi= 157
ECP= 200kPa
Vi= 157
ECP= 1000kPa
Vi= 169
ECP= 100kPa

Fig 5.9

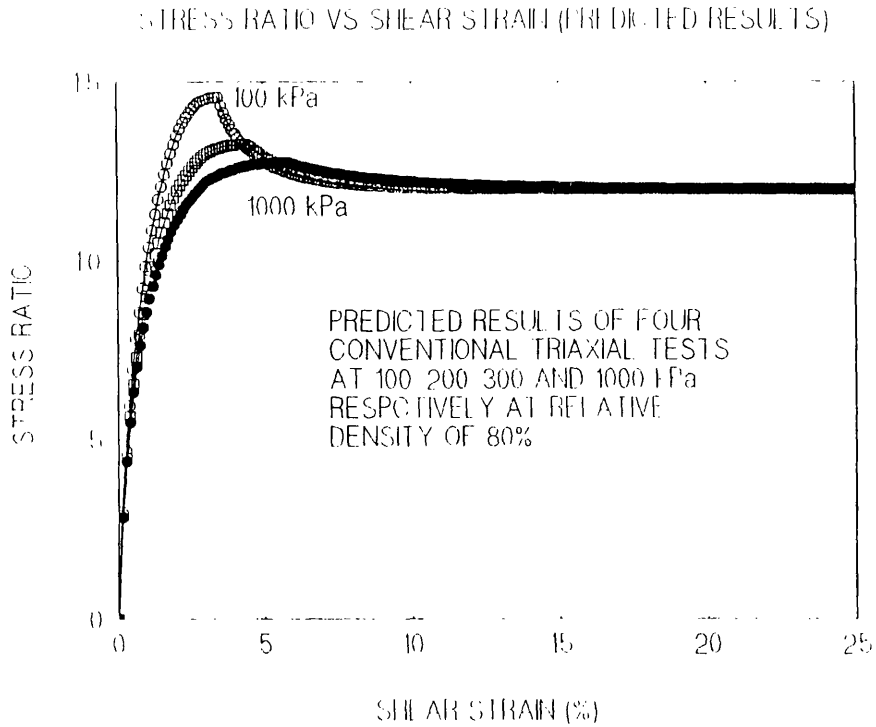
STRESS RATIO VS SHEAR STRAIN (PREDICTED RESULTS)
100 kPa
1000 kPa
PREDICTED RESULTS OF FOUR
CONVENTIONAL TRIAXIAL TESTS
AT 100 200 300 AND 1000 kPa
RESPECTIVELY AT RELATIVE
DENSITY OF 80%
STRESS RATIO
0
5
10
15
20
25
SHEAR STRAIN (%)

Fig 5.10

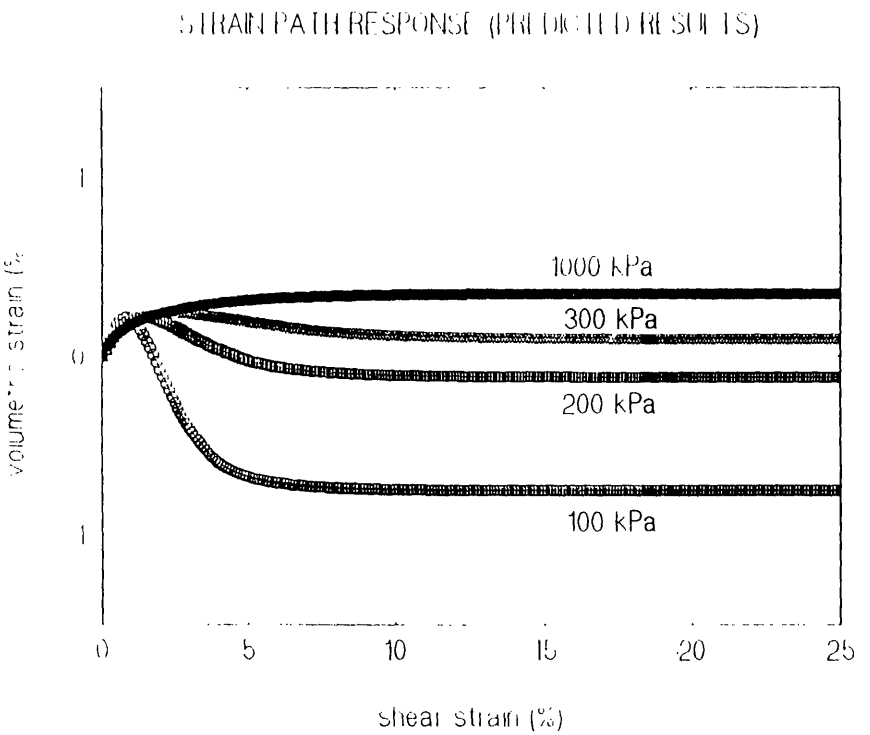
STRAIN PATH RESPONSE (PREDICTED RESULTS)
1000 kPa
300 kPa
200 kPa
100 kPa
1
0
1
0
5
10
15
20
25
shear strain (%)

Fig 5.11

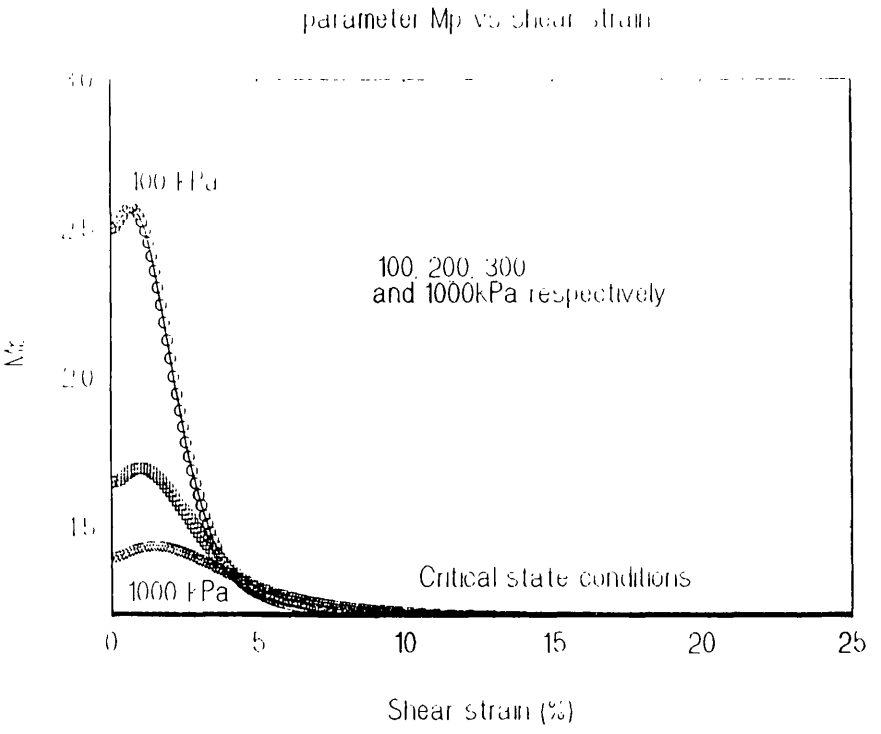
parameter Mp vs shear strain
100 kPa
100, 200, 300
and 1000kPa respectively
Critical state conditions
1000 kPa
20
15
0
5
10
15
20
25
Shear strain (%)

Fig 5.12

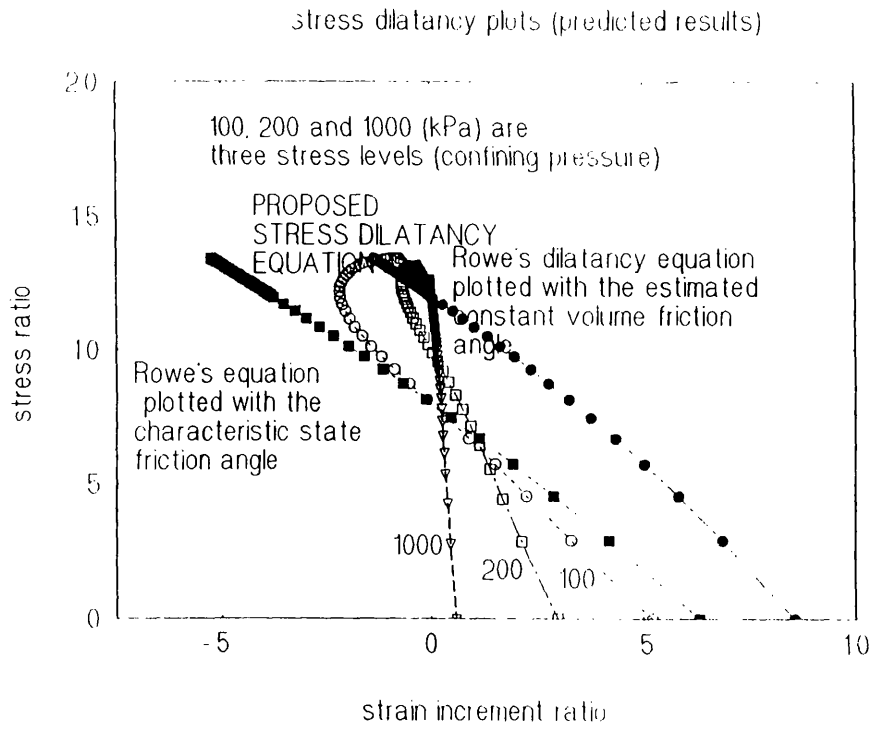
stress dilatancy plots (predicted results)
100, 200 and 1000 (kPa) are
three stress levels (confining pressure)
PROPOSED
STRESS DILATANCY
EQUATION
Rowe's dilatancy equation
plotted with the estimated
constant volume friction
angle
Rowe's equation
plotted with the
characteristic state
friction angle
1000
200
100
stress ratio
strain increment ratio
20
15
10
5
0
-5
0
5
10

Fig 5.13

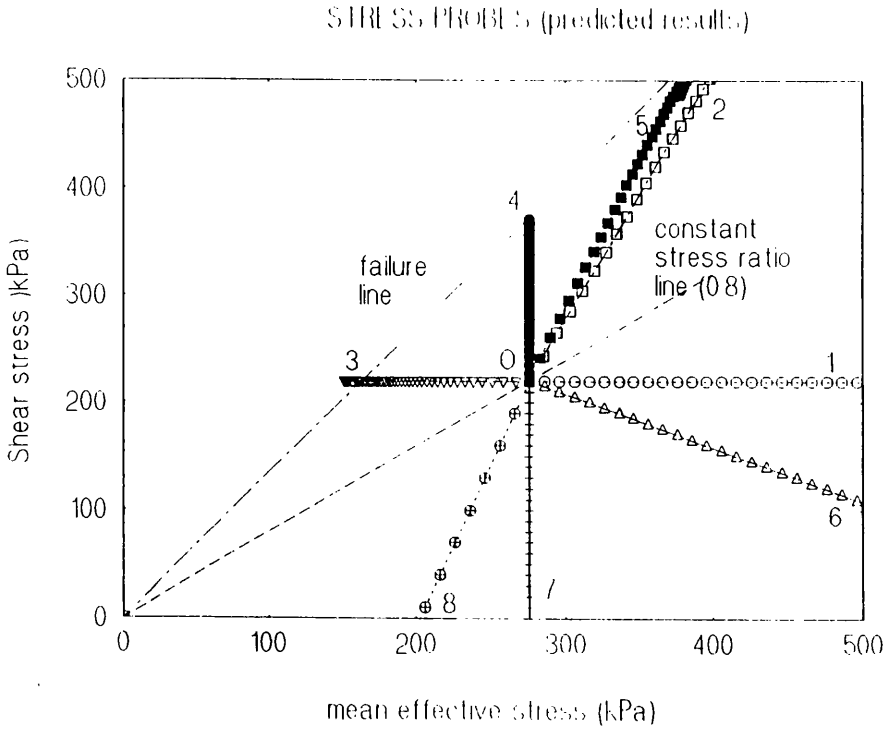
STRESS PROBES (predicted results)
Shear stress (kPa)
mean effective stress (kPa)
failure line
constant stress ratio line (0.8)
0
100
200
300
400
500
1
2
3
4
5
6
7
8

Fig 5.14

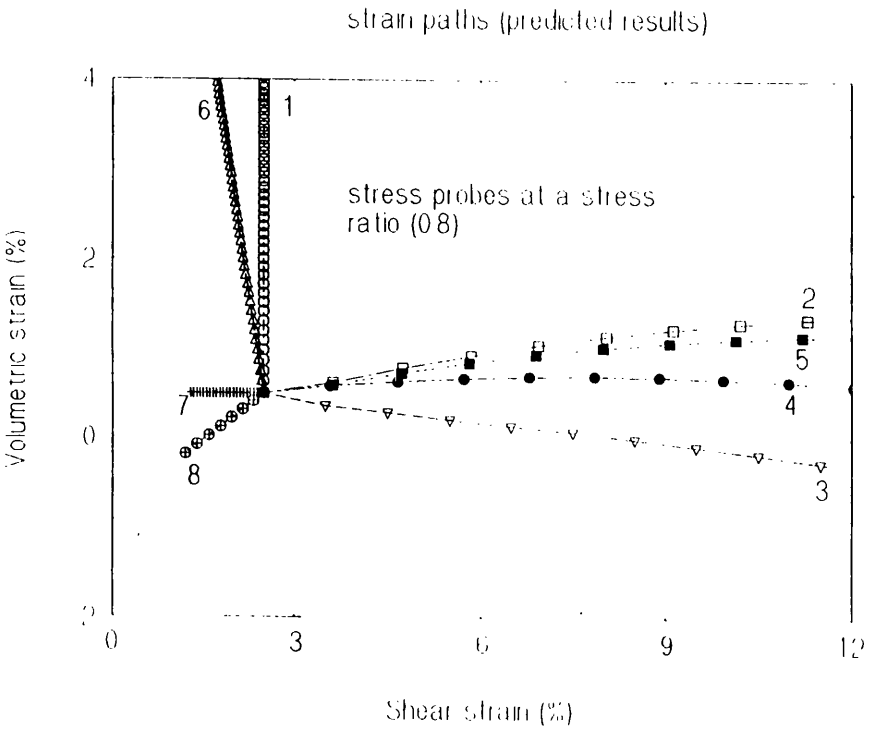
strain paths (predicted results)
stress probes at a stress ratio (0 8)
Volumetric strain (%)
Shear strain (%)
0
3
6
9
12
1
2
3
4
5
6
7
8

Fig 5.15

Stress path length vs strain path length

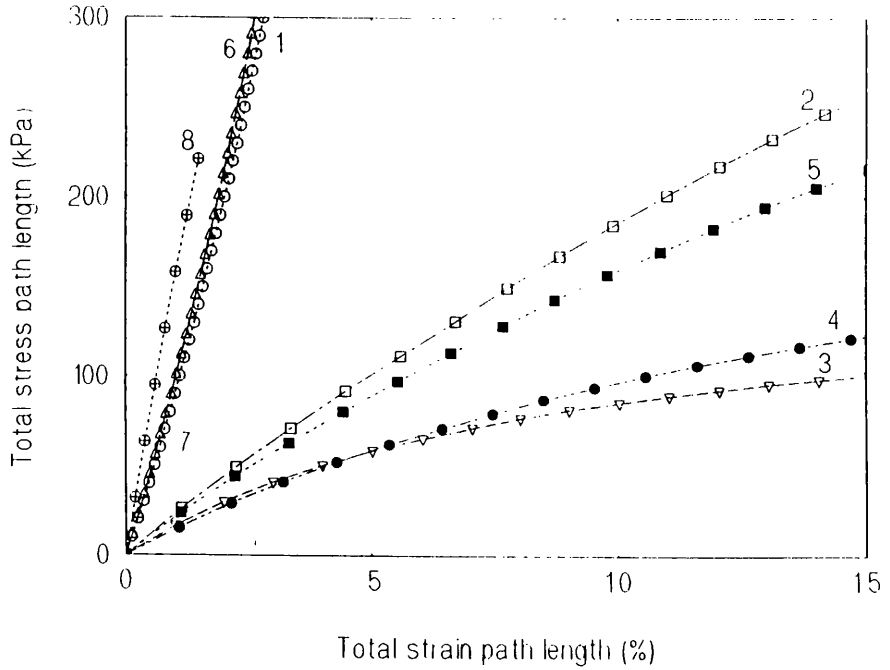

Fig 5.16

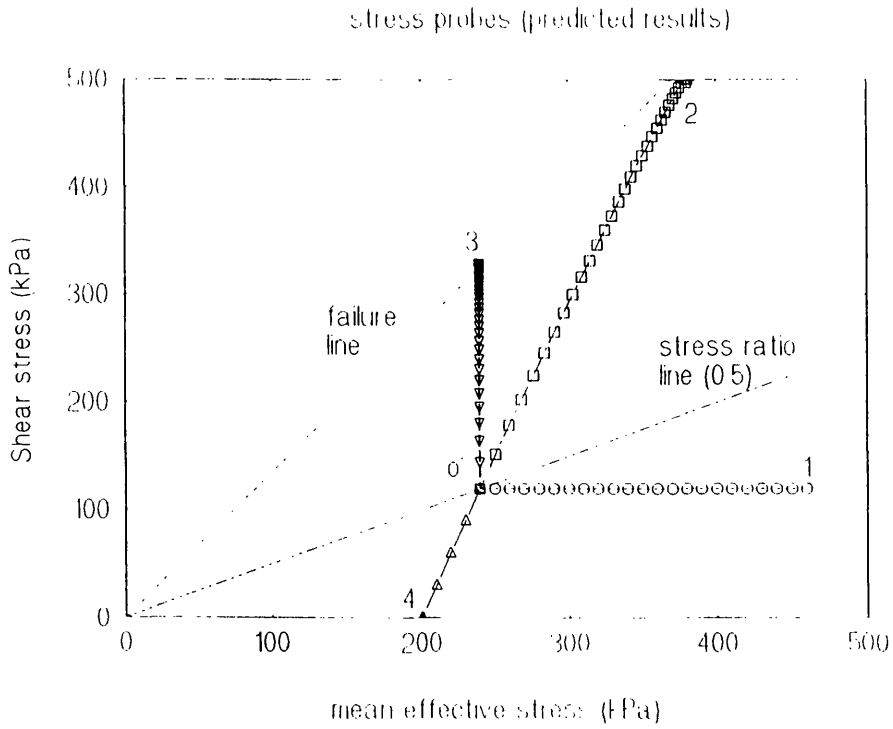
stress probes (predicted results)
Shear stress (kPa)
mean effective stress (kPa)
failure line
stress ratio line (0.5)
0
100
200
300
400
500
1
2
3
4
5

Fig 5.17

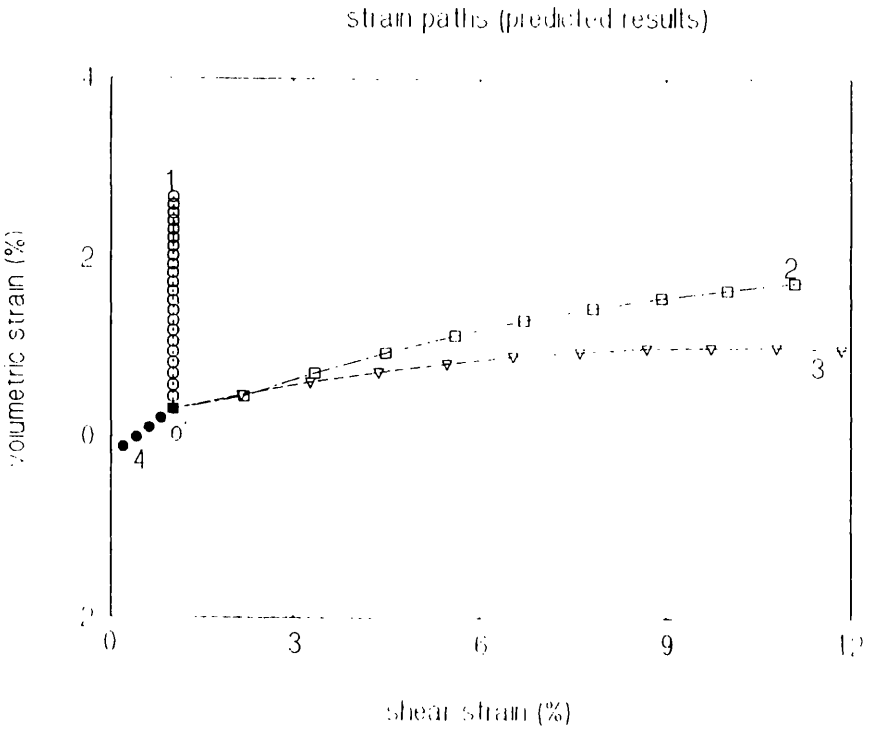
strain paths (predicted results)
volumetric strain (%)
shear strain (%)
0
3
6
9
12
1
2
3
4

Fig 5.18

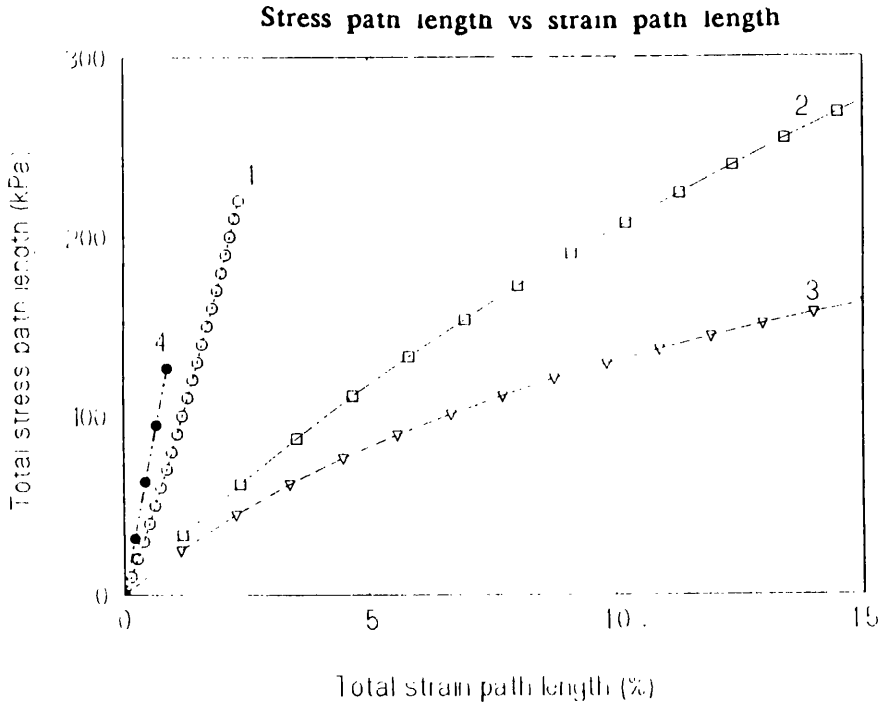
Stress path length vs strain path length
Total stress path length (kPa)
300
200
100
0
0
5
10
15
Total strain path length (%)
1
2
3
4

Fig 5.19

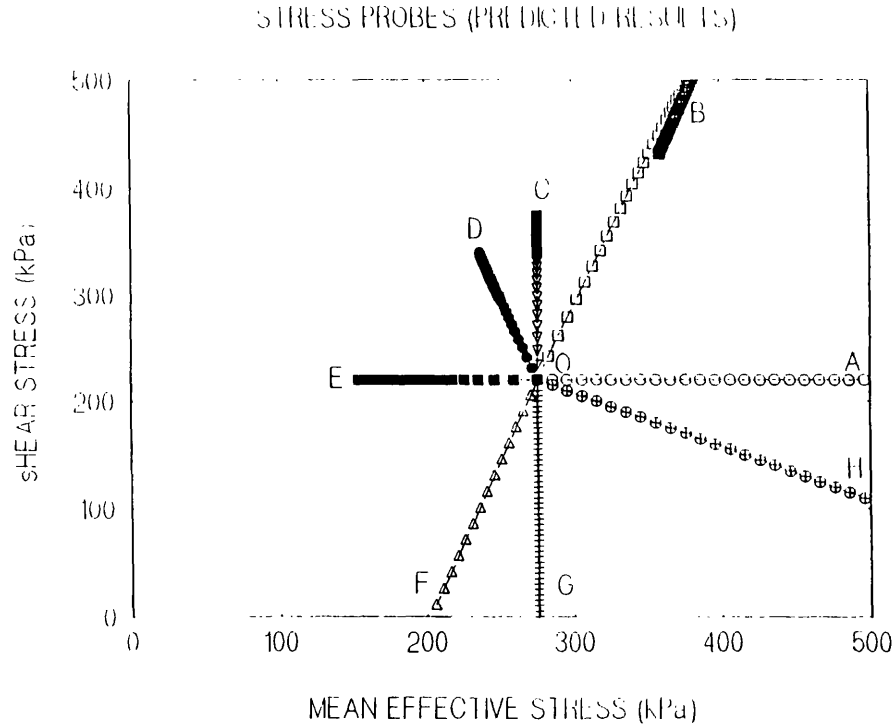
STRESS PROBES (PREDICTED RESULTS)
SHEAR STRESS (kPa)
MEAN EFFECTIVE STRESS (kPa)
0
100
200
300
400
500
A
B
C
D
E
F
G
H
O

Fig 5.20

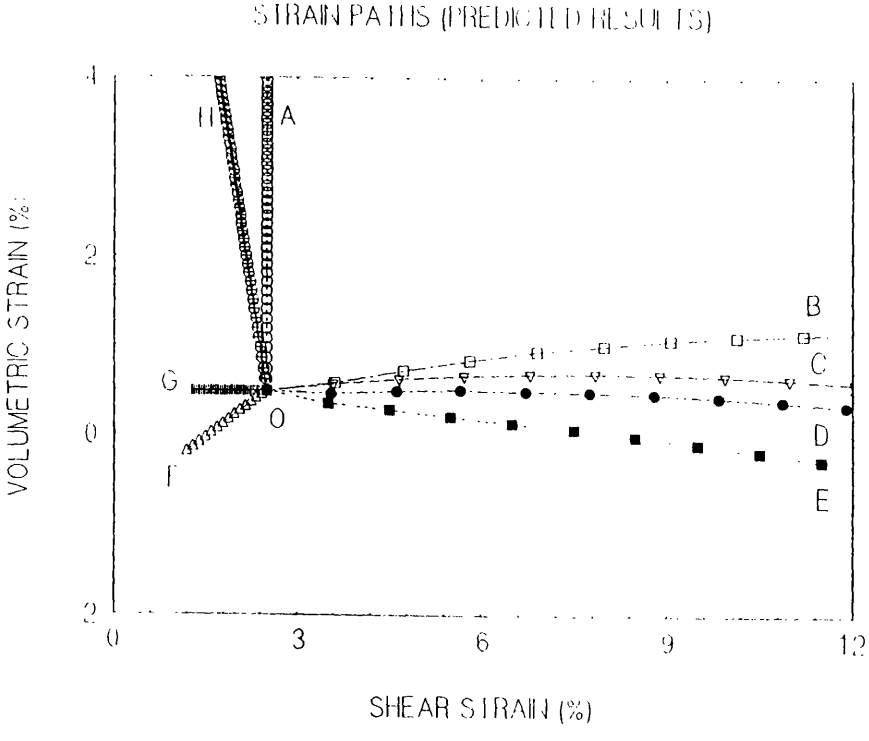
STRAIN PATHS (PREDICTED RESULTS)
VOLUMETRIC STRAIN (%)
SHEAR STRAIN (%)
A
B
C
D
E
F
G
H
O
0
3
6
9
12

Fig 5.21

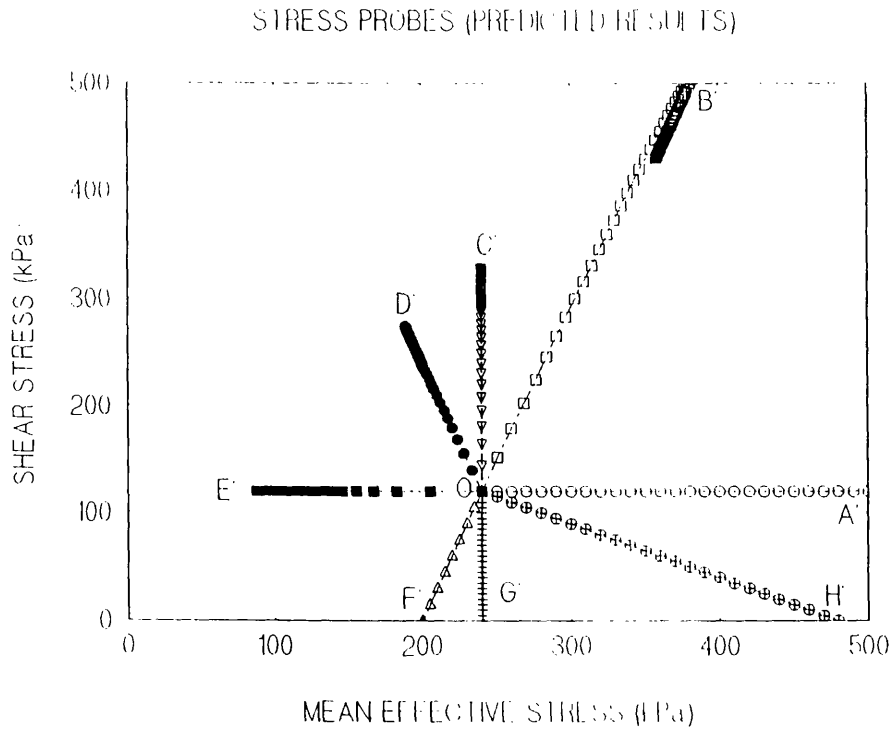
STRESS PROBES (PREDICTED RESULTS)
SHEAR STRESS (kPa)
MEAN EFFECTIVE STRESS (kPa)
0
100
200
300
400
500
A
B
C
D
E
F
G
H
O

Fig 5.22

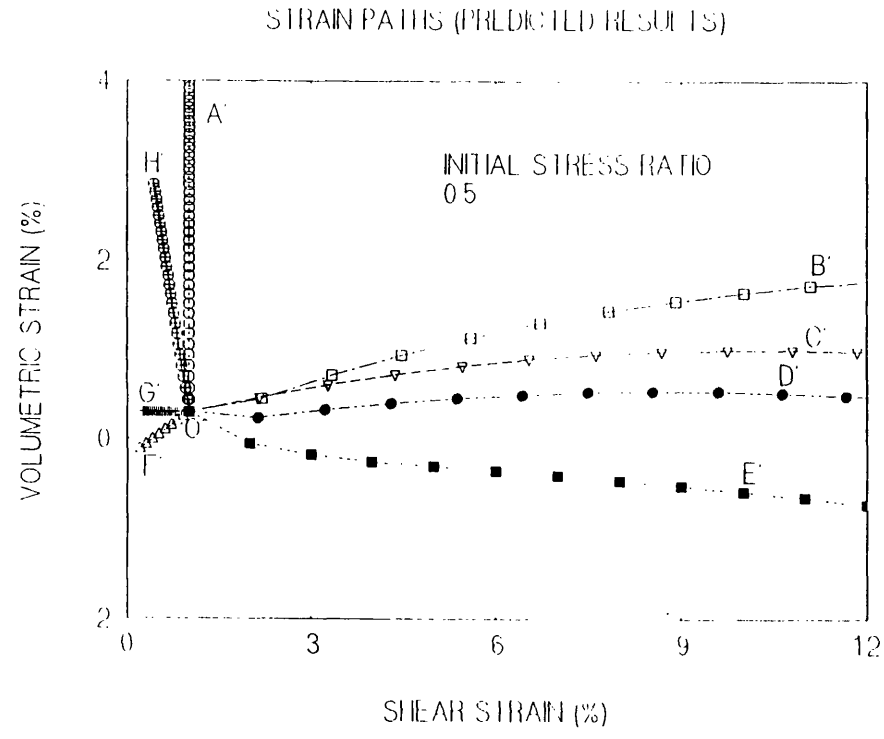
STRAIN PATHS (PREDICTED RESULTS)
INITIAL STRESS RATIO
05
A'
B'
C'
D'
E'
G'
H'
VOLUMETRIC STRAIN (%)
SHEAR STRAIN (%)
4
2
0
2
0
3
6
9
12

Fig 5.23

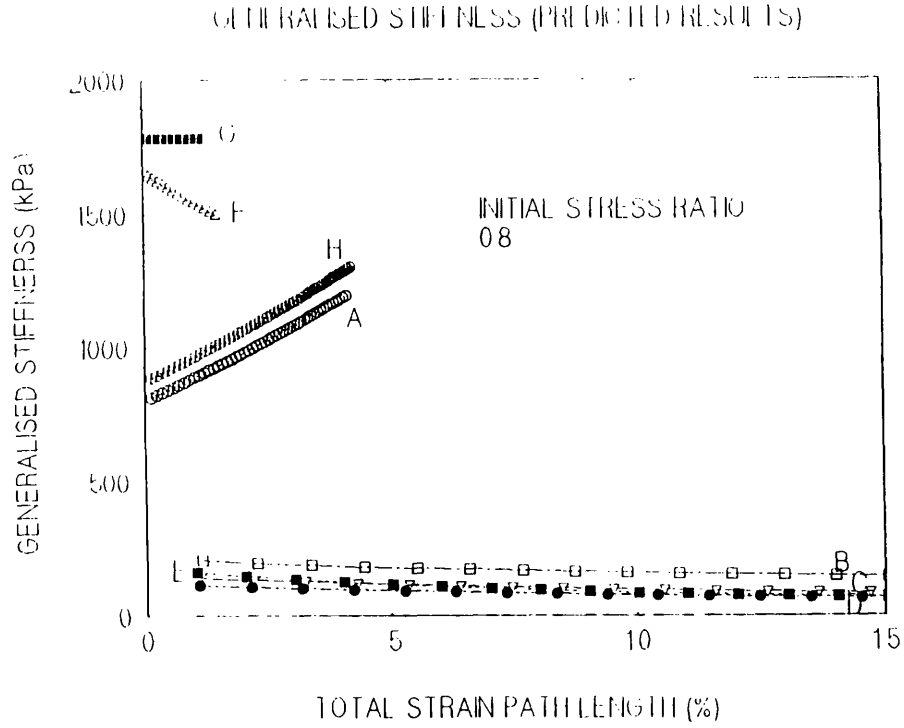
GENERALISED STIFFNESS (PREDICTED RESULTS)
GENERALISED STIFFNESS (kPa)
2000
1500
1000
500
0
INITIAL STRESS RATIO
08
G
F
H
A
B
C
D
E
0
5
10
15
TOTAL STRAIN PATH LENGTH (%)

Fig 5.24

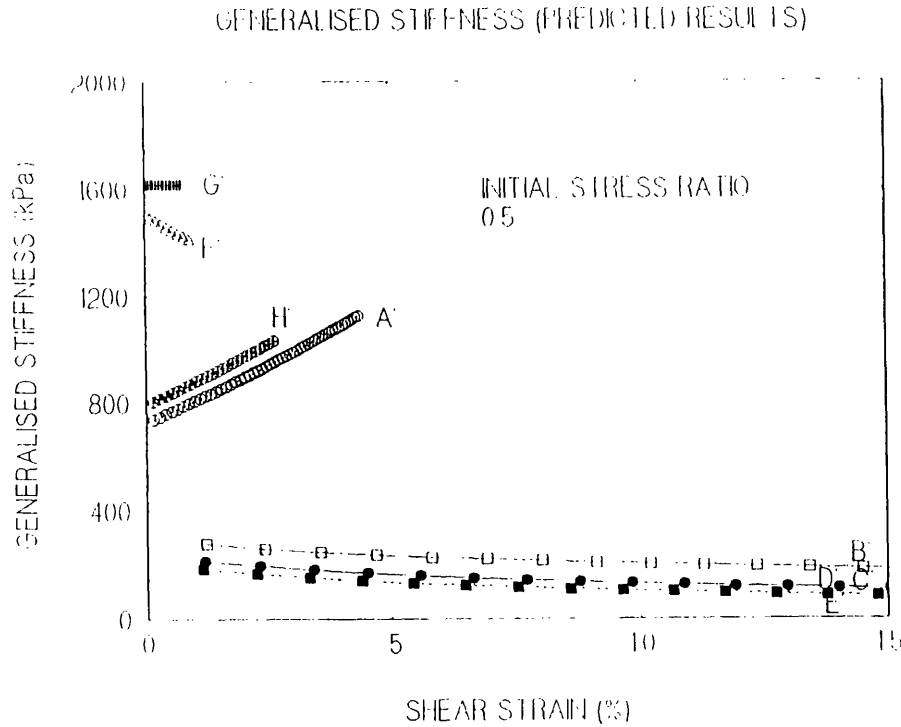
GENERALISED STIFFNESS (PREDICTED RESULTS)
GENERALISED STIFFNESS (kPa)
2000
1600
1200
800
400
0
INITIAL STRESS RATIO
0.5
G
F
H
A
B
C
D
E
0
5
10
15
SHEAR STRAIN (%)

Fig 5.25

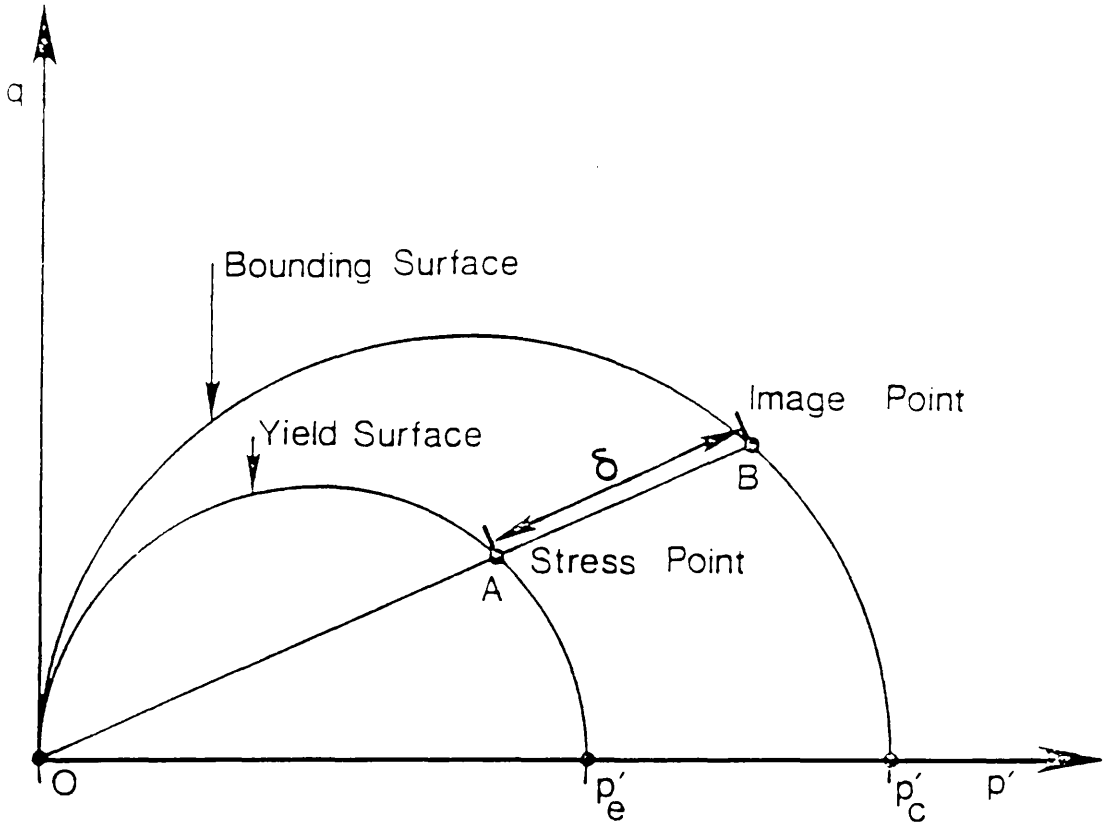

Fig 5.26

Yield and bounding surfaces for simplification of model of Dafalias and Herrmann (1980)

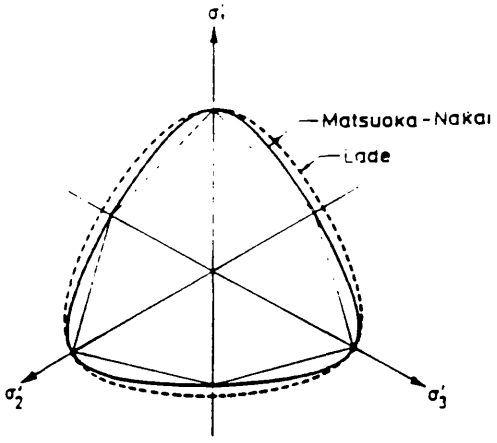

Fig 6.1 Sections of failures surfaces
in principal stress space (after Wroth and Houlsby, !985)

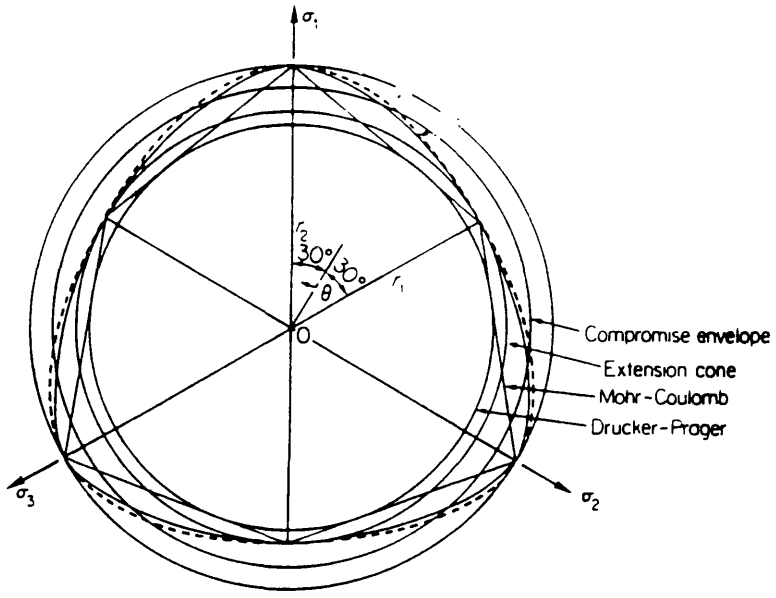

Fig 6.2 The π − plane section of Mohr − Coulomb with $\varphi = 20^0$ and various smooth approximation (after Zienkiewicz and Pande, 1977)

References

Alawaji, H., Alawi, M., Ko, H., Sture, S., Peters, J.F. and Wood, D.M. (1990) ‹perimental observations of anisotropy in some stress controlled tests on dry sand. In: elding, Damage and Failure of Anisotropic Solids, ed. Boehler, J.P. Mechanical ıgineering Publications, 251–264.

Al–Tabbaa, A. and Wood, D.M. (1989), 'An experimentally based 'buble' model for ıy', in S.Pietruszczak and G.N. Pande (eds), Numerical Models in Geomechanics JMOG III (London: Elsevier), pp.91–99.

Baldi, G., Hight, D.W. and Thomas, G.E. (1988), 'A Reevaluation of Conventional iaxial Test Methods', Advanced Triaxial Testing of Soil and Rock, ASTM STP 977, ›bert T. Donaghe, Ronald C. Chaney, and Marshall L. Silver, Eds., American Society : Testing and Materials, Philadelphia, pp. 219–263.

Banerjee, S., Davis, R.O. and Sribalaskandarajah, K. (1992), 'Simple double–hardening ›del for geomaterials', in Proc. ASCE, Journal of the Geotechnical Engineering 118(6), 9–901.

Barden, L. and Khayatt, A.J. (1966), 'Incremental strain rate ratios and strength of ıd in the triaxial test', Geotechnique, 16(4), 338–357.

Barden, L., Ismail, H. and Tong, P. (1969), 'Plane strain deformation of granular terial at low and high pressures', Geotechnique 19(4), 441–452.

Bardet, J.P., (1986), ' Modelling of sand behaviour with bounding surface plasticity', ımerical Models in Geomechanics NUMOG II, eds. Pande, G.N. and Van Impe, .F.M.Jackson & son, 79–90.

Been, K. and Jefferies, M.G. (1985), 'A state parameter for sands', Geotechnique (2), 99–112.

Been, K. and Jefferies, M.G. (1986), 'Discussion: A state parameter for sands', ɔotechnique 36(1), 127–32.

Bishop, A.W. and Henkel, D.J. (1962), 'The measurement of soil properties in the axial test (London: William Arnold))'.

Bishop, A.W. and Wesley, L.D. (1975), 'A hydraulic triaxial apparatus for controlled ·ess path testing', Geotechnique 25(4), 657–670.

Black, D.K. and Lee, K.L. (1973), 'Saturating laboratory samples by back pressure', in oc. ASCE, Journal of the Soil Mechanics and Foundations Division, 99, SM1, 75–93.

Burland, J.B. (1989), 'Ninth Laurits Bjerrum Memorial Lecture: Small is beautiful– the .ffness of soils at small strains', Canadian Geotechnical Journal 26(4), 499–516.

Burland, J.B. and Georgiannou, V.N. (1991), 'Small strain stiffness under generalised ress changes', Proc. Xth ECSMFE, Florence, In Press.

Chaney, R.C. and Mulilis, J.P. (1978), 'Suggested Method for Soil Specimen Remoulding r Wet Raining', Geotechnical Testing Journal, ASTM, vol. 1, No. 2, pp. 107–108.

Dafalias, Y.F. and Herrmann, L.R. (1980), 'A Bounding Surface Soil Plasticity Model', roc.Int.Symp. on Soils under Cyclic and Transient Loading, Swansea, 7–11 Jan., 35–345.

– Drescher, A. and Vardoulakis, I. (1982), 'Geometric softening in triaxial test on ranular material', Geotechnique (32), 291–304.

Drucker, D.C., Gibson, R.E. and Henkel, D.J. (1957), 'Soil mechanics and 'ork–hardening theories of plasticity', Trans. ASCE (122), 338–346.

Duncan, J.M. and Chang, C.Y. (1970), 'Non linear analysis of stress and strain in ɔils', Proc. ASCE J. Soil Mech. Found. Engg, (96), SM5, 1629–1653.

El–Sohby, M.A. (1969), 'Deformation of sands under constant stress ratios', In Proc. th Int.Conf.on Soil Mechs and Foundation Eng., Mexico (Mexico City: Sociedad Mexicana e Mecanica de Suelos), vol. 1, pp. 111–119.

Faruque, M.O. and Zaman, M.M. (1991), 'On the concept of characteristic states of ohesionless soil and constitutive modeling', Soils and Foundations 31(2), 164–174.

Frydman, S., (1972), 'An inquiry into the stress strain behaviour of particulate media', 'hesis for the degree of Doctor of Science in Technology, Haifa.

Goldscheider, M. (1975), 'Dilatanzverhalten von sand bei geknickten Verformungswegen', Mechanics. Research. Communications, 2, pp. 143–148.

Goldscheider, M. (1984), 'True triaxial tests on dense sand', in Proc. Int Workshop on Constitutive Behaviour of soils, Grenoble, sept. 6–8 1982, Rotterdam: Balkema.

- Goto, S. and Tatsuoka, F. (1988), 'Effects of end conditions on triaxial compressive strength for cohesionless soil', Advanced Triaxial Testing of Soil and Rock, ASTM STP 977, Robert T. Donaghe, Ronald C.Chaney, and Marchall L.Silver, Eds., American Society for Testing and Materials, Philadelphia, pp.692–705.

- Graham, J. and Houlsby, G.T. (1983), 'Anisotropic elasticity of a natural clay', Geotechnique (33), 165–180.

- Habib, P., and Luong, M.P. (1978), 'Sols pulverulents sous chargement cyclique', Materiaux et Structures Sous Chargement Cyclique, Association Amicale des Ingenieurs Anciens Eleves de l'Ecole Nationale des Ponts et Chaussees (Palaiseau, 28–29 Sept), 49–79.

- Head, K.H. (1982), 'Manual of Soil Laboratory Testing', vol. 2, Pentech Press (London: Plymouth).

- Head, K.H. (1984), 'Manual of Soil Laboratory Testing', vol. 1, Pentech Press (London: Plymouth).

- Head, K.H. (1986), 'Manual of Soil Laboratory Testing', vol. 3, Pentech Press London).

- Hettler, A. and Vardoulakis, I. (1984), 'Behaviour of dry sand tested in a large triaxial pparatus', Geotechnique 34(2), 183–198.

Hird, C.C., and Hassona, F. (1986), 'Discussion: A state parameter for sands', eotechnique 36(1), 124–7.

Horne, M.R. (1969), 'The behaviour of an assembly of rotund, rigid, cohesionless rticles, Part III', Proceedings of the Royal Society of London, A310, 21–34.

Houlsby, G.T. (1981), 'A study of plasticity theory and its applicability to soils', Phd
hesis, University of Cambridge.

Ishihara, K., Tatsuoka, F., and Yasuda, S. (1975), 'Undrained deformation and
uefaction of sand under cyclic stresses', Soils and Foundations 15(1), 29–44

Janbu, N. (1963), 'Soil compressibility as determined by oedometer and triaxial tests',
oc. 3rd Eur.Conf.Soil Mech.Found.Engg, 19–24, Wiesbaden.

Jardine, R.J. (1992), 'Some observations on the kinematic nature of soil stiffness', Soils
d Foundations 32(2), 111–124.

Khatrush, S.A. (1987), 'The yielding of a fine sand in triaxial stress space', PhD
hesis, University of Surrey.

Kirkpatrick, W.M. (1961), Discussion, Proceedings of the Fifth International Conference
Soil Mechanics and Foundation Engineering, vol. 3, pp. 131–133.

Koiter, W.T. (1953), 'Stress–strain relations, uniqueness, and variational theorems for
stic–plastic materials with a singular yield surface', Journal of Applied Mathematics
(3), 350.

Kolbuszewski, J.J. (1948a), 'An experimental study of the maximum and minimum
rosities of sands', in Proc. 2nd Int. Conf. on soil Mechs and Foundation Eng.,
tterdam 1, 158–65.

Kolbuszewski, J.J. (1948b), 'General investigation of the fundamental factors controlling
se packing of sands', Proc. 2nd Int. Conf. on soil Mechs and Foundation Eng,
tterdam 7, 47–49.

- Kondner, R.L. and Zelasko, J.S. (1963), 'Void ratio effects on the hyperbolic stress–strain response of sand', Laboratory Shear Testing of Soils, ASTM Standard Technical Publication No. 361, 250–257, Ottawa.

- Ladd, R.S. (1978), 'Preparing Test specimens Using Undercompaction', Geotechnical Testing Journal, ASTM, vol. 1, No. 1, pp. 16–23.

- Lade, P.V. (1972), 'The stress–strain and strength characteristics of cohesionless soils', PhD Thesis, University of Cambridge.

- Lade, P.V. (1977), 'Elasto–plastic stress–strain theory for cohesionless soil with curved yield surfaces', Int.J.Solids and Structures, 13, 1019–1035.

- Lee, K.L. and Seed, H.B. (1967), 'Drained strength characteristics of sands', in Proc. ASCE, Journal of the Soil Mechanics and Foundations Division, (93), SM6, 117–41.

- Lewin, P.I. and Burland, J.B (1970), 'Stress–Probe Experiments On Saturated Normally Consolidated Clay', Geotechnique 20(1), 38–56.

- Luong, M.P. (1979), 'Les phenomenes cycliques dans les sables', Journee de Rheologie: Cycles dans les sols–rupture–instabilites. (Vaulx–en–Velin: Ecole Nationale des Travaux Publics de L'Etat), Publication 2.

- Matsuoka, H. and Nakai, T. (1974), 'Stress–deformation and strength characteristics of soil under three different principal stresses', Proc. JSFE, No.232, 59–70.

- Miura, N., Murata, H. and Yasufuku, N. (1984), 'Stress–strain characteristics of sand in particle crushing region', Soils and Foundations 24(1), 77–89.

Miura, N. and Yamamoto, N. (1982a), 'On the yield curve of sand in particle crushing gions', Proc. JSCE, No. 326, 83–90.

Miura, S. and Toki, S. (1982b), 'A sample preparation method and its effect on static nd cyclic deformation–strength properties of sand', Soils and Foundations 22(1), 61–77.

Mulilis, J.P., Seed, H.B., Chan, C.K., Mitchell, J.K., and Arulanandan, K. (1977), Effect of sample preparation on sand liquefaction', Proc. ASCE., Journal of the eotechnical Engineering Division 103(GT2), 91–108.

Nakai, T. (1989), 'An Isotropic Hardening Elastoplastic Model For Sand Considering he Stress Path Dependency in Three–Dimensional Stresses', Soils and Foundations 29(1), 9–137.

Negussey, D. and Vaid, Y.P (1990), 'Stress dilatancy of sand at small stress ratio', Soils nd Foundations 30(1), 155–156.

Negussey, D., Wijewickreme, W.K.D. and Vaid, Y.P. (1987), 'Constant–friction angle granular materials', Canadian Geotechnical Journal 25(1), 50–55.

Nova, R. and Wood, D.M., (1979), 'A constitutive model for sand in triaxial mpression', International Journal For Numerical and Analytical Methods in eomechanics, vol. 3, 255–278.

Ohmaki, S. (1979), 'A mechanical model for the stress–strain behaviour of normally nsolidated cohesive soils', Soils and Foundations 3(19), 29–44.

Poorooshasb, H.B., Holubec, I., and Sherbourne, A.N. (1966), 'Yielding and flow of nd in triaxial compression: PartI', Canadian Geotechnical Journal 3(4), 179–90.

- Poorooshasb, H.B., Holubec, I., and Sherbourne, A.N. (1967), 'Yielding and flow of ınd in triaxial compression: Parts II and III', Canadian Geotechnical Journal 4(4), 76– 97.

- Prevost, J.H. and Griffiths, D.V. (1988), 'Parameter identification and implementation f a kinematic plasticity model for frictional soils', Proceedings of the Workshop on :onstitutive Laws for the Analysis of Fill Retention Structures, ed. Evgin, E. Department f Civil Engineering, University of Ottawa, 285– 358.

- Prevost, J.H. and Hoeg, K. (1975), 'Effective Stress– Strain– Strength Model for Soils', 'roc. ASCE, Journal of the Geotechnical Engineering Division 101(GT3), 259– 278.

- Rad, N.S. and Clough, W., (1984), 'New procedure for saturating sand specimens', in 'roc. ASCE, Journal of Geotechnical Engineering 110(9), 1205– 1218.

- Roscoe, K.H., and Burland, J.B (1968), 'On the generalised stress– strain behaviour of wet' clay', in J.Heyman and F.A.Leckie(eds), Engineering plasticity (Cambridge: :ambridge University Press), pp.186– 91.

- Roscoe, K.H., and Schofield, A.N. (1963), 'Mechanical behaviour of an idealised 'wet' lay', Proc. European Conf. on Soil Mechanics and Foundation Engineering. Wiesbaden Essen: Deutshe Gesellschaft fur Erd– und Grundbau e.V.), vol. 1, pp. 47– 54.

- Roscoe, K.H., Schofield, A.N., and Thurairajah, A. (1963), 'Yielding of clays in states vetter than critical', Geotechnique 13(3), 211– 40.

- Roscoe, K.H., Schofield, A.N., and Wroth, C.P. (1958), 'On the yielding of soils', ietechnique 8(1), 22– 52.

– Rowe, P.W. (1962), 'The stress–dilatancy relation for static equilibrium of an assembly of particles in contact', in Proc. Roy.Soc.London A269, 500–27.

– Rowe, P.W. (1971), 'Theoretical meaning and observed values of deformation parameters for soil', in R.H.G. Parry (ed), Stress–strain behaviour of soils (Proc. Roscoe Memorial Symp., Cambridge) (Henley–on–Thames: G.T.Foulis & Co.), pp. 143–94.

– Rowe, P.W. and Barden, L. (1964): 'Importance of free ends in triaxial testing', ASCE, Journal of Soil Mechanics and Foundations Division, vol. 90, SM1, 1–27.

– Schofield, A.N., and Wroth, C.P. (1968), Critical state soil mechanics (London: McGraw–Hill).

– Singh, S., Seed, H.B. and Chan, C.K. (1982), 'Undisturbed Sampling of Saturated Sands by Freezing', Journal of the Geotechnical Engineering Division, ASCE, vol. 108, No. GT2, pp. 247–264.

– Skempton, A.W. (1954b), 'The pore pressure coefficients A and B', Geotechnique 4(4), 143–47.

– Tatsuoka, F., (1972), 'Shear tests in a triaxial apparatus. A fundamental research on the deformation of sand', PhD Thesis, University of Tokyo (in Japanese).

– Tatsuoka, F., and Ishihara,K. (1974a), 'Yielding of sand in triaxial compression', Soils and Foundations 14(2), 63–76.

– Tatsuoka, F., and Ishihara,K. (1974b), 'Drained deformation of sand under cyclic stresses reversing direction', Soils and Foundations 14(3), 51–65.

– Tavenas, F., des Rosiers, J–P., Leroueil, S., LaRochelle, P., and Roy, M. (1979), 'The use of strain energy as a yield and creep criterion for lightly overconsolidated clays', Geotechnique 29(3), 285–303.

– Taylor, D.W., (1948), 'Fundamentals of soil mechanics', (New york: John wiley).

– Vaid, Y.P., Chern, J.C. and Tumi, H. (1985), 'Confining pressure, grain angularity and liquefaction', Proc. ASCE, Journal of the Geotechnical Engineering Division 111(10), 1229–1235.

– Vaid, Y.P. and Negussey, D. (1988), 'Preparation of reconstituted sand specimens', Advanced Triaxial Testing of Soil and Rock, ASTM STP 977, Robert T. Donaghe, Ronald C.Chaney, and Marchall L.Silver, Eds., American Society for Testing and Materials, Philadelphia, pp. 405–417.

– Vardoulakis, I. (1978), 'Equilibrium bifurcation of granular earth bodies', in Advances in analysis of geotechnical instabilities (Waterloo, Ontario: University of Waterloo Press), SM study 13, paper 3, pp.65–119.

– Vermeer, P.A. (1978), 'A double hardening model for sand', Geotechnique 28(4), 413–433.

– Vermeer, P.A., and Borst, R.de (1984), 'Non–associated plasticity for soils, concrete and rock', Heron 29(3), 1–64.

– Vesic, A.S., and Clough, G.W. (1968), 'Behaviour of granular materials under high stresses', in Proc. ASCE, Journal of the Soil Mechanics and Foundation Division, 94, SM3, 661–88.

– Wood, D.M (1984b), 'On stress parameters', Geotechnique 34(2), 282–7.

- Wood, D.M. (1990), 'Soil Behaviour and Critical State Soil Mechanics', Cambridge University Press.

- Wood, D.M. (1991), 'Approaches to modelling the cyclic stress–strain response of soils', in M.P.O'Reilly and S.F.Brown (eds.), Cycling Loading of Soils: from theory to design, 2, (Glasgow and London: Blackie and Son Ltd), pp. 19–69.

- Wroth, C.P. and Houlsby, G.T., (1985), 'Soil mechanics–property characterisation and analyses procedures', in Proc. 11th Int.Conf.on Soil Mechs and Foundation Eng., San Francisco (Rotterdam: A.A. Balkema), vol. 1, pp. 1–55.

- Yasufuku, N., Murata, H. and Hyodo, M. (1991), 'Yield characteristics of anisotropically consolidated sand under low and high stresses', Soils and Foundations 31(1), 95–109.

- Zienkiewicz, O.C. and Pande, G.N., (1977), 'Some useful forms of isotropic yield surfaces for soil and rock mechanics', in G. Gudehus (ed.), Finite Elements in Geomechanics, Ch.5, 179–190, New York: John Wiley and Sons.

- Zytynski, M. (1976), 'Private communication to C.P.Wroth'.